Summer 2013

Subtalar Joint Instability: Diagnosis and Conservative Treatment

Julie Choisne
Old Dominion University

SUBTALAR JOINT INSTABILITY: DIAGNOSIS AND CONSERVATIVE TREATMENT

by

Julie Choisne
M.S. July 2009, Ecole Superieur d'Ingenieur Leonard de Vinci, France

A Dissertation Submitted to the Faculty of
Old Dominion University in Partial Fulfillment of the
Requirements for the Degree of

DOCTOR OF PHYLOSOPHY

MECHANICAL AND AEROSPACE ENGINEERING

OLD DOMINION UNIVERSITY
August 2013

Approved by:

Stacie I. Ringleb (Director)

Sebastian Bawab (Member)

Matthew C. Hoch (Member)

Stephen B. Knisley (Member)

Gene Hou (Member)

ABSTRACT

SUBTALAR JOINT INSTABILITY: DIAGNOSIS AND CONSERVATIVE TREATMENT

Julie Choisne
Old Dominion University, 2013
Director: Dr. Stacie I. Ringleb

Subtalar instability may be caused by various ligamentous injuries. Combined instability at the ankle and subtalar joint is not adequately diagnosed. Further, isolated subtalar instability is usually misdiagnosed which may lead to long term damage to the joint. Developing a non-invasive and clinically practical tool to diagnose subtalar joint instability would be an important asset. The ability of an ankle brace, a common treatment for hindfoot instability, to promote stability for the subtalar joint was not well established. The purposes of this study were to 1) assess the kinematics of the subtalar, ankle, and hindfoot in the presence of isolated subtalar instability; 2) investigate the effect of bracing in a calcaneofibular ligament (CFL) deficient foot and with a total rupture of the intrinsic ligaments; 3) implement an optimization method to determine the subtalar joint axis in vivo and apply this method in the diagnosis of subtalar joint instability. Kinematics from nine cadaveric feet were collected with the foot placed in neutral, dorsiflexion and plantarflexion. Motion was applied with and without a brace on an intact foot and after sequentially sectioning the CFL and the intrinsic ligaments. A two-hinge joint optimization model was developed to approximate the ankle and subtalar joint axis during inversion based on the kinematics of the calcaneus and the tibia. The optimization determined subject-specific subtalar and ankle joint axis for each condition. Isolated CFL sectioning increased ankle joint inversion while sectioning the CFL and intrinsic ligaments affected subtalar joint stability. Additionally, examining the foot in dorsiflexion significantly reduced ankle and subtalar joint motion. The ankle brace limited inversion at both joints. The inclination and deviation angles of the optimized subtalar joint axis were similar to previous studies. The orientation of the subtalar and ankle joint axes did not change after ligament injury. The optimized subtalar and ankle

axes were significantly different than the 'true' subtalar and ankle joint axes determined from inversion-eversion. Future work would improve the optimization to look at the change in the angle of rotation around the optimized subtalar and ankle joint axes to detect subtalar joint instability.

To my beloved Nicolas and Lili

ACKNOWLEDGMENTS

I would like to acknowledge my doctoral committee for their patience and guidance with my research as well as my family and friends for their constant support. I would like to offer special recognition to my mentor Dr. Stacie Ringleb, who has been a great academic advisor and a personal leader to me. I want to thank her for guiding me through my research, encouraging me when I needed it and for all the support she has given me. I would also like to thank Dr. Matthew Hoch for advising me in the clinical aspect of my dissertation and for his important help in collecting data. And last, but not least, thank you to Dr. Sebastian Bawab for his guidance and mentorship throughout my doctoral studies.

I owe a very special thanks to my family and friends for their support and encouragement. A special consideration goes to Nicolas, who made this dissertation happen. Without his love and encouragement, this dissertation would never have seen the light. He has been on my side since the first day and has given me the strength to continue. A special wink to my daughter, Lili, who inspired me in my work and showed me that any obstacle can be overcome.

TABLE OF CONTENTS

LIST OF TABLES

LIST OF FIGURES

1 INTRODUCTION

The ankle joint complex is composed of the talocrural joint and the talocalcaneal joint. The talocrural joint, most commonly called the ankle joint, is formed by the articulation of the distal end of the tibia and fibula with the talus. The talocalcaneal joint, usually called subtalar joint, is the articulation between the talus and the calcaneus (heel bone) (Figure 1-1) [1].

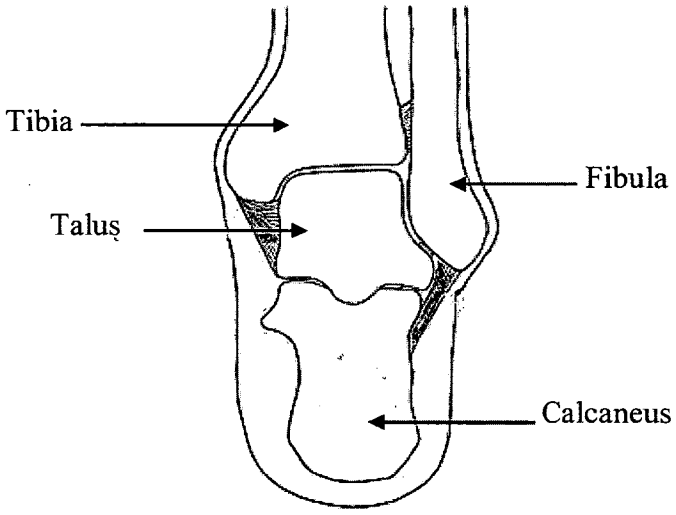

Figure 1-1: Posterior view of a right foot [2]

The primary function of the subtalar joint is to absorb the rotational forces of the weight bearing lower extremity during stance phase and therefore becomes the primary inverter of the foot. Its secondary role is to provide a shock absorption function for the body at heel strike [1, 3].

Subtalar joint stability can be affected by certain injuries and pathologies. The most common injuries that affect the subtalar joint are sprains and fractures. A lateral ankle sprain is one of the most common injuries with an estimated daily rate of 1 in

10,000 people in the United States [4] and was reported to account for 15 to 45% of sports-related injuries [5].

While lateral sprains are initially believed to happen at the ankle, most of these injuries actually occur at the subtalar or both joints. On a clinical examination, motion of the talus, a common bone in the ankle and subtalar joints (Figure 1-1), cannot be isolated, which makes it difficult for the examiner to differentiate between ankle and subtalar joint injury. Therefore, subtalar joint instability combined with ankle joint instability may not be adequately diagnosed, and isolated subtalar joint instability is usually ignored in the diagnosis [6].

Undiagnosed subtalar joint instability may lead to mechanical and functional instability of the hindfoot, which may lead to long term damage to the joint caused by abnormal kinematics. These pathologies include sinus tarsi syndrome [7], flexible flatfoot deformity [8] and Posterior Tibial Tendon Dysfunction (PTTD) [9]. Chronic ankle instability is the most common complication after an ankle sprain involving rupture of ligaments. It was associated with decreased quality of life and degenerative joint disease [10, 11]. Although conservative management is used to prevent the development of mechanical instability of the ankle, approximately 74% of hindfoot injuries result in chronic instability [12]. Among them, up to 80% are associated with subtalar joint instability [13-17]. Specifically, imaging studies demonstrated that 65% to 80% of ankle joint instability was combined with laxity of the subtalar joint [14, 15]. Additionally, 30% to 45% of foot surgeries presented subtalar joint instability intra-operatively while clinical procedures did not demonstrate any sign of instability at that joint [16, 17].

1.1 Injury mechanism

To help improve detection of subtalar joint instability, the mechanism of injury at this joint should be clarified. Keefe et al. [18] proposed that a forced hindfoot supination or inversion motion coupled with the ankle in neutral or dorsiflexion creates the injury. They believe that this motion creates a progressive injury to the calcaneofibular ligament (CFL), the lateral talocalcaneal ligament, the cervical ligament and the interosseous talocalcaneal ligament (ITCL). However, discrepancy in the literature exists regarding

whether deficiency of the CFL causes instability at the ankle or the subtalar joint. While several studies [19-22] documented the CFL as an important stabilizer of the subtalar joint, others found that CFL injury affected ankle joint stability instead [23-30]. Concerning the cervical ligament and the ITCL, only a few studies investigated their role in subtalar instability [21, 26, 29, 31-34]. Therefore, understanding the kinematics of the ankle and subtalar joint in inversion after injury to the subtalar joint ligaments is needed to help clinicians in their diagnosis.

1.2 Detection of instability

After an ankle sprain, a clinical procedure involves physical examination of the foot. A typical physical exam includes an anterior drawer stress test where an anterior force is applied to the heel while attempting to glide the talus anteriorly in the ankle mortise and an inversion stress test where the examiner rotates the calcaneus and talus into inversion. However, none of these procedures can differentiate the motion of the subtalar joint from the talocrural joint requiring advanced imaging techniques to delineate the source of instability [35, 36].

The same stress tests can be performed during an imaging evaluation. X-ray imaging is the most used technique with routine radiographs taken with antero-posterior, lateral and mortise views [16, 37-40]. However, these views and tests are not adapted to detect instability at the subtalar joint. Therefore, Broden [41] proposed a special view where the x-ray is centered over the lateral malleolus and the tube is angled at 10 - 20 degree towards the head with the patient's foot supine and the leg 45° internally rotated. While this technique was used to detect a possible subtalar tilt [14, 39, 42, 43], the overlap in the degree of subtalar opening between the symptomatic and asymptomatic is too high to differentiate between a healthy and unstable subtalar joint. 3D imaging techniques demonstrated that subtalar joint instability diagnosed using the Broden's view was not confirmed with a 3D CT scan of the same foot [43, 44]. Arthrography [15] and MRI techniques [27, 45] demonstrated good results in detecting subtalar joint instability; however, the first technique was too invasive, and the second one was time and cost

prohibitive. Therefore, current radiographical techniques do not meet clinical requirements to detect mechanical instability at the subtalar joint.

All of the aforementioned stress tests were performed with the foot held in a neutral position. In order to isolate motion at the subtalar joint, some studies proposed positioning the foot in dorsiflexion in order to lock the talus in the ankle mortise and therefore limit ankle joint motion [18, 46, 47]. One method dorsiflexed the foot at the ankle mortise while applying a varus stress on the calcaneus [47]. Another method consisted of positioning the foot in supination with forced manual dorsiflexion applied to the ankle to measure the relative position of the lateral process of the talus at the posterior articular facet of the calcaneus while using stress radiography [46]. Applying these techniques in vitro would improve the understanding of the mechanism behind these clinical evaluation strategies.

1.3 Non-operative treatment

In addition to the aforementioned need to explore techniques to evaluate subtalar joint instability, conservative treatment strategies for subtalar joint instability require further investigation. The application of an ankle brace was used after diagnosis of ankle and/or subtalar sprains [48]. The effects of ankle supports on ankle motion restriction were demonstrated *in vivo* [49-56] and their ability to reduce re-injury during athletic activities. Semi-rigid ankle braces limit inversion/eversion motion while keeping normal sagittal motion at the hindfoot [50, 51, 57]. Additionally, ankle braces also reduced talar tilt and frontal plane motion in passive and rapidly induced inversion [58, 59]. Despite these studies, limited evidence is available regarding the effects of ankle braces on subtalar joint instability. The effect of an ankle support after a total rupture of the lateral and intrinsic ligaments showed that the ankle brace significantly restricted inversion at the subtalar joint but not at the ankle joint [29]. However, the effect of the brace after isolated CFL injury was not investigated, and the applied moment was small (2 Nm) compared to moments applied during dynamic motion that may be more closely associated with an ankle sprain [60].

1.4 Three-dimensional kinematics of the subtalar joint

A step toward detecting and differentiating subtalar joint instability would be to further understand the three dimensional kinematics in the stable subtalar joint. Many investigators have investigated the kinematics of the ankle joint, but only few looked at the subtalar joint [61-68]. Moreover, a high discrepancy exists in the description of the subtalar joint range of motion in the 3 cardinal planes. For example, Beimers et al. [61] found that the greatest motion of the subtalar joint was from maximum inversion to maximum eversion with an angle of rotation of 37.1° while Siegler et al. [67] found that internal-external rotation was greater with an angle of rotation of 27.8°. A first explanation for this discrepancy is the difference in the experimental techniques and methods of analysis. This is supported by a previous study [26] which demonstrated differences in rotation angles for the same data set depending on the kinematics method used to analyze motion. A second explanation comes from the high inter-subject variability in the subtalar joint axis orientation that affects motion in the three cardinal planes. According to Close et al. [69] the orientation of the subtalar joint axis determines the amount of rotation found at the subtalar joint in a tri-planar motion. The subtalar joint axis is an oblique axis that describes motion in the three planes with the first motion around the subtalar joint axis being supination (combination of inversion, internal rotation and plantarflexion) and the second known as pronation (combination of eversion, external rotation and dorsiflexion). Investigators usually describe the orientation of the subtalar joint axis by referring to the inclination angle which is the angle between the axis and the plantar surface of the foot and by the deviation angle which is the angle between the projection of the axis on the transverse plane and the long axis of the foot [70]. Using 100 cadavers' feet, Inman et al. [71] demonstrated that the mean inclination angle was 42° and the mean deviation angle was 23° with a variation ranging from 20 to 68° for the inclination angle and from 4 to 47° for the deviation angle. The high variability in the orientation of the subtalar joint axis explains the discrepancy in kinematics reported at the subtalar joint. The development of a tool to create a subject specific kinematic model to approximate the subtalar axis during inversion may help in understanding how different injury mechanisms affect the stability of the subtalar joint.

Generating a tool to diagnose subtalar joint instability either manually or by using a model would be an important asset for clinicians. If subtalar instability can be diagnosed early, degeneration of the joint could be avoided, reducing the development of chronic ankle instability in the general population. Using an adequate conservative treatment after being diagnosed with subtalar instability may help in the reduction of recurrent lateral sprains.

1.5 Specific aims

This study had three specific aims and associated hypotheses to address the gaps in the literature described in the previous sections.

Aim 1: Investigate the 3D kinematics of both the intact and damaged ankle and subtalar joints in vitro.

The first step of this aim will be to determine the change in the subtalar joint and ankle joint kinematics after creating isolated subtalar instability. Inversion-Eversion will be applied to 1) the intact hindfoot, 2) after sectioning the calcaneofibular ligament (CFL) alone and 3) in combination with the cervical ligament and the interosseous talocalcaneal ligament (ITCL). The second step will be to understand the effect of foot sagittal position on frontal plane motion by moving the foot into inversion and eversion held in maximum dorsiflexion first and then maximum plantarflexion.

Hypothesis 1: Isolated injury at the CFL will increase inversion at the ankle joint while additional injury to the intrinsic ligaments (cervical and ITCL) will increase subtalar instability. Holding the foot in dorsiflexion and plantarflexion will decrease inversion and eversion range of motion in the hindfoot. Maintaining the foot in dorsiflexion should limit ankle motion for all injury conditions and allow for isolated subtalar range of motion. Having the foot in plantarflexion should increase ankle inversion compared to neutral and limited subtalar motion.

Aim 2: Assess how a semi-rigid, commercially available ankle brace, a commonly used conservative treatment for ligamentous ankle injuries, stabilizes the intact and unstable subtalar joint.

Hypothesis 2: The ankle brace will restrict motion in inversion/eversion in the ankle and subtalar joint without restricting plantarflexion and dorsiflexion but will not limit excessive internal/external rotation of the shank.

Aim 3: Determine the subtalar joint axis in vitro based on the kinematics of the calcaneus and the tibia.

The first step of this aim will be to estimate the subtalar joint axis and the ankle joint based on the hindfoot kinematics for initial guess to the optimization process. The subtalar joint axis will be approximated by holding the foot in dorsiflexion while applying inversion-eversion in order to minimize ankle motion. The ankle joint axis will be approximated based on plantarflexion-dorsiflexion motion which is known to have minimal subtalar rotation involved. The second step will be to develop a two-hinge joint optimization model to approximate the subtalar joint axis and ankle joint axis during inversion based on the kinematics of the calcaneus and the tibia using the approximated subtalar and ankle axes as initial guesses. The third step will be to use this optimization algorithm to determine the subtalar joint axis and the ankle joint axis after lateral ligamentous injury and see if the orientation of the two axes will significantly change after hindfoot instability was created.

Hypothesis 3: The two hinge-joint optimization algorithm will be satisfactory to approximate the subtalar joint axis in an intact foot but will not be able to account for the change in subtalar stability.

2 LITERATURE REVIEW

2.1 Introduction

The hindfoot is a unique complex part of the anatomy involving two hinge joints: a talocrural joint, most commonly called the ankle joint, and the talocalcaneal joint, also referred as the subtalar joint. The common bone of the two joints is the talus which is inaccessible to external tracking and makes its motion impossible to measure in vivo. Therefore, distinction between ankle and subtalar joint motion is difficult; consequently, differentiating between ankle and subtalar instability becomes impossible.

Subtalar joint stability can be affected after ligamentous injuries such as an acute ankle sprain or degenerative conditions such as Posterior Tibial Tendon Dysfunction (PTTD) [9], flexible flatfoot deformity [8], sinus tarsi syndrome [7] and Charcot foot in diabetes. In cases where subtalar joint instability is caused by trauma such as ankle sprains, it is generally assumed that the patient has lateral ankle instability, not subtalar joint instability. However, up to 80% of individuals with a history of lateral ankle sprain associated with ankle instability also demonstrated instability at the subtalar joint [13-17]. Furthermore, 74% of hindfoot injuries result in chronic joint instability with up to 75% specifically associated with subtalar joint instability [12]. This is a significant problem to address because lateral ankle sprain is the most common lower extremity injury with an estimated daily rate of 1 in 10,000 people in the United States [4], and it accounts for 15% to 45% of all reported sports-related injuries [5]. Repetitive articular trauma may lead to a mechanical and/or functional instability of the hindfoot and long term disability associated with degenerative joint conditions.

Subtalar joint instability may also be caused by pathologies including but not limited to PTTD, flexible flatfoot deformity, cerebral palsy, sinus tarsi syndrome, hemiplegia, rheumatoid arthritis and Charcot foot in diabetes. By the time patients are treated, severe osteoarthritis at the subtalar joint caused by abnormal cartilage loading

patterns or disability may be present. Osteoarthritis in the subtalar joint causes degradation in balance leading to an increased risk of falls and additional joint trauma.

Subtalar joint instability was first described by Rubin and Whitten [6] where they presented a method for evaluating instability at the subtalar joint using a tomography technique. After forcibly inverting the symptomatic foot, none of their patients demonstrated increase in subtalar tilt compared to the asymptomatic foot. In 1977, Brantigan et al. [72] confirmed Rubin and Whitten's work by demonstrating three cases of chronic subtalar joint with a subtalar tilt greater in symptomatic feet (57° ±5) than on the asymptomatic (38° ±6). None of the patients showed differences in talar tilt between the two feet. While Laurin et al. [20] investigated the stability of the subtalar joint in vitro, Chrisman and Snook [17] recognized the need for treatment in three young adults demonstrating ankle and subtalar instability. Later, Meyer et al. [15] confirmed the presence of subtalar instability in 80% of his patients with acute sprains using subtalar arthrography.

Subtalar joint instability combined with ankle joint instability are not adequately diagnosed and are usually detected after surgery. Isolated subtalar joint instability is usually neglected and can lead to inadequate treatment. A key to successful treatment is a differential diagnosis with stability testing of both joints.

2.2 Anatomy

2.2.1 The ankle joint complex

The subtalar joint is composed of 3 articular surfaces: the anterior, middle and posterior facets. Hyer et el. [73] described the middle and anterior facets as conjoined in 56% of cases. The anterior/middle and posterior facets are separated by the sinus tarsi and the tarsal canal. The anterior subtalar joint is composed of the anterior part of the talus, the anterior part of the calcaneus and the posterior surface of the navicular. The posterior facet of the subtalar joint is formed by the posterior facet of the talus and calcaneus with a convex-concave shape to increase the bony stability of the joint. [74]

Harper et al. [75] categorized the subtalar joint ligamentous structures into three layers. The superficial layer is formed by the lateral root of the extensor retinaculum, the CFL and the lateral talocalcaneal ligament; the intermediate layer is composed of the intermediate root of the retinaculum and the cervical ligament; finally, the medial root of the inferior extensor retinaculum and the ITCL constitute the deep layer.

A complete understanding of the ligamentous structures in the foot is required to understand the injury pattern and help in diagnosing subtalar joint instability.

2.2.2 Ligaments of the foot

Recognizing the anatomic location of the lateral ligaments of the foot is important to understanding their role in hindfoot stability.

The lateral ankle ligament structure is composed of the anterior talofibular ligament (ATFL), the calcaneofibular ligament (CFL) and the posterior talofibular ligament (PTFL). The three ligaments find their insertion close to each other on the distal fibula and are oriented in the three different spatial directions. The most lateral stabilizing structures are the ATFL and CFL. The ATFL is the weakest of the lateral ankle ligaments [76]. Its attachment is localized on the anterior edge of the lateral fibula and extends slightly superiorly, anteriorly and medially to the lateral aspect of the talus. In plantarflexion, the ATFL is parallel to the long axis of the foot that may be a reason for why this ligament is more subject to injury while the foot is in plantarflexion. The CFL is perpendicular to the posterior facet of the subtalar joint and is responsible for the maintenance of congruity between the talus and the calcaneus. It extends obliquely from the anterior edge of the distal fibula to the mid lateral surface of the calcaneus. The CFL is almost parallel to the subtalar joint axis [77].

The main ligaments situated in the sinus tarsi and tarsal canal are the cervical ligament and the interosseous talocalcaneal ligament (ITCL). They are commonly called the intrinsic ligaments in opposition to the lateral ligaments named extrinsic ligaments. The cervical ligament joins the neck of the talus to the lateral edge of the calcaneus. It is laterally interlinked to the extensor retinaculum. It has been described as the strongest

ligament connecting the talus and calcaneus [78]. The ITCL is found in the sinus tarsi and is divided into 2 branches (like a "Y" shape) directed antero-medially across the sinus tarsi and provides a strong stabilization system to the subtalar joint [7]. According to some authors [33, 79], the ITCL seems to play an important role in subtalar joint stability, especially in supination and has been shown to restrict anterior displacement of the calcaneus. It has also been described [7] as the pivot point of the subtalar joint similar to the role of the cruciate ligaments in the knee.

2.3 Biomechanics

2.3.1 Normal range of motion of the subtalar joint

Understanding the biomechanics of the intact subtalar joint is necessary in order to determine the pathomechanics at this joint. The subtalar joint was widely described as a hinge joint [71, 80]. This plane of rotation is lying on a slant with respect to the subtalar joint axis. Rotation about this plane produces a combination of eversion, external rotation and slight dorsiflexion on one side called pronation and a combination of inversion, internal rotation and plantarflexion on the other side termed supination. Leardini et al. [81] reported the kinematics in the ankle joint complex during passive motion to investigate the presence of a preferred path of motion at the unloaded intact hindfoot prescribed by the articular surfaces and the ligaments. The authors used a flexing rig to move the ankle complex throughout its range of passive flexion. They found that most of the motion occurred at the ankle joint in the sagittal plane but also in the transverse and frontal planes. However, when deviation load was applied to the calcaneus, most of the motion occurred at the subtalar joint showing its typical range of motion; 8° of plantar/dorsiflexion, 8° of inversion/eversion and 11° of internal/external rotation. In another study [82], the same authors found that 70 to 90% of the motion occurred at the subtalar joint during supination/pronation.

The subtalar joint has a tri-planar range of motion. Its main motion happens in the frontal plane where inversion/eversion occurs. Then internal and external rotation is described as the rotation along the long axis of the tibia perpendicular to the transverse

plane and the third motion is plantarflexion/dorsiflexion which is the motion occurring in the sagittal plane.

Motion at the subtalar joint can be described individually in the three anatomical planes. Siegler et al. [67] investigated kinematics in the hindfoot complex. Using a motion tracking system, they determined the range of motion at the ankle joint and the subtalar joint during plantarflexion/dorsiflexion, inversion/eversion and internal/external rotation. Based on the motion of the calcaneus and tibia, the authors found that the ankle joint accounts for 80% of plantarflexion/dorsiflexion motion, the subtalar joint has a bigger range of motion during inversion/eversion (73.5%) and that both joints contribute equivalently to internal/external rotation (50%/50%) of the hindfoot. Maximum dorsiflexion and plantarflexion of the foot are associated with 5.37° and 8.97° of subtalar joint motion respectively. Contribution of the subtalar joint during inversion and eversion were 15.04° and 8.5°. During internal rotation the subtalar joint rotated 15.65°, and during external rotation the subtalar joint motion was 12.24°.

Lundberg et al. [63] investigated the range of motion of the subtalar joint in the 3 cardinal planes in vivo using stereo photogrammetry. They found that external rotation was the largest motion detected in the subtalar joint with an average of 11.6° followed by inversion with 9.9°. Applying 20° of internal rotation to the foot resulted in the smallest amount of subtalar joint rotation with 2.1°. Eversion, plantarflexion and dorsiflexion motion resulted in less than 5° of subtalar motion. In a previous study [62, 64, 65], the same authors looked at the 3D kinematics of the ankle and subtalar joint for each motion. When applying plantarflexion/dorsiflexion, they concluded that most of the sagittal motion happened at the ankle joint with small rotation occurring at the subtalar joint. They found that in 30° of plantarflexion, the subtalar joint rotated 2.2° of plantarflexion, 2.4° of internal rotation and 1.3° of inversion. In 30° of dorsiflexion, motion of the subtalar joint was even smaller with 1.8° of plantarflexion, 1.4° of internal rotation and 1.3° of inversion. After applying supination/pronation to the foot, most of the motion occurred at the talonavicular and subtalar joint. In 20° of supination, the subtalar joint rotated of 5.1° of plantarflexion, 5.6° of internal rotation and 5.5° of inversion while in 20° of pronation, motion of the subtalar joint was smaller with 2.7° of dorsiflexion, 1.8°

of external rotation and 2.7° of eversion. When studying the influence of leg rotation on the kinematics of the joints of the foot, Lundberg et al. [65] found that internal rotation was mainly induced by the rotation of the talus in the ankle mortise and external rotation happens at the subtalar joint. In 20° of tibia internal rotation, the subtalar joint rotated 1.1° of dorsiflexion, 1.2° of external rotation and 0.9° of eversion. With 10° of external rotation applied to the hindfoot, motion of the subtalar joint was larger with 6.4° of plantarflexion, 7.4° of internal rotation and 5.2° of inversion.

Siegler et al. [68] and Sheehan et al. [45] used MRI to study the kinematics of the ankle and subtalar joint. Siegler et al. compared the ankle and subtalar joint in vitro and in vivo kinematics and found greater motion in vitro at the ankle joint with similar rotations at the subtalar joint. When a 3.4Nm inversion moment was applied to the foot, the subtalar joint rotated 9° ±4 in vivo and 8.3° ±4 in vitro. Subtalar joint response to a 150N anterior drawer force was 1.7mm ±1.5 in vivo and 1.3mm ±1 in vitro. After moving the foot in the sagittal plane, Sheehan found that most of plantarflexion/dorsiflexion motion occurred at the ankle with small motion detected at the subtalar joint. For most subjects, plantarflexion was coupled with inversion and little internal rotation.

Tujithof et al. [83] investigated the normal ranges of motion of the ankle and subtalar joint using a 3D CT stress test. Rotation of the subtalar joint was greater than the ankle joint when inversion/eversion was applied with a 37.3° of rotation between extreme eversion to extreme inversion and 35.5° between extreme combined eversion and plantarflexion to extreme combined plantarflexion and dorsiflexion.

Most ankle joint motion happens in the sagittal plane motion with small rotation happening at the subtalar joint while most subtalar joint motion happens in the frontal plane. Motion in the transverse plane occurs at the 2 joints with greater contribution of the subtalar joint in external rotation than internal rotation. During supination/pronation, 70 to 90% of the motion comes from the subtalar joint with a rotation of 5.1° in plantarflexion, 5.6° in internal rotation and 5.5° in inversion during supination and 2.7° of dorsiflexion, 1.8° of external rotation and 2.7° of eversion during pronation.

2.3.2 Pathomechanics of the subtalar joint

The CFL was described as the main stabilizer of the subtalar joint [19-22] and an important structure in maintaining subtalar joint stability. Other studies showed that rupture of the CFL did not affect the stability between the talus and calcaneus but increased ankle joint motion instead [23-30]

Martin et al. [28] examined the role of the CFL and cervical ligament during physiologic loading and determined the effect of CFL deficiency on the cervical ligament. They assessed the talar and subtalar tilt as well as inversion ROM in the hindfoot before and after sectioning the CFL. They found a significant 63% increase in talar tilt after sectioning the CFL and a not significant 17% increase in subtalar tilt. The maximum inversion rotation at the tibio-calcaneal joint was recorded during the combination of dorsiflexion and inversion with an intact ROM of 27.7° and a CFL deficient ROM of 33°.

Cass et al. [25] investigated the 3D kinematics at the ankle joint and subtalar joint on a stable foot and after sectioning the ATFL alone, the CFL alone, both combined and adding the PTFL. The foot was placed in stress supination combined with plantar/dorsiflexion positions. Results for maximal inversion and internal rotation of the intact subtalar joint were 18.7° and 19° respectively, regardless of the degree of flexion. Sectioning ligaments did not affect motion at the subtalar joint. The main motion of the hindfoot occurred at the subtalar joint when the foot was intact. After sectioning ligaments, increase of rotation was observed mainly at the ankle joint. After sectioning the CFL alone, the amount of inversion in the neutral position doubled at the ankle joint.

Rosenbaum et al. [24] and Fujii et al. [30] determined the degree of rotational instability at the subtalar and ankle joint after sequentially sectioning the ATFL and the CFL. Rosenbaum found that cutting the ATFL and both ligaments increased significantly the range of motion at the ankle joint in inversion/eversion and internal/external rotation but not at the subtalar joint. Injury at the lateral ligament does not affect plantar/dorsiflexion range of motion in either joint. Fujii [30] assessed ankle joint stability after applying an inversion torque and an internal rotation torque through the

range of sagittal plane motion. Rosenbaum did not find any increase in subtalar joint motion in inversion or internal rotation with any flexion angle. Sectioning the ATFL increased ankle internal rotation and an additional injury to the CFL increased ankle inversion ROM. Placing the foot in dorsiflexion reduced internal rotation and inversion ROM while having the foot in plantarflexion increased the range of ankle inversion. Hollis et al. [23] came to the same conclusion that the ankle was more lax in plantarflexion and more stable in dorsiflexion when inversion is applied to the foot. A section of the ATFL and CFL increased ankle joint motion in all sagittal positions while subtalar motion was not affected.

Ringleb et al. [27] used an MRI to identify the increase in ankle and subtalar joint inversion after sectioning the ATFL and CFL. They found a significant 100% increase in inversion at the ankle joint and a non-significant 29% increase at the subtalar joint after sectioning the CFL in addition to the ATFL. Choisne et al. [26] found a 150% increase in ankle inversion after sectioning the ATFL and CFL without affecting subtalar motion.

Kamiya et al. [29] investigated the influence of ligament injury on subtalar joint stability. The authors applied a 2N.m inversion/eversion and internal/external rotation torque to the tibia with the calcaneus fixed on an intact foot and after sequentially sectioning the CFL, the cervical ligament and the ITCL and after applying an ankle brace to the hindfoot. Kinematics of the tibia, fibula, talus and calcaneus were recorded with no load applied to the tibia. Results at the subtalar joint demonstrated a non-significant increase of 12.6% in the frontal plane and 17% in the transverse plane during inversion after sectioning the CFL. When internal rotation and eversion was applied, no increase was observed between the intact condition and subtalar joint injury. On the other hand, applying external rotation to the injured foot significantly increased motion at the subtalar joint after sectioning the CFL with an increase of 1.4° compared to intact which is not clinically significant. Ankle joint inversion significantly increased by 283% after sectioning the CFL while ankle eversion and transverse rotation were not affected.

Other studies found that the CFL does not influence ankle stability but contributes to subtalar instability. Kjaersgaard-Andersen et al. [22] investigated the role of the CFL

on the subtalar joint stability by applying an inversion moment to the hindfoot combined with incremental position of plantarflexion-dorsiflexion. They determined subtalar joint motion before and after fixing the ankle joint on impact and after sectioning the CFL. Before fixing the ankle joint, motion of the hindfoot joint decreased in dorsiflexion on the intact foot, but larger inversion rotations were detected between intact and CFL cut in dorsiflexion. After fixing the ankle joint, motion in the sagittal plane was restricted to 7.5° plantarflexion and 5° dorsiflexion. At the subtalar joint, a significant increase in inversion was found from 5° plantarflexion to 2.5° dorsiflexion only after sectioning the CFL. The rotation differences between an intact and an injured foot increased with dorsiflexion. Regardless of the foot position in the sagittal plane, most of the differences in inversion between the two conditions were found to take place in the subtalar joint, with a maximum increment of 77% at 5° dorsiflexion. The authors concluded that with the ankle joint at maximal dorsiflexion, the talus is interlocked in the ankle mortise and inversion of the hindfoot only takes place in the subtalar joint.

Weindel et al. [21] fixed the ankle joint to study subtalar joint kinematics in an intact foot and after sectioning in sequence (1) and inverse sequence (2) the bifurcate ligament, the inferior extensor retinaculum, the ITCL, LTCL and CFL. They applied motion to the foot in plantarflexion/dorsiflexion, external/internal rotation and inversion/eversion. The authors found statistically significant increase in motion during inversion/eversion after sectioning the inferior extensor retinaculum in the first sequence and significant increase in internal/external rotation after cutting the LTCL. In the inverse sequence (2), dissection of the CFL lead to a significant increase in rotation in all motions; however, the increase did not exceed 1° of rotation; that is not clinically significant.

The main drawback of these two studies [21, 22] was that they fixed the ankle joint in a neutral position that might allow for abnormal subtalar motion. [19, 20] assessed the subtalar tilt and the talar tilt in CFL deficient hindfoot using roentgenograms and X-rays. They found that sectioning the CFL produced an increase in the subtalar tilt without any excessive mobility at the ankle joint. Variability of the orientation of the CFL may explain the discrepancy in literature on the influence of the CFL on subtalar

joint stability. Trouilloud et al. [84] investigated the anatomy of 26 ankles and found that 35% ankles (Type A) had a CFL that blends with the lateral talocalcaneal ligament and diverges at the talar or calcaneal insertion. In 25% (Type B) a distinct lateral talocalcaneal ligament was present anterior to the CFL. In 42% (Type C) the lateral talocalcaneal ligament is absent. Sectioning the CFL in ankles presenting a type B did not affect the kinematics of the subtalar joint while in type A and C CFL deficiency affected subtalar stability.

The ITCL is found in the sinus tarsi and provides a strong stabilization system to the subtalar joint [7, 79, 85]. The ITCL seems to play an important role in subtalar joint stability [21, 26, 29, 31-34]. Discrepancy exists in the literature about the percentage of inversion increase after sectioning the ITCL. Fixing the ankle joint to study the subtalar motion might be a cause for this discrepancy. Some studies [21, 31, 32] investigated the 3D kinematics of the subtalar joint with a fixed ankle. Kjaersgaard-Andersen et al. [31] measured the range of motion in the 3 planes after sectioning the cervical ligament or the ITCL. The maximum increase in motion observed after cutting the cervical ligament was 1.7° and 1.8° after sectioning the ITCL, which is not clinically significant. However, the authors stated that percentage increase after cutting one of the two ligaments is large enough, especially during inversion-eversion, to correlate clinical subtalar instability to lesions of these ligaments with a 31% increase in internal-external rotation and 23% increase in inversion-eversion at the subtalar joint. Weindel et al. [21] sectioned in sequence (1) and inverse sequence (2) the bifurcate ligament, the inferior extensor retinaculum, the ITCL, LTCL and CFL. Statistically significant increases were detected during inversion/eversion after sectioning the inferior extensor retinaculum in the first sequence, in internal/external rotation after cutting the LTCL and in the sagittal plane after sectioning the bifurcate ligament. The second sequence showed statistical differences after the CFL was cut in the 3 planes. They never found any significant increase after sectioning the ITCL with an increase of 27% in the first sequence and 24% in the second sequence. Knudson et al. [32] investigated the contribution of the ITCL on the stabilization of the subtalar joint during supination-pronation. A 29% significant increase in supination was found after sectioning the ITCL using the helical axis description. Another cause of literature discrepancy on ITCL deficient subtalar joint

inversion ROM would be the use of a closed kinetic chain device. Kamiya et al. [29] investigated the influence of ligament injury after sequentially sectioning the CFL, the cervical ligament and the ITCL. Results at the subtalar joint demonstrated a significant increase of 33% in inversion after sectioning the cervical ligament in the frontal plane. Significant 45% and 57% increases in rotation were found in the frontal and transverse plane respectively after sectioning the ITCL. When internal rotation and eversion were applied, no increase was observed between the intact condition and subtalar joint injury. The sagittal position of the foot is another factor for discrepancy in the literature. Choisne et al. [26] investigated the influence of ATFL, CFL, cervical ligament and ITCL sectioning on subtalar, ankle and hindfoot joints kinematics. Significant increase in inversion (102%), supination (72%) and inversion with the foot in maximum dorsiflexion (67%) at the subtalar joint was detected after sectioning the ITCL.

2.3.3 Determination of the subtalar joint axis

Motion at the subtalar joint is tri-planar and allows for motion in inversion/eversion, internal/external rotation and limited plantarflexion/dorsiflexion. The subtalar joint has also been described as a hinge joint with an oblique axis passing through the head of the talus and a point on the posterior-lateral calcaneus. Motions around this axis are called supination and pronation with supination being a combination of inversion, internal rotation and plantarflexion and pronation combine eversion, external rotation and dorsiflexion of the calcaneus with respect to the talus. The inclination and deviation angles are usually reported to describe the orientation of the subtalar joint axis. The inclination angle is defined as the angle between the subtalar joint and the plantar surface of the foot, and the deviation angle is formed with the projection of the subtalar joint axis on the transverse plane and the midline of the foot [70]. Numerous studies attempted to localize the subtalar joint axis, but none of them demonstrated conclusively accurate techniques nor found wide-spread clinical use.

In vitro studies

Manter [80] was the first to investigate the subtalar joint axis of rotation in relationship to the cardinal planes of the body. The results of measurement of the subtalar joint axis showed a mean deviation angle of 16° that ranged from 8 to 24° and a mean inclination angle of 42° with a range between 29 and 47° depending on foot specimens. He was the first to conclude that motion at the subtalar joint consisted of rotation in a direction oblique to the axis of the joint that implies a screw like rotation of the subtalar joint. When the calcaneus is fixed, pronation of the foot causes the talus to turn clockwise and advance along the joint axis; its forward displacement would be 1.5mm every 10 degrees of rotation.

Root et al. [86] improved the technique developed by Manter [80] to determine the subtalar joint axis. The orientation of the subtalar joint was similar to the one reported by Manter with a mean inclination angle of 41° ±8° (22-55°) and a mean deviation angle of 17° ±2° (8-29°).

Inman et al. [71] described the motion between the talus and calcaneus as a rotatory motion about a single oblique axis. From 100 cadaver feet, they estimated this oblique axis to point from a postero-lateral-distal to an antero-medial-proximal direction. The inclination of this axis with the transverse plane was found to be 42° ±9°, and the deviation from the midline of the foot in the horizontal plane was found to be 23° ±11°. A high inter-specimen variability in the orientation of the subtalar joint axis was detected with a variation between 20° and 68° in inclination angle and from 4° to 47° in deviation angle.

Engsberg et al. [87] were the first to investigate subtalar joint kinematics by locking the talocrural joint and using a 6 DOF apparatus. The authors used Euler angles to move an apparatus in different positions with different loads for a total of 243 experiments on 9 specimens. They determined the mean helical axis between all motions and found a large inter- and intra-specimen variability in the location and orientation of the helical axis unit vector. They stated that the subtalar joint axis was a multi-axial type joint, and using the subtalar joint axis to prevent or treat of injury was not appropriate.

Lewis et al. [88] presented a novel technique to approximate the subtalar joint axis location by passively immobilizing the ankle joint and using the helical axis between the tibia and the calcaneus. They investigated kinematics of the hindfoot in vitro by comparing the helical axis unit vector computed from the talus and calcaneus bone motions to axes computed from the tibia and calcaneus. To compare the helical axis location and direction, they calculated the angle between the calcaneus-talus and calcaneus-tibia axes that ranged from 1.7° to 27.4°, and the minimum distance between the 2 axes ranged from 0.2 to 5.2mm. The inclination angle was 30.6 ±6.4° at the tibiocalcaneal joint and 38.2 ±6.2° at the subtalar joint. The deviation angle was 23.2 ±10.4° at the tibiocalcaneal joint and 21.3 ±3.6° at the subtalar joint. The method to approximate the subtalar joint axis by locking the ankle joint using the kinematics from the tibia and calcaneus was acceptable for 4 of the 6 specimens. For the 2 remaining specimen they needed to reduce motion at the ankle joint.

In vivo studies

Close et al. [69] investigated the importance of the subtalar joint axis on foot kinematics. According to the authors, the orientation of the subtalar joint axis accounts for the variations in the type of foot. They classified the human foot according to the position of the subtalar joint axis. For example, they determined that a cavus foot presents a significant medial deviation inferior to 16°, and a flatfoot has a subtalar joint axis deviated from more than 16°. The position of the axis determines also the amount of motion found at the subtalar joint. Therefore, for a cavus foot, the total range of supination and pronation will not exceed 11° while for a normal foot the average range of motion is 24°, and for a flatfoot it is greater than 28°.

Lundberg et al. [63] analyzed the position and orientation of the talocalcaneal joint axis during plantar/dorsiflexion, internal/external rotation and inversion/eversion using stereo photogrammetry. They determined the talocalcaneal joint axis using the helical axis method. They found that the mean deviation of the joint axis ranged from 23° during internal rotation to 37° in external rotation with a maximum variability between subjects found in dorsiflexion. The inclination angle ranged from 29° in eversion to 38°

in external rotation and high standard deviation during pronation. Individual variation was considerable especially during internal rotation that produced the smaller rotations.

Lewis et al. [89] applied their method previously developed in vitro [90] to living volunteers to approximate the subtalar joint axis using the location and orientation of the tibiocalcaneal helical axis. They changed their technique to reduce motion at the ankle joint using a 3D rigid body dynamic model to determine the line of action that would minimize ankle joint motion by setting the angular acceleration equal to 0. Subtalar joint axes were located using a dynamic MRI, and tibia-calcaneus motion was recorded using skin-mounted markers on the tibia and calcaneus. The MRI test showed that errors in locating the true subtalar axis using the tibiocalcaneal axis were 6 ±3.5° and 2.5 ±1.4mm. The inclination and deviation angles of subtalar joint axes were 33.4 ±10.7° and 18 ±10.4° respectively. This study demonstrated that the subtalar joint axis found from tibia-calcaneus bone motion closely approximated the true subtalar joint axis.

Clinical techniques

Kirby et al. [91] described two clinical methods to determine the position of the subtalar joint axis in relation to the plantar surface of the foot. The first method was a palpation technique that consisted of holding the fifth metatarsal with one thumb and applying pressure on the plantar calcaneus to the forefoot with the other thumb until no motion occurred at the subtalar joint. The other method used the range of motion technique that relied on the fact that for a foot with a normal subtalar joint axis position, the forefoot rotates about the subtalar joint axis in relation to the leg. These techniques required a highly skilled examiner and patience and have not been validated using cadavers or invasive techniques in vivo.

Phillips et al. [92] combined the palpation technique developed by Kirby et al. [91] and a mathematical model to construct the subtalar joint axis into a 3D linear equation. The method did not require special instruments or high skills of clinical examination. The authors determined the subtalar joint axis in 62 individuals and used it to calculate the torque produce at the subtalar joint during pronation and supination. However, neither validation nor comparison was used in their research.

Mathematical Optimization

Van den Bogert et al. [93] computed a subject specific 3D model of the ankle joint complex to approximate the joints axes by implementing 2 ideal hinge joints (talocrural and talocalcaneal joints) and expressed the 6DOF model using 12 model parameters describing the locations of the joint axes. They used an optimization method to fit the model parameters. They tested their model on 14 normal subjects in vivo by only tracking motion from the tibia and calcaneus. The low fit errors of the model suggest that this 2 axes optimization model of the hindfoot provided a good approximation to the kinematics of the unloaded ankle joint complex. The predicted inclination and deviation angles for the subtalar joint were similar to cadaver studies with an inclination angle of 37.4 ±2.7° and a deviation angle of 18 ±16.2°. The high variability in the subtalar joint deviation angle indicated uncertainty in the optimization method and makes the optimization procedure not sufficiently accurate for determining the subtalar joint axis.

Lewis et al. [90] developed a motion-based optimization method for locating the talocrural and subtalar joint axes. The computational method fitted a two-revolute model and used 12 model parameters corresponding to physiological ankle and subtalar joint landmarks and input the motion of the calcaneus relative to the tibia from reflective markers placed on cadaver feet. The optimization method performed well when compared to a 2 revolute mechanical linkage with differences in helical axis location ranging from 1° to 5°. However, when comparing the helical axis from the model to the cadaver bone motion, the difference in helical axis location exceeded 20°. They concluded that the optimization method based on 2 revolute joints failed to locate the subtalar joint axis because of the non-revolute behavior of the subtalar joint.

2.4 Mechanism of injury

Lateral ankle sprain are usually the result of a forced weight-bearing inversion of the rearfoot. If plantarflexion of the foot is combined with the inversion motion, the ATFL will most likely be the first ligament to rupture as with the foot in plantarflexion the ATFL becomes parallel to the foot axis. If dorsiflexion of the foot is coupled to the

inversion motion, stress will immediately injure the CFL as with dorsiflexion of the ankle the CFL becomes parallel to the foot.

Meyer et al. [15] described 2 mechanisms of injury. The first one is forceful supination combined with plantarflexion of the foot that first tears the ATFL, followed by disruption of the CFL or the ITCL. The second situation is a forceful supination combined with dorsiflexion of the ankle that leads to rupture of the CFL, the cervical ligament and the ITCL.

Freeman [94] investigated the causes for the foot to 'give way' after an ankle sprain. Functional instability of the foot can be caused by antero-posterior instability of the talus in the ankle mortise, instability at the subtalar joint, inferior tibio-fibular diastasis, peroneal muscle weakness and a "weak spot" in the ligament. The author investigated a group of 62 patients with a recent ankle sprain for a year. 14 patients showed a mechanically unstable foot after 1 year, but from these 14 only 6 complained of functional instability. 24 patients complained of functional instability without displaying any mechanical instability. No antero-posterior instability of the talus was found, nor subtalar joint instability, calf muscle weakness, tibio-fibular diastasis nor ligament 'weak spot'. However, most patients displayed adhesion formation. Mechanical instability of the ankle may have accounted for functional instability in 6 patients. 17 patients noted a sensation of 'give way' although no clinical or radiological abnormality was found after a year.

Laurin et al. [20] investigated the function of the lateral ankle in a cadaver study. They found that by sectioning the CFL alone, forced inversion produced a tilt in the subtalar joint and not in the ankle; additional damage to the talocalcaneal ligament increased the subtalar tilt without affecting the ankle joint. In a second experiment they sectioned the ATFL first and observed that the ankle joint was unstable with an obvious talar tilt. Additional damage at the CFL produced a tilt at the subtalar joint as well. Their conclusions are 1) the CFL supports both joints but its main role is to maintain subtalar joint stability and 2) the ATFL is important in the stability of the ankle joint and not the subtalar joint. According to the author, it is possible that an ankle sprain involves injury

to both ligaments; consequently, instability at the ankle joint would be associated with instability at the subtalar joint. However, if the CFL is torn first, further strain to the ankle will not necessarily involves damage to the ATFL and an isolated subtalar joint instability would be observed.

Exact injury pattern remains unclear, but it is apparent that force supination combined with dorsiflexion of the ankle is a common mechanism of subtalar joint injury. Dorsiflexion of the ankle seems to lock the talus into the ankle mortise without protecting the more distal ligaments. Isolated chronic laxity of the subtalar joint is common in athletes especially in sports with abrupt impact such as basketball and volleyball. This impact is associated with a sudden deceleration of the calcaneus with inertial progression of the talus that causes a "whiplash" mechanism of injury to the ITCL [7].

2.5 Diagnosis techniques

Differentiating between ankle and subtalar instability is almost impossible as the clinical symptoms of both are very similar. Most patients presenting to the clinician may give a history of an acute inversion injury or chronic ankle sprain which resulted in difficulty walking on uneven surfaces. Symptoms of subtalar joint instability are associated with a feeling of 'giving way' or 'rolling over' and lead to limitations in daily and sporting activities. Other symptoms include recurrent swelling, stiffness and pain situated in the sinus tarsi [7]. Patients may become dependent on ankle supports or braces and may change their daily activities to avoid situations that would stress their ankle [18].

2.5.1 Physical examination

Physical examination on acute subtalar sprain is difficult to perform; lateral ecchymosis/hematoma, swelling and tenderness are usually present and are comparable to signs associated with ankle instability. With later presentation the symptoms disappear with less pain allowing the clinician to examine the foot for subtalar instability. Despite the remaining stiffness, an increase in hindfoot inversion range of motion and anterior translation might be detected. A typical physical exam includes an anterior drawer stress test where an anterior force is applied to the heel while attempting to glide the talus

anteriorly in the ankle mortise and an inversion stress test where the examiner rotates the calcaneus and talus into inversion. Despite these tests, it remains difficult to differentiate between an isolated subtalar injury and a combination of ankle and subtalar instability.

Some studies investigated the outcome of the anterior drawer test and inversion stress test on cadavers before and after sectioning the ATFL and CFL. Bahr et al. [95] investigated the lateral ligament forces induced in neutral, 10 degree dorsiflexion and 10 and 20 degree plantarflexion combined with 1) anterior drawer and 2) inversion at the ATFL and CFL. They performed the tests on an intact foot and after sequentially sectioning the ATFL and CFL to analyze the changes in kinematics after injury. Results showed that on the intact foot forces induced at the CFL increased with dorsiflexion and increased at the ATFL with plantarflexion during anterior drawer and talar tilt tests. After sectioning the ATFL, significant increase in anterior displacement was found with the foot in plantarflexion. Sectioning the CFL induced a significant increase in inversion while the foot was in dorsiflexion, neutral and 10 degree plantarflexion. Fujii et al. [96] investigated the accuracy of the two stress manual techniques to diagnose hindfoot instability. On an intact foot and after sequentially sectioned the ATFL and CFL they analyzed the kinematics of the calcaneus relative to the tibia with the foot in neutral and 20° plantarflexion. They found statistical differences among cadavers, examiners and positions. Significant increase was found in anterior displacement after sectioning the ATFL and in inversion after cutting the ATFL and CFL; however, the differences were not clinically significant. They concluded that these methods are not sensitive enough to demonstrate ATFL injury or combined ATFL/CFL injury.

Another study looked at the differences between in vitro and in vivo experiments. Kerkhoffs et al. [35] tested a measurement device for anterior laxity in the hindfoot. In vitro, increase in anterior drawer was found after cutting the ATFL, CFL and PTFL. In vivo experiments included patients with prior ligament injuries and a control group; there was no detectable laxity difference between the 2 groups. The range of measured laxity was so large that it was not possible for the authors to define a limit above what a ligament injury can be diagnosed.

Pearce et al. [36] compared subtalar joint motion measured externally from a goniometer and using CT scan on healthy feet during supination and pronation of the foot. The external subtalar joint motion was 45.8° from full eversion to full inversion while the subtalar rotation measured on the CT scan was 10.9°. Differences in subtalar joint rotation between the 2 methods may include motion of the ankle joint when measuring externally the subtalar joint motion as the motion of the talus cannot be measured externally. Also, only antero-posterior and lateral views of the foot were used to calculate subtalar joint motion. The author concluded that physical examination is not suitable to assess subtalar joint motion as it involves ankle joint rotation as well.

Looking at the flexibility of the hindfoot instead of the range of motion might help in determining between ankle and subtalar joint instability. Flexibility is defined as the displacement in the direction of the applied load relative to the applied load. [97] measured the flexibility characteristics of the ankle complex in anterior drawer, inversion-eversion and internal-external rotation in vitro and in vivo. In vitro, flexibility was recorded on an intact foot and after serially sectioning the ATFL and CFL. In vivo, they tested the injured and non-injured feet. Isolated ATFL injury produced an increase greater than 60% in anterior drawer translation without any increase in inversion. ATFL and CFL injuries produced an increase of 57% in flexibility in inversion and a significant increase in internal rotation and coupled internal rotation and inversion motion. From the 4 patients with ATFL injury tested in vivo, the Ankle Flexibility Tester detected an increase of at least 21% in the injured joint flexibility during anterior drawer. One patient that demonstrated a tear of the CFL from the MRI evaluation showed an increase of 21% in injured ankle flexibility during inversion. The results from in vitro and in vivo studies indicated that the Ankle Flexibility Tester developed by the authors is able to detect significant changes in flexibility in patients with lateral ligament injuries.

There are some disadvantages in the manual anterior drawer test and inversion stress test. First, the soft tissue surrounding the bones structure may affect the interpretation of bones positions especially when the foot is swelling. Second, the manual load applied by the investigator is not recorded and will be different depending on the practitioner. Third, the displacement is not recorded as well and means that results will be

intuitive depending on the investigator and his experience. These three points may explain why results are subjective, hard to transmit and difficult to compare.

Another examination maneuver was described by Thermann et al. [47] where he suggested positioning the foot in dorsiflexion for evaluation of the posterior subtalar joint stability. This position should lock the talus in the ankle mortise and therefore limit ankle motion. After an inversion and internal rotation stress is applied to the heel a medial shift of the calcaneus in relation to the talus should be perceptible in case of subtalar instability.

After clinical examination, the presence of the subtalar joint is usually demonstrated radiographically; however, the methods used are not generally adequate to detect instability at the subtalar joint.

2.5.2 Imaging techniques

Radiography

- ❖ Ankle joint

The same stress tests as for the physical examination can be performed during imaging evaluation. X-ray imaging is the most used technique with routine radiographs taken with antero-posterior, lateral and mortise views. However, the wide range of talar tilt and anterior displacement values between the injured and uninjured ankles makes interpretation of the results difficult.

Several studies [98-105] used these tests before performing surgical exploration for diagnosing lateral ligament rupture. Some studies [98, 100, 102-106] were looking at patients with acute ankle sprain. Only one [105] found significant benefit in using stress views; the others concluded that x-ray stress tests were not reliable enough to make a diagnosis. The last study which investigated patients with chronic ankle instability [101] concluded that talar tilt and anterior drawer stress tests were not useful in the diagnosis of chronic ankle instability. Therefore, talar tilt and anterior drawer tests don't have any clinical relevance for diagnosing hindfoot instability.

Cass et al. [38] investigated the stress inversion test using computerized tomography on intact and unstable cadaver feet. Talar tilt was measured in the intact specimen and after sectioning the ATFL, the CFL and the interosseous ligaments in combination of two. Talar tilt occurred after the ATFL and CFL were sectioned with a mean angle of 20.6° and a range between 10° and 34°. Sectioning either the ATFL or CFL alone did not demonstrate talar tilt, neither cutting the interosseous ligament. However, testing on cadavers does not take into account muscle activation that might limit inversion and therefore decrease the talar tilt observed in this study.

Christensen et al. [37] designed the so called 'Telos device' to perform the inversion and anterior drawer stress examinations. The device allows for constant load applied to the ankle, inversion-eversion motion and 18 degree internal leg position to access mortise view. When inversion-eversion is applied for diagnosis, the ankle is kept in a neutral position to isolate the CFL. During the anterior drawer test, the foot is in plantarflexion to easily access the ATFL. There are many disadvantages of the manual technique in executing stress views such as the radiation exposure to the personnel, the patient motion during the examination and the lack of reproducibility of the force required to elicit a true talar tilt and anterior drawer tests result. Using a mechanical device (as the Telos) allowed withdrawing all the previous disadvantages, but it is expensive and time consuming to set up the apparatus and test the patient accurately. Even though the Telos device produces constant torque, it will not detect the firm endpoint that is different in each individual. Clinicians will be more sensible to acquire the endpoint by applying a different amount of torque.

The anterior displacement and talar tilt are widely used to detect instability in the hindfoot; however, these techniques are mainly applied to detect ankle joint instability and are not adequate for detecting additional or isolated subtalar instability. Riegler et al. [16] examined 22 patients presenting with chronic lateral instability of the hindfoot that failed non-operative management. Preoperative stress radiographs showed a talar tilt difference between symptomatic and asymptomatic feet ranged from 4 to 16° with an 8° mean and an increase in varus angulations in the injured foot. During surgery, significant

subtalar instability was found in five patients while radiographs did not detect any increase in subtalar tilt.

- ❖ Subtalar joint

Broden [41] was the first to examine subtalar joint roentgenograms by performing projections in two planes perpendicular to one another at a 45° angle to the longitudinal axis of the foot. This projection consists of turning the foot 45° inward with the ankle in neutral flexion-extension position and the patient supine. The central ray is directed 2-3cm below the anterior part of the lateral malleolus with a 40° angle. Brantignan et al. [72] reported good results using Broden's view to detect greater subtalar tilt in symptomatic feet while Harper [39] could not distinguish between normal and instable subtalar tilts. Brantignan et al. [72] reported 3 cases of chronic subtalar joint. The inversion stress test was performed on the symptomatic and asymptomatic feet using the Broden's view with tomography. Subtalar tilt was greater in symptomatic feet (57° ±5) than on intact (38° ±6). Harper [39] performed a series of stress radiographs on patients with complaint of inversion instability of the foot. Additionally, asymptomatic individuals were evaluated to better define a normal range of motion for this study. Patients were evaluated by a physical examination and radiographs of the stress Broden's view of the subtalar joint. Stress tests revealed 13 out of 14 subtalar instabilities with a joint opening ranging from 5 to 9 mm with a mean of 8 mm. Divergence of the articular surfaces averaged 12° in the symptomatic feet ranging from 7° to 22°. In asymptomatic patients, the stress Broden's view revealed an average of 7mm lateral opening of the subtalar joint in 14 of the 18 feet and an articular divergence of 9° ranging from 0 to 20°. They concluded that instability of the subtalar joint is not correlated with apparent opening of the joint laterally during inversion stressing.

Saltzman et al. [107] investigated the reliability of dorsoplantar and lateral radiographic measurement on 50 asymptomatic patients' feet. Lateral and AP talocalcaneal views were examined by 6 examiners using subjective and quantitative measurements. No differences in measurement were found for determining the AP talocalcaneal angle. The quantitative technique was more reliable for determining the

lateral talocalcaneal angle. The inter-observer differences in quantitative angle values were large in both talocalcaneal angles with an error of 13° in an 80% confidence interval in the AP view and 7° in the lateral view. The magnitude of the inter-observer error sets the outside limit on the intrinsic errors of measurement.

Kato et al. [108] developed a method to measure the anterior drawer displacement of the calcaneus with respect to the talus to detect subtalar joint instability. They performed radiography on patients with subtalar instability, ankle instability and a control group. They measured the subtalar joint displacement, ankle joint displacement, talar tilt and facet angle in each patient and found that the average of subtalar joint displacement was higher in patients with subtalar instability. The displacement of the ankle, the talar tilt and the facet angle were smaller in people with subtalar instability than the ankle instability group and the control group. However, the standard deviations of the measurement were high; consequently, the differences were not clinically significant.

Ishii et al. [46] investigated a new method to detect subtalar joint instability by measuring the transposition of the lateral process of the talus at the posterior facet in a supinate foot hold in maximum dorsiflexion. They looked at the mean displacement in a control group, recurrent ankle sprain group and amputated ankles and found a significant difference in displacement between the control group and symptomatic patients. The displacement found in the cadaver feet were similar to the one found in the control group. After sectioning the CFL, displacement matches result from patients with non-recurrent sprains and cutting the interosseous talocalcaneal ligament gave similar results than in patients with recurrent sprains. They considered that a transposition superior of 44% confirm the presence of mechanical subtalar instability.

Few studies examined subtalar tilt using mechanical device. Rubin et al. [6] suggested inverting the foot to diagnose subtalar joint instability in a method similar to the talar tilt test. By using a device similar to the telos, no significant subtalar tilt difference between an intact and an injured foot was found in any of the 26 patients. Löfvenberg et al. [109] evaluated subtalar joint stability in patients with chronic lateral instability of the hindfoot. Roentgen stereo photogrammetric (implantation of bone

marker) analysis was used during inversion tests, applied manually first and with a 5Nm torque. A reduction of the ankle and subtalar joint rotation was registered using a predetermined torque. With either manual or automatic inversion torque applied to the foot, no subtalar joint rotation differences were found between the symptomatic and asymptomatic feet. Yamamoto et al. [110] investigated the reliability of using inversion stress radiographs with the Telos device as a subtalar joint diagnostic technique by measuring the subtalar tilt angle. First they determined the intra-observer error, 1.4° and 0.8°, and an inter-observer error of 1.1°. Second they evaluated the subtalar tilt angle on normal ankles, on acute injured ankles and on chronic hindfoot injuries. They found significant increase in subtalar tilt between normal and injured ankles, from 5.2° to 9.7° for acute injuries and 10.3° for chronic instability. Subtalar tilt angle range in normal ankles was from 0° to 9° while for acute injured ankles the range was from 5° to 15° and for chronic from 5° to 16°. They suggested that the subtalar tilt angle measurement is a good technique to diagnose instability at the subtalar joint as the differences between intact and injured foot were significant. However the range of subtalar tilt angle cannot distinguish between intact and injured foot.

Results of stress radiography are closely related to the mechanical device and load applied to the foot, the position of the foot and if anesthesia has been used.

2.5.3 Fluoroscopy

Louwerens et al. [42] investigated the possibility of subtalar joint instability in patients that present chronic lateral instability of the foot. Radiographic measurement of talar and subtalar tilt were assessed on 33 patients with 55 symptomatic feet and 10 controls. The Broden's view was performed under fluoroscopy in neutral position, applying moderate inversion and after forced inversion. Statistically significant increase in talar tilt was found between the symptomatic feet and the control group after forced inversion; however, this difference was not significant with patients with unilateral complaints between the symptomatic and asymptomatic contra lateral foot. No significant differences were reported in the subtalar tilt between symptomatic and asymptomatic feet in either position of the foot.

Hertel et al. [14] investigated ankle and subtalar joint instability in patients with lateral ankle sprain history. The authors used stress fluoroscopy and physical examination to examine 12 subjects with history of unilateral ankle sprain and 8 controls. Physical examination included the anterior drawer test, talar tilt test and medial subtalar glide test. Fluoroscopy was performed with AP view and lateral modified Broden's view with and without inversion stress. Nine patients demonstrated abnormal talar tilt in their symptomatic feet with stress fluoroscopy. From these 9 patients, 3 did not demonstrate talar tilt differences on the physical examination and 2 of the 3 did not show anterior drawer differences. By physical examination, subtalar instability was found in 7 patients; only 4 demonstrated subtalar tilt in stress fluoroscopy and 2 bilateral laxity. They concluded that a combination of imaging and physical examination may be useful in detecting instability in the ankle and subtalar joint.

The major disadvantage of this technique is the potential risk of radiation-induced cancer to the patient.

2.5.4 Arthrography

Ankle arthrography may be recommended to better quantify lateral ligament damage. This technique requires the injection of a contrast liquid into the ankle joint or the sinus tarsi. Normally the contrast should remain into the joint capsule; if a leak appears then instability is present.

Meyer et al. [15] performed a radiographic study on 40 patients with acute ankle sprains. Anterior drawer stress and inversion stress tests were considered positive if the talar slippage was more than 8mm and the lateral tilt exceeded 15°. Given the uncertainty of radiographs in the evaluation of ligamentous injury, Meyer evaluated the integrity of the subtalar joint by arthrography. Eight patients were diagnosed with an ATFL rupture because of a positive anterior drawer stress test, a negative inversion stress test and a normal arthrogram. The 32 remaining patients had an abnormal arthrogram and following the radiographic test results, they were classified into four groups. The first group involved possible rupture of the ATFL, PTFL and CFL and presented a positive anterior drawer stress test, a positive inversion stress test and a leak in the lateral capsule. The

second group tore off the ATFL, interosseous and maybe cervical ligament and presented a positive anterior drawer stress test, a negative inversion stress test and a leak in the sinus tarsi. The third group had an intact ATFL but the CFL, cervical ligament and interosseous ligament were torn and presented a negative anterior drawer stress test, a slightly positive inversion stress test and a leak in the lateral capsular and sinus tarsi. The last group presented a complete tear of all ligaments of the posterior tarsus with all tests being positive with additional leak to the lateral and sinus tarsi.

Arthrography is usually not recommended because of the invasive nature of this procedure.

2.5.5 3D CT scan

Sijbrandij et al. [43] investigated the possibility of using helical CT scan to evaluate subtalar tilt with inversion stress view. 10 patients with unilateral instability were examined clinically first, then with the Broden's view on plain stress radiography and using a helical CT scan. Only patients presenting subtalar joint instability on physical examination were part of the study. Using the Broden's view demonstrated a subtalar tilt between 6° and 18° on the symptomatic foot and 4-12° for the contrary stable foot. Using the CT scan with a Broden's view did not show any subtalar tilt in symptomatic and asymptomatic feet. However, by using the CT scan with a traditional inversion stress they found that the postero-lateral part of the subtalar joint demonstrated tilt between 8° and 13° in asymptomatic feet and between 6° and 12° in symptomatic feet. They concluded that none of the methods demonstrated useful tools to detect subtalar joint instability because of the high range of subtalar tilt.

2.5.6 MRI

Ringleb et al. [27] evaluated the effect of ligamentous damage and reconstruction in vitro on the hindfoot using a 3D stress MRI technique. Inversion and anterior drawer stress tests were applied on intact feet, after sequentially sectioning the ATFL and CFL. A significant increase in inversion was found at the ankle joint after sectioning both

ligaments. No significant increase was detected during anterior drawer test. Subtalar joint stability was not affected by the damage occurring at the ATFL and CFL.

Sheehan et al. [45] investigated the accuracy of the fast-PC MRI technique on the ankle joint complex kinematics on normal feet and on ankles with a Stieda process. The kinematics in ankles with a Stieda process were altered compared to normative population especially at the subtalar joint. External calcaneal-tibia measurement was not able to determine the change in kinematics for ankles with Stieda process.

2.6 Conservative treatment

The most common treatment after a mild or moderate acute ankle sprain is the application of the RICE principal including rest, ice, compression and elevation immediately after injury. Then a short period of immobilization followed by an early return to weight bearing using tape or ankle brace with progressive range of motion exercises, neuromuscular and proprioceptive ankle training are advised [48, 111].

2.6.1 In vivo studies

Healthy volunteers

Zhang et al. [52] assessed the effectiveness of 3 ankle braces in limiting inversion motion applied to the hindfoot. One lace-up brace (ASO) and 2 semi-rigid braces (Element and Functional) including one with a subtalar locking system (Element brace) were used on 19 healthy volunteers. The reductions in total passive inversion-eversion range of motion were 67%, 48% and 57% for the Element, Functional and ASO braces respectively. All braces were effective in resisting hindfoot inversion motion with the semi-rigid type of braces being more effective than soft lace-up braces overall. One limitation would be that they used separate static trials across shoed and braced conditions that may contribute to differences in range of motion as the foot might not be placed in the same neutral position for each condition. They did not record subtalar joint motion as they measured motion in vivo; therefore, they did not demonstrate why the

element brace that included a subtalar locking system was more effective. Also, the heel cup incorporated into the element brace might be uncomfortable in dynamic conditions.

Thonnard et al. [60] evaluated the torque generated by a semi-rigid brace and a Push Brace support during inversion. They compared the angle-torque relationship of 12 healthy volunteers between barefoot and braced ankles under static and dynamic applied inversion. They found that mean dynamic torques were generally greater than the static ones. No differences in torque measurement were found after induced fast inversion while passive inversion braced ankle demonstrated an additional linear increase compared to barefoot. They concluded that braces are unable to absorb the mechanical energy produced in a sprain situation.

Nishikawa [57] investigated the degree of protection provided by ankle support to the ankle joint ligaments as well as their ability to perform plantarflexion and dorsiflexion compared to barefoot. Angular velocity and acceleration were assessed on 11 healthy volunteers after sudden 10° of inversion, eversion, plantarflexion and dorsiflexion applied through a rocking platform. Supports used in this study included tape, a lace-up ankle brace and a semi-rigid brace. All supports decreased inversion maximum velocities compared to barefoot of 25%, 32% and 34% for the tape, lace-up and semi-rigid brace respectively. The semi-rigid brace was the only one that did not affect plantarflexion/dorsiflexion angular acceleration. The authors speculated that the decrease in inversion velocity at the braced ankles reduced the force being applied to the ligaments. They concluded that ankle supports provided protection against inversion sprain. A 10° of hindfoot inversion might not be a good approximation of what an ankle sprain would produce; therefore, their conclusion could be premature.

Siegler et al. [55] assessed the 3 dimensional flexibility and restriction of 4 common braces (2 lace-on and 2 stirrup). Angular displacement and applied torque were recorded on 10 healthy volunteers with and without wearing ankle braces. Maximum angular positions and segmental flexibility were assessed in the transverse plane and frontal plane. Range of motion and performance index were evaluated in the sagittal plane. All ankle braces provided significant support in inversion, eversion and internal

rotation. The active ankle was overall better in limiting motion. The active ankle's hinge joint located at the malleoli helped in reducing resistance in sagittal motion.

Eils et al. [53] compared brace support in combination with a shoe and in a simulated barefoot condition using a cut-out shoe. The aim of this study was to evaluate the passive stability characteristics of 3 ankle stabilizing supports (tape, lace-up brace and a stirrup brace) with and without the influence of a sport shoe. Passive motion was applied in the 3 cardinal planes using individual torque for each of the test direction. All supports restricted motion in all directions alone or in combination with a sport shoe. They concluded that using a brace in combination with a shoe provided an additional stabilizing effect.

Tang et al. [54] investigated the effect of a semi-rigid ankle brace in reducing the ankle angular displacement and angular velocity during a simulated 23° supination sprain injury. A significant 35% reduction in inversion displacement and 40% in angular velocity were found after applying the brace. They concluded that the use of an ankle brace provided an external force to resist sudden supination motion of the ankle therefore helping the peroneal muscles and lateral ligaments. This study did not report the actual supination angular displacement and velocity or their definition of supination in the anatomical coordinate system.

Volunteers with Chronic Ankle Instability (CAI)

Eils et al. [59] tested 10 different ankle braces on 34 subjects with CAI during 6 DOF passive ankle ROM and during a simulated inversion sprains using a tilting platform. All braces restricted motion in the 3 anatomical planes with a higher motion constraint using the semi-rigid braces. Stirrup design restricted rapidly induced inversion more effectively than the other designs.

2.6.2 In vitro studies

Bruns et al. [58] demonstrated in vivo and in vitro the stabilizing effect of several ankle braces and peroneal muscle strength. In vitro experiments consisted of assessing the extent of the talar tilt and the anterior drawer sign after sectioning the ATFL and CFL

and after applying 4 braces. In another experiment they applied a 75N and 150N muscular strength to the peroneus longus and peroneus brevis in an ATFL and CFL deficient feet. The in vivo experiment consisted of measuring talar tilt and anterior drawer sign on 32 active sportmen with CAI with and without an ankle brace or a tape bandage. In vitro experiments demonstrated that the stabilization of the braces on ligamentous deficient feet was not sufficient to return to normal talar tilt and anterior drawer sign. After applying 150N strength to the peroneal tendons, they found a significant difference compared to no strength added. The in vivo experiment demonstrated a reduction of instability after application of the ankle supports. External ankle supports as well as peroneal muscle strength can partially stabilize the unstable ankle.

Bruns et al. [112] analyzed the influence of randomly selected ankle braces on sagittal and transverse planes motion on ATFL and CFL deficient feet. Significant increase in rotation was found between intact and unstable hindfoot in the 2 planes of motion. External ankle supports significantly decreased sagittal motion and internal rotation, but only 6 of them limited external rotation.

Tohyama et al. [50] determined the effect of ankle braces on hindfoot inversion with and without an axial load applied to the tibia. They evaluated hindfoot inversion on 6 intact ankles at 0° and 20° plantarflexion, with and without a 178N axial load and compared 3 different braces. Adding an axial load decreased ankle inversion rotation of 30% and 36% in 20° and 0° of plantarflexion. Sagittal foot position did not influence inversion range of motion. All braces, regardless of axial load and sagittal foot position, significantly reduced ankle inversion with a higher stability when using a semi-rigid brace. Using a brace in 20° plantarflexion gave more stability at the ankle than in neutral.

3 METHODS

Maximum inversion and eversion range of motion at the subtalar, ankle and hindfoot joint were investigated on nine intact feet and after sectioning the calcaneofibular ligament (CFL) alone and in combination with the cervical ligament and interosseous talocalcaneal ligament (ITCL). A semi-rigid ankle brace was placed on each foot after each condition and its restrictive characteristics were determined for each joint. Inversion-eversion motion was applied for each of six conditions with the foot placed in neutral sagittal position, in maximum dorsiflexion and in maximum plantarflexion.

An optimization method was developed to determine the subtalar and ankle joint axes during an inversion motion applied to the intact foot and after each ligament sectioning. The optimization initial guesses were 1) the approximated subtalar joint axis calculated by the mean helical axis of the hindfoot from inversion-eversion with the foot placed in dorsiflexion in order to limit ankle joint motion and 2) the approximated ankle joint axis calculated by the mean helical axis of the hindfoot from plantarflexion-dorsiflexion.

The optimization method was a two-hinge joint axes model represented by the subtalar and ankle joint axes. The inputs were the initial guesses from the approximated subtalar and ankle joint axes and the experimentally measured kinematics of the tibia and calcaneus during inversion. The outputs were the optimized subtalar and ankle joint axes which best represented the experimental motion of the calcaneus with respect of the tibia.

3.1 Loading device description

A six degree of freedom positioning and loading device was previously developed and manufactured (Figure 3-1) [113]. The device allowed for rotation and translation in the three cardinal planes and for loading the tibia and tendons in the foot. It was designed to enable motion of a physiologic stable and unstable hindfoot; it fits a 45 cm shank length, 12cm foot width , 25 cm foot length, and allows for 70° of inversion, 25° of

eversion, 50° of plantarflexion, 25° of dorsiflexion and 90° of internal and external rotation respectively. Line levels were attached to the device and used to make sure the foot returned to a neutral position after each trial.

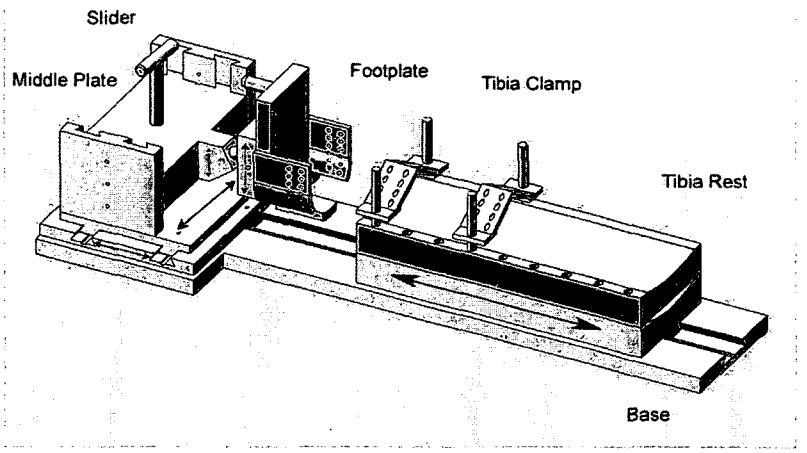

Figure 3-1: Positioning and loading device showing the direction of translation motions. [114]

The device was designed to apply loads in a similar fashion as a clinical examination. Therefore, motion of the foot was controlled manually by a certified athletic trainer who applied forces to the foot plate using a handle. The device was instrumented with a 6 degree of freedom force/torque transducer (ATI mini45, ATI Industrial Automation, Apex, NC) to accurately measure the applied force and therefore produce repeatable output. Additionally, the device allowed for Achilles tendon loading and for axially loading the tibia.

3.2 Data collection

Nine fresh-frozen cadaveric lower extremities (7 left, 2 right, age 66±9 years, 3 female and 6 male) were sectioned 20cm above the lateral malleolus. The hindfoot was examined manually by an athletic trainer after the foot was properly thawed to confirm that no instability or other pathology was present. An incision placed on the lateral side of the ankle exposed the ligaments. The Achilles tendon was sectioned and sutured to a 22N weight to roughly approximate the tendon tension during a manual examination.

Each specimen was placed into the six degree-of-freedom positioning and loading device described above. The tibia and fibula were fixed using a clamp and stainless steel k-wires. A 22N axial load was applied to the tibia to counterbalance the weight applied to the Achilles tendon. The calcaneus was fixed to the foot plate using bone screws in order to eliminate skin motion artifact from the measurements. The foot plate was moved with one hand using a handle to apply forces. The athletic trainer was instructed to move and stress the hindfoot similar to what would occur during a clinical evaluation.

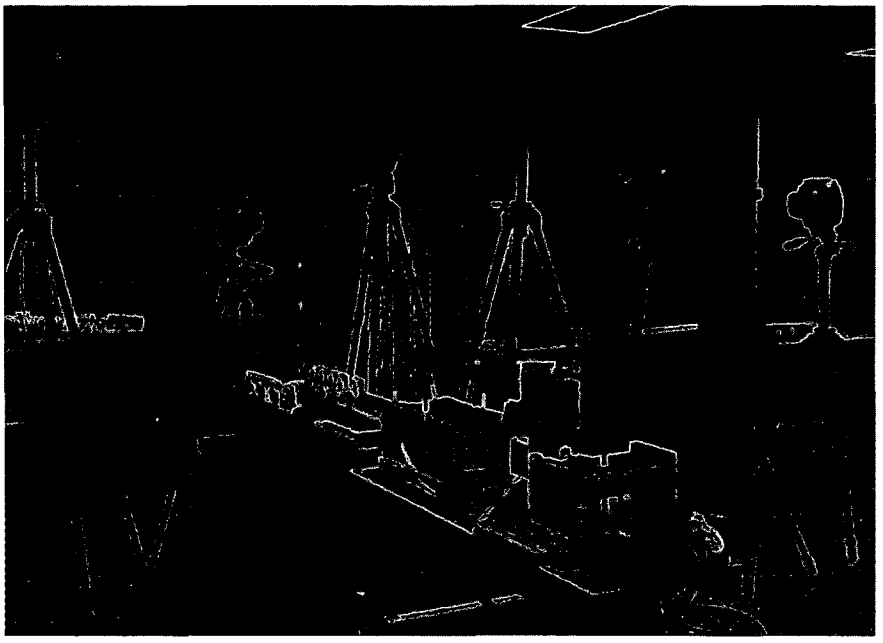

Figure 3-2: Data collection set up including the 6 digital cameras and the 6 DOF kinematics and kinetics device.

Kinematic data were collected from the tibia, talus and calcaneus with a 6 camera Motion Analysis Eagle System (Figure 3-2) (Motion Analysis Corporation, Santa Rosa, CA) in combination with the MotionMonitor (Innovative Sports Training, Chicago, IL). Custom-made sensors composed of four retroreflective markers each were screwed on the lateral side of the calcaneus, on the neck of the talus and proximal part of the tibia (Figure 3-3). The talus sensor was placed anteromedially to keep the extensor retinaculum intact. The athletic trainer re-evaluated the foot and ankle after screw

insertion to ensure motion restrictions were not created. The bony landmarks were digitized with the specimen held in an anatomically neutral position to define the anatomic coordinate system for each bone [115]. Specifically, three points were defined for each bone in order to create the two first axes attached to the bone coordinate system. The third axis was defined as the cross-product of the two axes and ensured the coordinate system was Cartesian. The three points for the tibia were first the proximal medial end of the tibia; the second point was the medial malleolus which created an axis along the tibia (Y-axis); the third point was the lateral malleolus which created the malleoli axis (Z-axis) with the second point. The talus and calcaneus coordinate system was created using the same points as no landmark was accessible on the talus. The first point was the most distal point of the calcaneus; the second point was the tip of the second phalanx which created the long axis of the foot (X-axis); the third point was the distal point of the talus near the talus marker incursion which created the second axis (Y-axis).

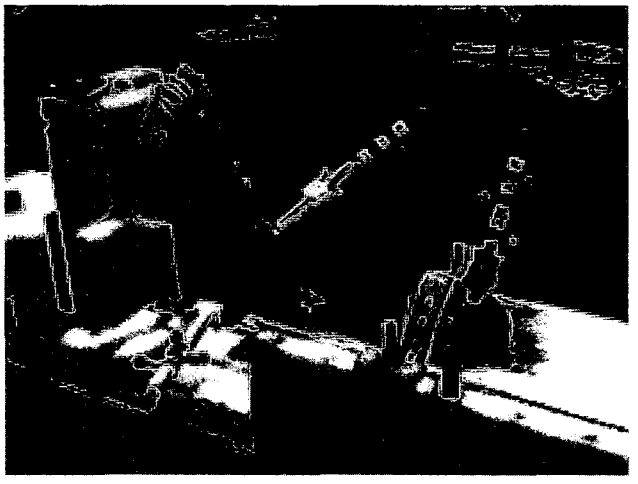

Figure 3-3: Cadaver foot attached to the 6DOF loading and positioning device. The semi-rigid ankle brace was fitted to the foot and the calcaneus, talus and tibia marker clusters were screwed onto each bone.

3.3 Experimental Protocol

Inversion and eversion were applied to the hindfoot with the foot placed in 1) neutral, 2) maximum dorsiflexion and 3) maximum plantarflexion. Plantarflexion and dorsiflexion motion was also applied to the foot in order to determine the ankle joint axis needed for the optimization procedure. Motions were applied with and without a semi-rigid ankle brace (Active Ankle T2, Cramer Products, Gardner, KS) on an intact hindfoot and after each ligament was sectioned. For each foot sagittal position and condition, the foot was manipulated to the end range of inversion and eversion until no further motion at the joint complex could be observed. Ligamentous injury was created by sectioning the calcaneofibular ligament (CFL) in isolation and in combination with the intrinsic ligaments (i.e. the cervical ligament and the interosseous talocalcaneal ligament) (Figure 3-4). A previous study [26] demonstrated that the cervical ligament by itself did not increase motion in the frontal plane at either joint; therefore, the cervical ligament was cut in combination with the ITCL.

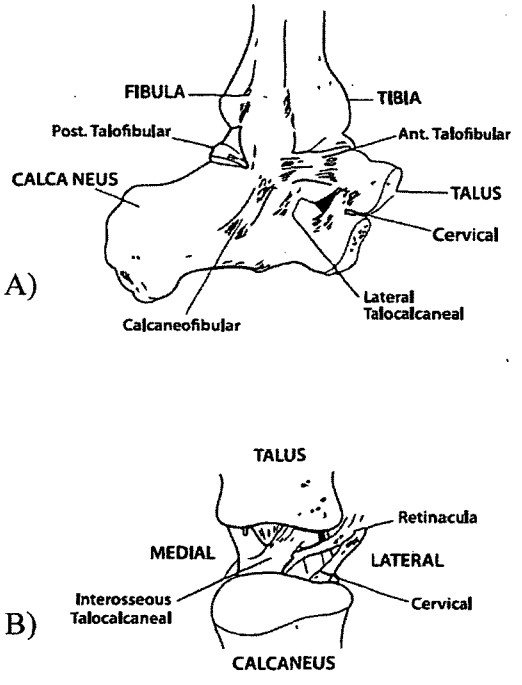

Figure 3-4: A: Representation of the lateral ligament complex of the ankle joint (joint between the talus and the tibia) and the subtalar joint (joint between the calcaneus and the talus) including the

anterior talofibular ligament (ATFL), the calcaneofibular ligament (CFL) and the cervical ligament. B: Representation of ligaments in the tarsal sinus on frontal section including the cervical ligament and the interosseous talocalcaneal ligament (ITCL). [116]

Motion of the calcaneus with respect to the talus (subtalar joint), motion of the talus with respect to the tibia (ankle joint) and motion of the calcaneus with respect to the tibia (hindfoot joint) were analyzed. The rotation matrices and the Euler angles for the three joints were exported from the MotionMonitor (Innovative Sports Training, Chicago, IL). Data truncation into one cycle of motion was performed with the hindfoot rotation angles. Euler angles for each joint and condition were normalized into a 100% motion which enabled the comparison between conditions. Rotations were calculated from neutral to maximum motion. Sensor data were exported from The MotionMonitor using an X-Z'-Y" Euler rotation sequence for the subtalar joint and a Z-X'-Y" Euler sequence for the ankle and hindfoot joint [26]. Rotation matrices of subtalar, ankle and hindfoot joints from anatomical data were exported to calculate each joint mean helical axis for the intact foot condition, after sectioning the CFL and after additional sectioning of the intrinsic ligaments.

The optimization method was used on six of the nine specimens as the noise in the kinematics of the three other specimens was too important and may have affected the results of the optimization. A mean helical axis (MHA) was calculated at the subtalar joint and ankle joint during inversion-eversion. These MHAs represent the true subtalar joint and ankle joint axes from inversion-eversion. They will be compared to the optimized subtalar joint and ankle joint axes by looking at the difference in inclination angle and deviation angle as well as the angle between the MHA and the joint optimized. These differences will be more commonly called angular errors. Absolute angular errors will be the absolute differences between the two axes.

The hindfoot MHA was calculated from dorsiflexed inversion-eversion and from plantarflexion-dorsiflexion to approximate the subtalar joint axis and ankle joint axis respectively and will be used as initial guesses for the optimization method. In order to ensure that hindfoot MHA is able to accurately approximate the subtalar joint axis, the difference in inclination and deviation angle as well as the angle between the dorsiflexed

inversion-eversion hindfoot MHA and the dorsiflexed inversion-eversion subtalar MHA will be computed. The same differences will be assessed between the hindfoot and ankle joint MHAs from plantarflexion-dorsiflexion.

3.4 Coordinate system

The body reference frame for the tibia, talus and calcaneus were defined according to the recommendations from the International Society of Biomechanics (ISB)[117]. The Y axis was defined as the perpendicular to the plane of the foot and pointing toward the tibia, the X axis as the anterior/posterior axis and the third axis, Z pointing laterally (Figure 3-5). Consequently, inversion/eversion occurs about the X-axis, internal/external rotation about the Y-axis and plantarflexion/dorsiflexion about the Z-axis.

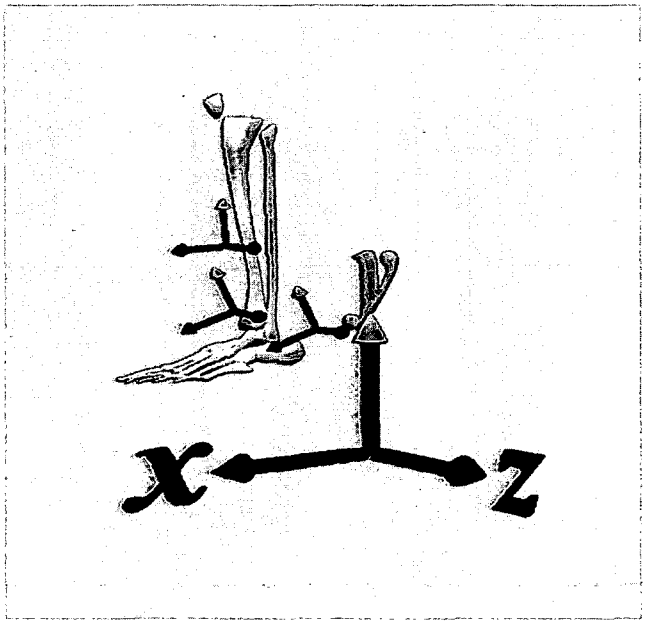

Figure 3-5: Left foot represented through the MotionMonitor (Innovative Sports Training, Chicago, IL) showing the world coordinate axes with X axis being the long axis of the foot pointing anteriorly, Y axis being the longitudinal axis of the tibia pointing upward and Z being the cross product between X and Y. The coordinate systems of the tibia, talus and calcaneus are also represented.

3.5 Euler angles calculation

Motion between two rigid bodies can be described as a sequence of three successive rotations from an initial position at which the two rigid bodies coordinate system coincide. Euler angles are defined as these three successive angles of rotation about pre-defined axes. The Euler angles method, in which rotations take place in a described sequence, is commonly used in biomechanics. The sequence used to calculate the rotations are important as finite rotations in 3D are non-commutative [118, 119]. A previous study [26] demonstrated the importance of the sequence of rotation used at the subtalar joint. The International Society of Biomechanics recommends the same sequence for the ankle and subtalar joint; however, the main motion of the ankle joint happens in the sagittal plan around the Z axis while subtalar joint motion occurs mainly in the frontal plane around the X axis. We decided to calculate the subtalar joint rotation angles based on a X-Z'-Y'' Euler sequence of rotation.

The Euler angles are expressed as elements of the 3×3 rotation matrix calculated from the three rotation matrices depending on the sequence of rotation.

For a single rotation of α radians about the X axis, the rotation matrix is expressed as in Equation 1.

$$R_x(\alpha) = \begin{bmatrix} 1 & 0 & 0 \\ 0 & \cos\alpha & -\sin\alpha \\ 0 & \sin\alpha & \cos\alpha \end{bmatrix} \qquad \textbf{Equation 1}$$

For a single rotation of β radians about the Y axis, the rotation matrix is expressed as in Equation 2.

$$R_y(\beta) = \begin{bmatrix} \cos\beta & 0 & \sin\beta \\ 0 & 1 & 0 \\ -\sin\beta & 0 & \cos\beta \end{bmatrix} \qquad \textbf{Equation 2}$$

For a single rotation of θ radians about the Z axis, the rotation matrix is expressed as in Equation 3.

$$R_z(\theta) = \begin{bmatrix} \cos\theta & -\sin\theta & 0 \\ \sin\theta & \cos\theta & 0 \\ 0 & 0 & 1 \end{bmatrix}$$ **Equation 3**

At the subtalar joint, the sequence of rotation used is X-Z'-Y'', consequently the rotation matrix at the subtalar joint can be calculated as showed in Equation 4.

$$[R]_{subtalar} = [R_{Y''}]_{cal/tal} \cdot [R_{Z'}]_{cal/tal} \cdot [R_X]_{cal/tal}$$ **Equation 4**

where $[R_X]_{cal/tal}$ is the rotation matrix of the calcaneus relative to the talus around the X axis.

Where $[R_{Z'}]_{cal/tal}$ is the rotation matrix of the calcaneus relative to the talus around the Z' axis.

Where $[R_{Y''}]_{cal/tal}$ is the rotation matrix of the calcaneus relative to the talus around the Y'' axis.

At the ankle joint, the sequence of rotation used is Z-X'-Y''; consequently the ro$[R]_{ankle} = [R_{Y''}]_{tal/tib} \cdot [R_{X'}]_{tal/tib} \cdot [R_Z]_{tal/tib}$ted as shown in Equation 5.

$$[R]_{ankle} = [R_{Y''}]_{tal/tib} \cdot [R_{X'}]_{tal/tib} \cdot [R_Z]_{tal/tib}$$ **Equation 5**

At the hindfoot, the sequence of rotation is the same as the ankle joint, Z-X'-Y'' and the rotation matrix at the hindfoot is presented in Equation 6.

$$[R]_{Hindfoot} = [R_{Y''}]_{cal/tib} \cdot [R_{X'}]_{cal/tib} \cdot [R_Z]_{cal/tib}$$ **Equation 6**

In addition to the sequence dependency of the method, the main drawback of the Euler angle is gimbal lock. This is a mathematical singularity that occurs when the second rotation equals ± 90°.However, gimbal lock should not occur in the range of motion that are calculated in the hindfoot. The Euler angles provide a representation of joint orientation in terms of three anatomies and offer clinically meaningful parameters.

3.6 Determination of the joint axis

3.6.1 Helical axis calculation

Motion between two rigid bodies can also be described as a rotation about, and a translation along, an axis, commonly called the Helical Axis (Figure 3-6). To completely describe the movement, it is necessary to determine the four parameters described below:

- **n** is the unit vector describing the orientation of the Helical Axis
- **p** represents a point on the Helical Axis to locate it in space
- θ determine the amount of rotation around the Helical Axis
- **t** is the amount of translation along the Helical Axis.

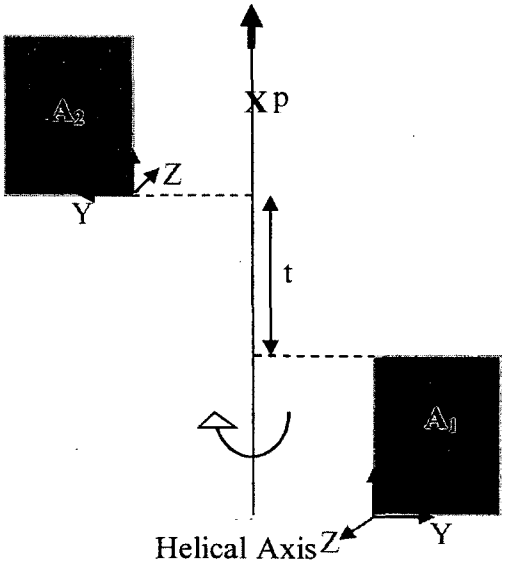

Figure 3-6: The generalized helical axis representing a rigid body A in position 1 and after translating (t) along and rotating (θ) around the helical axis ($\vec{n}$) to position 2.

The Helical Axis parameters can be calculated from the rotation matrix for a selected angular displacement from one coordinate frame to the next as described below [120-123].

The following transformation matrix (Equation 7) describes the rotation and translation between two rigid bodies.

$$T = \begin{bmatrix} R_{11} & R_{12} & R_{13} & t_1 \\ R_{21} & R_{22} & R_{23} & t_2 \\ R_{31} & R_{32} & R_{33} & t_3 \\ 0 & 0 & 0 & 1 \end{bmatrix} \quad \textbf{Equation 7}$$

where **R** is the rotation matrix and **t** the translation vector.

For a given rotation and displacement, all points on the helical axis remain on the helical axis; therefore, for any point **p** on the helical axis we have (Equation 8 and Equation 9)

$$[p] = [R][p] \quad \textbf{Equation 8}$$

Or

$$[R - I][p] = [0] \quad \textbf{Equation 9}$$

where **I** defines the identity matrix

If $\vec{n}$ is that particular point $\vec{p}$ with a magnitude of unity, then the components of $\vec{n}$ become the direction cosines of the Helical Axis (Equation 10).

$$\begin{bmatrix} R_{11} - 1 & R_{12} & R_{13} \\ R_{21} & R_{22} - 1 & R_{23} \\ R_{31} & R_{32} & R_{33} - 1 \end{bmatrix} \begin{bmatrix} n_X \\ n_Y \\ n_Z \end{bmatrix} = \begin{bmatrix} 0 \\ 0 \\ 0 \end{bmatrix} \quad \textbf{Equation 10}$$

Equation 10 is solved, yielding Equation 11 and Equation 12, which can be used to determine $\boldsymbol{\theta}$, the rotation about the helical axis (Equation 13).

$$R_{11} = n_X^2(1 - cos\theta) + cos\theta \quad \textbf{Equation 11}$$

and

$$R_{12} = n_Y(1 - cos\theta) - n_Z sin\theta. \qquad \textbf{Equation 12}$$

Then we can determine $\boldsymbol{\theta}$ as

$$\theta = cos^{-1}\left(\frac{R_{11} - n_X^2}{1 - n_X^2}\right). \qquad \textbf{Equation 13}$$

The sign of $\boldsymbol{sin\theta}$ gives the sign of $\boldsymbol{\theta}$.

The same process is used to determine the translation. If the point **p** is on the Helical Axis, this point will translate on the helical axis from position 1 to position 2 leading to Equation 14 and Equation 15.

$$\begin{bmatrix} p_X^2 \\ p_Y^2 \\ p_Z^2 \\ 1 \end{bmatrix} = [R] \begin{bmatrix} p_X^1 \\ p_Y^1 \\ p_Z^1 \\ 1 \end{bmatrix} \qquad \textbf{Equation 14}$$

and

$$\begin{bmatrix} p_X^2 - p_X^1 \\ p_Y^2 - p_Y^1 \\ p_Z^2 - p_Z^1 \end{bmatrix} = K \begin{bmatrix} n_X \\ n_Y \\ n_Z \end{bmatrix} \qquad \textbf{Equation 15}$$

where **K** is the magnitude of the translation.

Equation 16 is used to determine a point on the helical axis and the translation component.

$$\begin{bmatrix} R_{11} - 1 & R_{12} & R_{13} \\ R_{21} & R_{22} - 1 & R_{23} \\ R_{31} & R_{32} & R_{33} - 1 \end{bmatrix} \begin{bmatrix} p_X^1 \\ p_Y^1 \\ p_Z^1 \end{bmatrix} = \begin{bmatrix} Kn_X - t_X \\ Kn_Y - t_Y \\ Kn_Z - t_Z \end{bmatrix} \qquad \textbf{Equation 16}$$

where $\vec{\boldsymbol{t}}$ is the translation vector.

Finally, substituting $\boldsymbol{p_Z^1 = 0}$ on the Helical Axis gives the point where the axis intersects the X-Y plane.

The Helical axis method is a good approach to provide information about the actual axes of rotation in a joint and linear translation of one bone with respect to another. However, the Helical axis parameters are sensitive to noise in spatial coordinates and to the magnitude of the rotation angle that might be an issue when determining the helical axis unit vector and the point on the helical axis.

3.6.2 Determination of the mean helical axis (MHA)

A mean helical axis (MHA) at the subtalar joint and the ankle joint were calculated from data collected during inversion/eversion with the foot held in maximum dorsiflexion for the subtalar joint MHA and from data collected during plantarflexion/dorsiflexion for the ankle joint MHA. The MHAs were used to define the axes of rotation for the ankle and subtalar joint. Using a custom program written in Matlab, the MHA was defined from four helical axes calculated for each joint. Each Helical axis described motion between 2 instants of time:

1. from neutral position to maximum motion 1(inversion/dorsiflexion)
2. from maximum motion 1 back to neutral position
3. from neutral to maximum motion 2 (eversion/plantarflexion)
4. from maximum motion 2 back to neutral

The mean helical axis will be calculated using a least squares fit as follow. For a group of four helical axes, the central direction $\vec{u}$ should have a minimum square s_θ of angles from all axes. The sum of squares of angles may be approximated by using Equation 17.

$$s_\theta = \sum_{i=1}^{4} (u' \widetilde{U}_i^2 u) \qquad \textbf{Equation 17}$$

where s_θ is the sum of squares of angles from all Helical Axes, $\vec{u}$ is the central direction, or mean Helical Axis and $\widetilde{U}_i$ are the skew-symmetric direction matrices (Equation 18).

$$\widetilde{U_i} = \begin{bmatrix} 0 & -u_Z & u_Y \\ u_Z & 0 & -u_X \\ -u_Y & u_X & 0 \end{bmatrix}$$

Equation 18

Setting the partial derivative of the sum of squares with respect to the central direction equal to zero will minimize the sum of squares by the Eigen solution (Equation 19).

$$\left(\sum_{i=1}^{4} \widetilde{U_i^2}\right) u = 0$$

Equation 19

$\vec{u}$= eigenvector of $\sum_{i=1}^{4} \widetilde{U_i^2}$ for the smallest eigenvalue.

This mean the helical axis $\vec{u}$, represents the joint axis of rotation throughout the applied motion. The subtalar joint axis and the ankle joint axis will then be calculated and the inclination angle and deviation angle will be determined to represent the orientation of each joint axis (Figure 3-7).

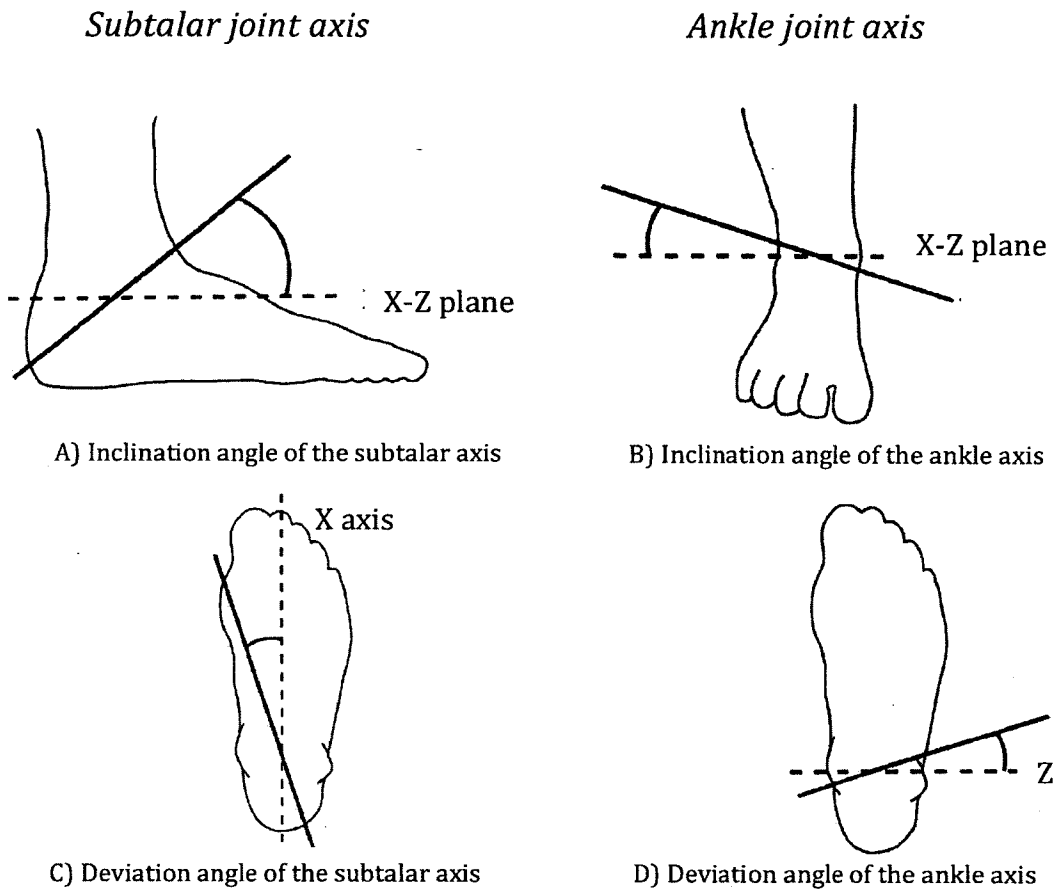

Figure 3-7: A&B) The inclination angle is the angle between the joint axis and the transverse plane (X-Z plane). C) The subtalar joint deviation angle is the angle between the projection of the subtalar joint axis on the transverse plane and the X axis representing the long axis of the foot. D) The ankle joint deviation angle is the angle between the projection of the ankle joint axis on the transverse plane and the Z axis representing the axis passing through the malleoli. [90]

The inclination angle was described as the angle between the axis and the plantar surface of the foot (Figure 3-7) and was calculated as follows (Equation 20).

$$\alpha_{inc} = \sin^{-1}\left(\frac{|\overrightarrow{Y_{cal}}.\vec{u}|}{|\overrightarrow{Y_{cal}}|.|\vec{u}|}\right)$$

Equation 20

where α_{inc} is the inclination angle, $\overrightarrow{Y_{cal}}$ is the Y component of the calcaneus coordinate system, and $\vec{u}$ is the joint axis unit vector.

The deviation angle (Figure 3-7) of the subtalar joint axis was described as the angle between the projection of the axis on the transverse plane and the long axis of the foot (X axis) and was determined as follows (Equation 21 and Equation 22). The deviation angle of the ankle joint axis is described as the angle between the projection of the ankle axis on the transverse plane and the axis passing through the malleoli (Z axis) and was determined as in Equation 21 and Equation 22 (by replacing the X axis with the Z axis).

First the projection of the unit vector on the transverse plane (X-Z plane) is determined using Equation 21.

$$\overrightarrow{v_{proj}} = \vec{u} - (\overrightarrow{Y_{cal}}.\vec{u}) \times \overrightarrow{Y_{cal}}$$

Equation 21

Then the deviation angle can be assessed using the projection vector calculated in Equation 22.

$$\beta_{dev} = \cos^{-1}\left(\frac{|\overrightarrow{X_{cal}}.\overrightarrow{v_{proj}}|}{|\overrightarrow{X_{cal}}|.|\overrightarrow{v_{proj}}|}\right)$$

Equation 22

where β_{dev} is the deviation angle, $\overrightarrow{X_{cal}}$ is the X component of the calcaneus coordinate system.

In addition to the subtalar MHA, a hindfoot MHA calculated from motion of the calcaneus with respect to the tibia, was determined while the foot was dorsiflexed and inversion/eversion was applied. It is expected that the difference between the two axes' orientation will be minimal enough that the hindfoot MHA will be used as a good approximation of the subtalar MHA for the optimization input. The same approach was used on the ankle joint MHA; another hindfoot MHA calculated this time from plantarflexion-dorsiflexion will be used as the ankle joint axis for the optimization input.

To measure the difference in orientation between two axes we can calculate the angle between the axes using Equation 23.

$$\gamma_{bet} = \cos^{-1}\left(\frac{|\overrightarrow{u_{sj}}.\overrightarrow{u_{hf}}|}{|\overrightarrow{u_{sj}}|.|\overrightarrow{u_{hf}}|}\right)$$ **Equation 23**

where γ_{bet} is the angle between the subtalar joint axis and the hindfoot joint axis, $\overrightarrow{u_{sj}}$ is the subtalar joint axis unit vector and $\overrightarrow{u_{hf}}$ is the hindfoot joint axis unit vector.

The inclination and deviation angles were compared between the subtalar/ankle joint axis and hindfoot joint axis in the intact foot and after sequentially sectioning the calcaneofibular ligament (CFL), the cervical ligament and the interosseous talocalcaneal ligament (ITCL). Differences in inclination and deviation angles between the subtalar/ankle joint axis and hindfoot joint axis were determined to ensure that each joint axis can be approximated by their respective hindfoot joint axis. Also, the angle between the subtalar and the hindfoot joint axis calculated during dorsiflexion in combination with inversion/eversion and between the ankle and hindfoot joint axis from plantarflexion-dorsiflexion were calculated to ensure minimal error in the approximation of the each joint axis location.

In addition to the dorsiflexed inversion/eversion and plantarflexion-dorsiflexion MHAs, the MHAs at the subtalar joint and ankle joint were determined during neutral inversion-eversion to compare the calculated MHAs with the axes resulting from the optimization.

3.7 Optimization

An optimization method [93, 124] was developed to implement a two-axes model represented by the subtalar joint axis and ankle joint axis to represent inversion motion at the hindfoot. The algorithm consisted of a two-tiered optimization with one inner optimization using a Gauss-Newton algorithm and one outer optimization using a Levenberg-Marquardt algorithm. The inputs to the algorithm were the 3D kinematics of the tibia and calcaneus experimentally measured and the initial guesses for the 12 joint location parameters. The joint parameters were defined by the orientation and the position of the subtalar joint axis and the ankle joint axis (5 parameters each) and the 2 last parameters represented the angle and separation distance between the two joint axes.

The outer optimization was used to adjust the 12 parameters. The inner optimization computed the two joint angles for each time frame such that the differences between the model and the measured kinematics were minimized.

3.7.1 Mathematical model

We already mentioned that coordinate transformation representing rotation and translation can be expressed using a transformation matrix (see Equation 24). The matrix ${}^{i}T_{j}$ transforms the j-CS intothe i-CS.

$$ {}^{i}T_{j} = \begin{bmatrix} R_{11} & R_{12} & R_{13} & t_1 \\ R_{21} & R_{22} & R_{23} & t_2 \\ R_{31} & R_{32} & R_{33} & t_3 \\ 0 & 0 & 0 & 1 \end{bmatrix} \qquad \textbf{Equation 24} $$

where **R** is the rotation matrix and **t** the translation vector. With that in mind we can detail the coordinate transformation of the model.

The two-hinge joint model was developed using the ankle joint axis and the subtalar joint axis (Figure 3-8) approximated by the hindfoot mean helical axis calculated from dorsiflexion inversion-eversion motion for the subtalar axis and from plantarflexion-dorsiflexion for the ankle joint axis. The model consists of 4 coordinate systems: the tibia coordinate system (CS_{Tibia}), the ankle joint coordinate system (CS_{Ankle}), the subtalar joint coordinate system ($CS_{Subtalar}$) and the calcaneus coordinate system ($CS_{Calcaneus}$). The Z_{Ankle} axis coincides with the ankle joint axis, and the $X_{Subtalar}$ axis coincides with the subtalar joint axis. The X_{Ankle} axis runs along the shortest common perpendicular between the ankle joint axis, and the subtalar joint axis and the $Z_{Subtalar}$ axis lies on the same line in the opposite direction (Figure 3-8). The tibia coordinate system is attached to the tibia and the calcaneus coordinate system is fixed to the calcaneus. We want to analyze the motion of the moving calcaneus with respect to the fixed tibia.

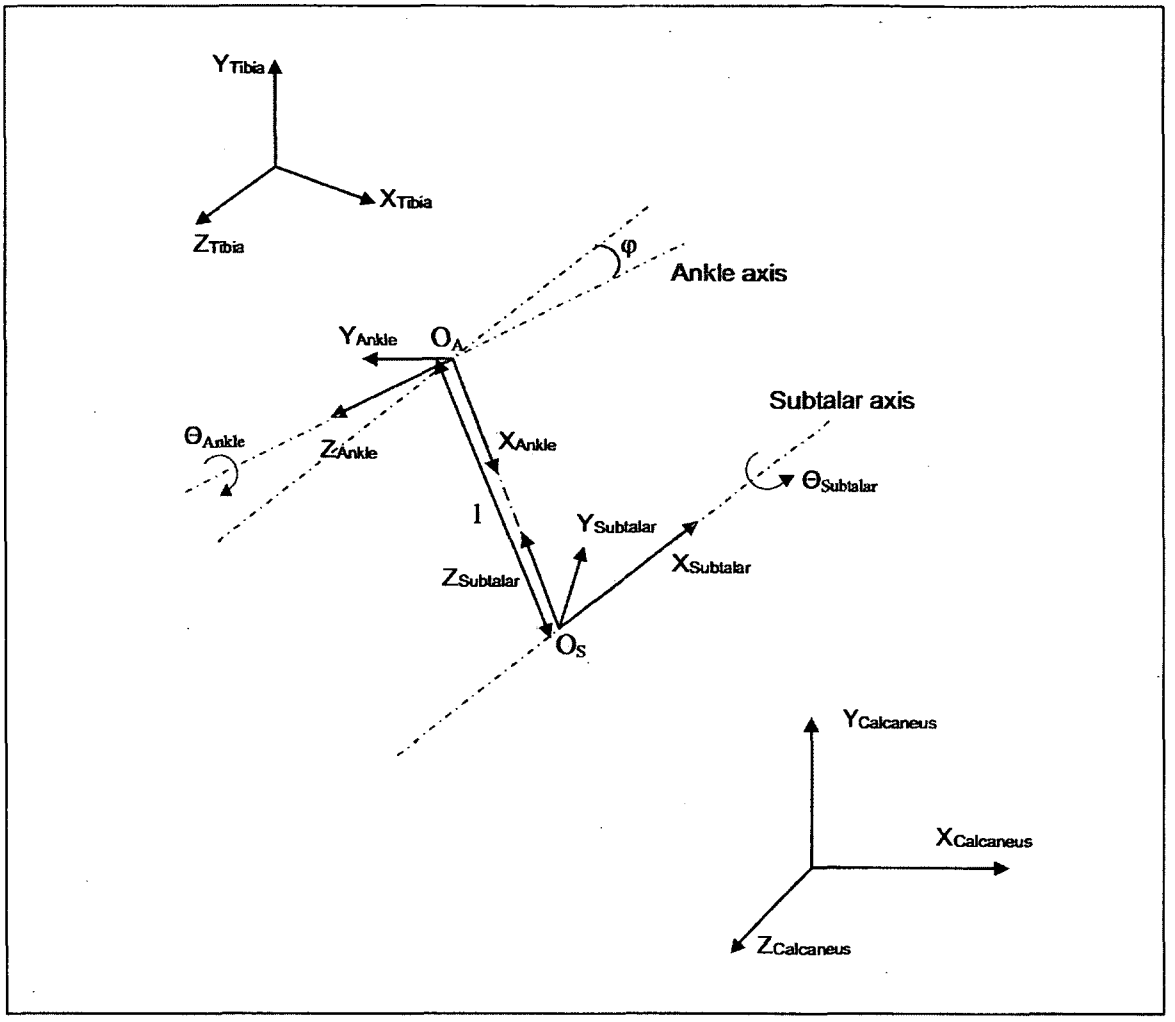

Figure 3-8: Two-axis model of the hindfoot showing the coordinate system used in the mathematical formulation of the optimization algorithm.

The transformation matrix between CS_{Tibia} and CS_{Ankle} includes a 3-Dimensional translation vector from the Origin of CS_{Tibia} to the Origin of CS_{Ankle} (O_A) and a 3-D rotation. The first rotation occurs around the ankle joint axis of θ_A radians. Then, 2 additional rotations can be performed byα_1 radian around X' and $\alpha_2$radian of rotation around Y''. The matrix ${}^{Tibia}T_{Ankle}$ depends on 6 parameters and can be decomposed as in Equation 25.

$$ {}^{Tibia}T_{Ankle} = {}^{Tibia}T_0 \ * \ {}^{0}T_{Ankle} $$

Equation 25

with ${}^{Tibia}T_0$ representing the translation vector and the rotation α_1 and α_2 as described in Equation 26. ${}^0T_{Ankle}$ is the transformation matrix describing the single rotation θ_A around the ankle joint axis (Equation 27).

$$ {}^{Tibia}T_0 = \begin{bmatrix} 1 & 0 & 0 & t_1 \\ 0 & 1 & 0 & t_2 \\ 0 & 0 & 1 & t_3 \\ 0 & 0 & 0 & 1 \end{bmatrix} * \begin{bmatrix} \cos\alpha_2 & 0 & \sin\alpha_2 & 0 \\ 0 & 1 & 0 & 0 \\ -\sin\alpha_2 & 0 & \cos\alpha_2 & 0 \\ 0 & 0 & 0 & 1 \end{bmatrix} * \begin{bmatrix} 1 & 0 & 0 & 0 \\ 0 & \cos\alpha_1 & -\sin\alpha_1 & 0 \\ 0 & \sin\alpha_1 & \cos\alpha_1 & 0 \\ 0 & 0 & 0 & 1 \end{bmatrix} \quad \textbf{Equation 26} $$

$$ {}^0T_{Ankle} = \begin{bmatrix} \cos\theta_A & -\sin\theta_A & 0 & 0 \\ \sin\theta_A & \cos\theta_A & 0 & 0 \\ 0 & 0 & 1 & 0 \\ 0 & 0 & 0 & 1 \end{bmatrix} \quad \textbf{Equation 27} $$

The transformation matrix between the ankle joint coordinate system and the subtalar joint coordinate system is represented by a rotation of φ radians about the $Z_{subtalar}$ axis with a translation of l along the same axis and a rotation of $\pi/2$ around the rotated Y' axis (Equation 28). φ is the angle between the subtalar and ankle joint axis and l is the distance separating the two axes.

$$ {}^{Ankle}T_{Subtalar} = \begin{bmatrix} 0 & 0 & 1 & 0 \\ \sin\varphi & \cos\varphi & 0 & 0 \\ -\cos\varphi & \sin\varphi & 0 & l \\ 0 & 0 & 0 & 1 \end{bmatrix} \quad \textbf{Equation 28} $$

To represent the transformation matrix between the subtalar joint CS and the calcaneus CS, we need a translation vector and 3 rotations. The first two rotations (α_3 and α_4) will bring the X-axis along the subtalar joint axis, and the third rotation will represent the rotation around the subtalar axis. Therefore, we can decompose the transformation matrix between the calcaneus and subtalar CS as shown in Equation 29.

$$ {}^{Subtalar}T_{Calcaneus} = {}^{Subtalar}T_1 * {}^1T_{Calcaneus} \quad \textbf{Equation 29} $$

with ${}^1T_{Calcaneus}$ representing the translation vector and the rotation $\alpha_3$around the Z axis and α_4 around the rotated Y axis as described in Equation 30. ${}^{Subtalar}T_1$ is the

transformation matrix describing the single rotation θ_S around the subtalar joint axis (Equation 31).

$$ {}^{1}T_{Calcaneus} = \begin{bmatrix} 1 & 0 & 0 & t_4 \\ 0 & 1 & 0 & t_5 \\ 0 & 0 & 1 & t_6 \\ 0 & 0 & 0 & 1 \end{bmatrix} * \begin{bmatrix} \cos\alpha_4 & 0 & \sin\alpha_4 & 0 \\ 0 & 1 & 0 & 0 \\ -\sin\alpha_4 & 0 & \cos\alpha_4 & 0 \\ 0 & 0 & 0 & 1 \end{bmatrix} * \begin{bmatrix} \cos\alpha_3 & -\sin\alpha_3 & 0 & 0 \\ \sin\alpha_3 & \cos\alpha_3 & 0 & 0 \\ 0 & 0 & 1 & 0 \\ 0 & 0 & 0 & 1 \end{bmatrix} \quad \textbf{Equation 30} $$

$$ {}^{Subtalar}T_{1} = \begin{bmatrix} 1 & 0 & 0 & 0 \\ 0 & \cos\theta_S & -\sin\theta_S & 0 \\ 0 & \sin\theta_S & \cos\theta_S & 0 \\ 0 & 0 & 0 & 1 \end{bmatrix} \quad \textbf{Equation 31} $$

According to the model described previously, the relative motion of the calcaneus with respect to the tibia can be written as in Equation 32.

$$ {}^{Tibia}T^{model}_{Calcaneus} = {}^{Tibia}T_0 \cdot {}^{0}T_{Ankle} \cdot {}^{Ankle}T_{Subtalar} \cdot {}^{Subtalar}T_1 \cdot {}^{1}T_{Calcaneus} \quad \textbf{Equation 32} $$

According to this model we have 14 variables; 12 are the optimization model parameters and 2 are the kinematic variables representing the subtalar and ankle joint angles. More precisely, the 12 parameters include the 6 translations (t1, t2, t3, t4, t5 and t6), 4 rotations (α_1, α_2, α_3, α_4) and the 2 parameters relating the ankle joint and subtalar joint axes (l and φ). The kinematic variables are θ_A and θ_S which represent the angles around the ankle and subtalar joint axis respectively. The 12 model parameters are constant but different between individuals and the 2 kinematic variables change with motion.

The experimental transformation matrix representing the motion of the calcaneus with respect to the tibia was calculated based on the position and orientation of the calcaneus and tibia with respect to the laboratory CS as shown in Equation 33.

$$ {}^{Tibia}T^{Exp}_{Calcaneus} = \left[{}^{Lab}T^{Exp}_{Tibia}\right]^{-1} {}^{Lab}T^{Exp}_{Calcaneus} \quad \textbf{Equation 33} $$

In order to compute the two joint angles for each time frame such that the differences between the model and the measured kinematics were minimized, we need to

relate ${}^{0}T_{Ankle}$ and ${}^{Subtalar}T_{1}$ to the experimental data. Therefore we used the experimental data from Equation 33, Equation 26, Equation 30 and Equation 32 into Equation 34.

$$B = \left[{}^{Tibia}T_{0}\right]^{-1} \cdot {}^{Tibia}T^{Exp}_{Calcaneus} \cdot {}^{1}T_{Calcaneus} \qquad \textbf{Equation 34}$$

This matrix B can be related to the matrix described in Equation 35.

$${}^{0}T_{1} = {}^{0}T_{Ankle} \cdot {}^{Ankle}T_{Subtalar} \cdot {}^{Subtalar}T_{1} \qquad \textbf{Equation 35}$$

${}^{0}T_{1}$ is a function of l, φ (constant) and θ_A, θ_S.

Once θ_A and θ_S fit the experimental data we need to optimize the 12 model parameters. A set of three Euler angles were extracted from the model (${}^{Tibia}T^{model}_{Calcaneus}$) and the experimental data (${}^{Tibia}T^{Exp}_{Calcaneus}$) at each frame and were compared.

3.7.2 Optimization method

The 12 model parameters were optimized to fit the model to the experimental inversion motion of the calcaneus with respect to the tibia. The 2-hinge joint model has only 2 degree of freedom however any motion of the foot requires 6 degree of freedom to be described exactly. The 12 model parameters will be optimized to perform the experimental inversion motion as well as possible without using the kinematics of the talus. The optimization algorithm is as follows and explained in Appendix 1:

1) Start with the 12 model parameters initial guess from the hindfoot mean helical axes approximating the subtalar axis and the ankle.

2) For each frame calculate the ${}^{Tibia}T^{Exp}_{Calcaneus}$ and estimate the subtalar joint angle θ_S and ankle joint angle θ_A from the experimental data using Equation 34.

3) Using an 'inner-optimization' the model joint kinematic variables (θ_S, θ_A) were adjusted from Equation 35 at each time frame for best closure. The inner optimization

used a Gauss-Newton algorithm to minimize the differences between the joint kinematics variables from the model and the experimental data.

4) The three Euler angles describing the experimental motion of the calcaneus with respect to the tibia and the three Euler angles from the model were measured and compared. The residuals at each frame (k) consisted of the differences in these Euler angles (ζ_i) as well as the differences in the origin location (O_i) of the calcaneus. Therefore the function F to minimize can be written as Equation 36 with the primed terms denoting the experimental quantities and the unprimed terms the model quantities.

$$F_{min} = \sum_{k=1}^{100} \sum_{i=1}^{3} [(\zeta_i - \zeta_i')_k^2 + (O_i - O_i')_k^2] \qquad \textbf{Equation 36}$$

An iterative least-square optimization algorithm was used to minimize F as a function of the 12 model parameters. The search for the minimum was terminated when the estimated relative errors were less than 10^{-5}.

3.8 Statistics

3.8.1 Foot kinematics analysis

A 2-way repeated measure ANOVA (condition*sagittal foot position) was used to investigate the interaction between the foot position in the sagittal plane and the maximum inversion and eversion rotation detected in each ligament and bracing condition. A separate 2-way repeated measure ANOVA (ligament*bracing) was used to analyze the differences in moments applied around the inversion-eversion axis on the foot between each ligament sectioned (intact, CFL cut, CFL cut with the intrinsic ligaments) with and without a brace applied (bracing condition). In the presence of a significant interaction or main effect, Fisher's LSD and Cohen's d effect sizes were applied for post hoc comparisons. The significance level for all analyses was alpha = 0.05 and an effect size greater than 0.8 were required for clinical relevance. Statistical analyses were conducted using SPSS (Version 20, SPSS Inc., Chicago, IL).

3.8.2 Cohen's effect size

Effect size quantifies the size of the difference between two groups. The effect size d is the standardized mean difference between two conditions and is calculated as in Equation 37.

$$d = \frac{\mu_1 - \mu_2}{SD_{pooled}} \qquad \textbf{Equation 37}$$

where d is the effect size, μ_1 is the mean for condition 1, μ_2 is the mean for condition 2 and SD_{pooled} is the pooled estimate standard deviation which is calculated as in Equation 38.

$$SD_{pooled} = \sqrt{\frac{(n_1 - 1)SD_1^2 + (n_2 - 1)SD_2^2}{n_1 + n_2 - 2}} \qquad \textbf{Equation 38}$$

where n_1 and n_2 are the size of our sample for condition 1 and condition 2; SD_1 and SD_2 are the standard deviation for condition 1 and condition 2.

Values calculated for effect size are generally low but can range from -3 to 3. The standard interpretation of effect size was offered by Cohen and is described as 0.2 being small, 0.5 being moderate and 0.8 and higher being large. For example, having an effect size of 0.8 indicates that 79% of the results from condition 1 would be below the mean of condition 2.

3.8.3 Foot axes analysis

A 2-way repeated measure ANOVA (condition*joint axis) was used to investigate the interaction between each ligament condition with the calculated mean helical axis from inversion-eversion and the resulting optimized joint axis inclination and deviation angles at the subtalar joint and ankle joint.

4 RESULTS

The foot kinematics analysis section displays the inversion and eversion range of motion for each condition (i.e. intact, injury at the calcaneofibular ligament (CFL) and additional injury to the intrinsic ligaments) with and without a brace at each foot sagittal position (i.e. neutral, maximum dorsiflexion and maximum dorsiflexion). No significant interaction was found between the foot condition and the foot position; however, a significant main effect was found for the foot condition and for the foot position. Briefly, significant increase in inversion was found at the ankle after sectioning the CFL and at the subtalar joint after sectioning the CFL, cervical ligament and interosseous talocalcaneal ligament (ITCL). Significant decrease in inversion range of motion was found after placing the foot in dorsiflexion compared to the neutral position for the subtalar and ankle joint. Placing the foot in plantarflexion also decreased subtalar joint range of motion in inversion and eversion compared to the neutral position.

The foot axes analysis section first presents the results for the calculation of the mean helical axis (MHA) at the subtalar joint, ankle joint and hindfoot. At the subtalar joint a MHA was calculated from dorsiflexed inversion/eversion motion and from inversion-eversion and compared to ensure that the differences in the orientation of the two axes were minimal. We found an angle of 7.30° between the two axes in the intact condition; 6.57° after sectioning the CFL and 6.77° after all ligaments were cut. The dorsiflexed inversion/eversion hindfoot MHA was calculated and compared to the dorsiflexed inversion/eversion subtalar MHA, and we found a 14.61° angle between the hindfoot and subtalar axes in intact, 15.67° after CFL sectioning and 18.30° after all ligaments were cut. As the differences in MHA between the subtalar and hindfoot were small, the dorsiflexed inversion/eversion hindfoot MHA was used to approximate the subtalar joint axis orientation needed as initial guess for the optimization. The plantarflexion-dorsiflexion hindfoot MHA was used to approximate the ankle joint axis needed as an initial guess for the optimization.

In the second part, the results of the optimization for the subtalar joint and ankle joint axes were presented, and their orientation was compared with the MHA calculated at the subtalar and ankle joint during inversion-eversion. The angle between the subtalar MHA and the optimized axis was 25.30° in intact, 19.16° after sectioning the CFL and 30.92° after all ligaments were cut. For the ankle joint the angle between the MHA and the optimized axis was 39.35° in intact, 53.59° after sectioning the CFL and 53.27° after all ligaments were cut. The statistical analyses looking at the differences between the MHA and optimized axis and the differences in ligament conditions for each joint showed only a statistical difference between the subtalar joint MHA and the subtalar optimized axis inclination angle ($p=0.006$) and a significant difference in the ankle MHA and its resulting optimization axis deviation angle ($p=0.003$).

4.1 Foot kinematics analysis

No significant interaction was found between the foot conditions (i.e., intact, ligaments cut and/or brace applied) and the position of the foot in the sagittal plane for the subtalar joint in inversion ($M=11.203$, $SE=0.653$, $F(10)=1.589$, $p=0.125$, $CI=[9.698,12.708]$) and eversion ($M=-6.918$, $SE=0.657$, $F(10)=1.663$, $p=0.104$, $CI=[-8.433,-5.404]$) (Table 4-1A), the ankle joint in inversion ($M=4.085$, $SE=0.831$, $F(10)=1.511$, $p=0.151$, $CI=[2.169,6.001]$) and eversion ($M=-1.623$, $SE=0.238$, $F(10)=0.819$, $p=0.611$, $CI=[-2.172,-1.074]$) (Table 4-1B) and for the hindfoot in inversion ($M=15.127$, $SE=1.176$, $F(10)=1.928$, $p=0.053$, $CI=[12.417,17.838]$) and eversion ($M=-8.121$, $SE=0.708$, $F(10)=1.470$, $p=0.166$, $CI=[-9.754,-6.488]$) (Table 4-1C). Individual results can be found in Appendix 2.

Table 4-1: Mean rotation (standard deviation) of the rotation angle at the A) Talocalcaneal joint, B) Talocrural joint, C) Tibiocalcaneal joint. (Inv = Inversion, Ev = Eversion, DF = Dorsiflexion, PF = Plantarflexion). No significant interaction was found between the foot condition and the foot position.

A)

Subtalar	Intact		CFL cut		CFL+cevical+ITCLcut	
	Barefoot	Bracing	Barefoot	Bracing	Barefoot	Bracing
Inv (°)	13.46 (3.48)	10.20 (2.22)	15.18 (3.81)	10.11 (2.37)	17.73 (4.29)	12.55(3.21)
Ev (°)	8.55 (3.74)	6.05 (3.48)	9.52 (3.94)	7.02 (2.99)	9.12 (3.43)	8.6 (3.43)
DF+Inv (°)	10.31 (2.91)	7.74 (2.60)	11.78 (4.39)	7.68 (1.41)	12.42 (3.82)	8.53 (3.17)
DF+Ev (°)	8.18 (1.84)	5.32 (2.30)	8.18 (3.30)	7.17 (2.68)	10.31 (2.57)	8.28 (2.88)
PF+Inv (°)	12.16 (2.94)	7.28 (3.84)	12.83 (2.38)	7.91 (2.38)	14.88 (4.11)	8.91 (2.56)
PF+Ev (°)	4.31 (1.73)	3.90 (1.36)	5.40 (2.39)	3.99 (1.47)	5.57 (1.70)	5.08 (2.05)

B)

Ankle	Intact		CFL cut		CFL+cevical+ITCLcut	
	Barefoot	Bracing	Barefoot	Bracing	Barefoot	Bracing
Inv (°)	3.43 (3.08)	2.34 (2.36)	8.22 (4.68)	4.42 (4.02)	8.64 (5.44)	4.61 (3.53)
Ev (°)	1.91 (1.12)	1.48 (0.89)	1.83 (1.43)	1.47 (1.62)	1.81 (0.79)	1.49 (0.87)
DF+Inv (°)	1.85 (1.56)	0.95 (0.93)	4.81 (2.90)	2.25 (2.04)	5.24 (4.62)	1.73 (1.65)
DF+Ev (°)	1.04 (0.85)	1.20 (0.70)	1.06 (0.45)	1.31 (0.84)	1.52 (0.62)	1.08 (0.89)
PF+Inv (°)	3.35 (1.72)	2.17 (1.90)	6.16 (3.52)	3.48 (2.09)	6.12 (3.75)	3.77 (2.75)
PF+Ev (°)	2.04 (1.54)	1.54 (1.00)	2.67 (2.37)	1.91 (1.36)	2.16 (1.34)	1.71 (0.77)

C)

Hindfoot	Intact		CFL cut		CFL+cevical+ITCLcut	
	Barefoot	Bracing	Barefoot	Bracing	Barefoot	Bracing
Inv (°)	16.65 (3.63)	12.39 (3.93)	23.29 (6.12)	14.60 (5.56)	26.28 (6.48)	17.11(5.45)
Ev (°)	10.25 (4.01)	6.96 (3.28)	11.09 (3.16)	8.21 (3.23)	10.47 (3.14)	9.44 (3.15)
DF+Inv	11.68 (2.41)	7.71 (2.09)	16.42 (5.10)	9.73 (2.77)	17.55 (3.98)	10.11 (2.69)
DF+Ev	8.29 (2.61)	5.84 (1.87)	8.93 (3.26)	8.05 (3.50)	11.05 (3.26)	8.92 (3.28)
PF+Inv	15.54 (4.17)	9.31 (5.01)	19.00 (5.57)	11.40 (4.08)	20.98 (7.69)	12.54 (4.70)
PF+Ev	6.14 (2.44)	5.33 (1.35)	7.70 (3.17)	5.66 (2.19)	7.27 (2.11)	6.58 (1.88)

Significant condition main effect (Figure 4-1) was present for inversion at the subtalar joint ($F(5)=22.430$, $p<0.001$), ankle joint ($F(5)=23.027$, $p<0.001$) and hindfoot ($F(5)=35.102$, $p<0.001$) and for eversion at the subtalar joint ($F(5)=10.707$, $p<0.001$) and

hindfoot ($F(5)=11.754$, $p<0.001$). Post-hoc analyses showed that isolated injury at the CFL significantly affected ankle joint ($p=0.002$, $d=2.03$) and hindfoot ($p=0.009$, $d=1.74$) inversion range of motion. Combined injury of the CFL with the intrinsic ligaments (cervical and ITCL) significantly increased subtalar inversion ($p=0.007$, $d=1$).

The use of a semi-rigid ankle brace significantly limited inversion motion in the intact condition ($p=0.001$, $d=1.66$ for the subtalar joint and $p<0.001$, $d=1.69$ for the hindfoot), after the CFL was sectioned ($p=0.002$, $d=2.02$ for the subtalar joint; $p=0.001$, $d=1.02$ for the ankle joint; $p=0.001$, $d=1.76$ for the hindfoot) and after the CFL and intrinsic ligaments were damaged ($p<0.001$, $d=1.71$ for the subtalar joint; $p=0.001$, $d=1.01$ for the ankle joint; $p<0.001$, $d=1.72$ for the hindfoot). The semi-rigid ankle brace also limited eversion motion at the subtalar joint ($p=0.009$, $d=0.93$) and hindfoot ($p=0.02$, $d=0.91$) in the intact condition and after sectioning the CFL at the hindfoot only ($p=0.007$, $d=0.84$). Applying the brace on a combined CFL and intrinsic ligaments deficient foot did not limit eversion at the subtalar joint ($p=0.07$) nor hindfoot ($p=0.024$, $d=0.54$). On the contrary, using the brace after complete tear of all ligaments increased eversion motion at the subtalar joint ($p=0.004$, $d=1$) and hindfoot ($p=0.006$, $d=1.05$) compared to using the brace on the intact foot.

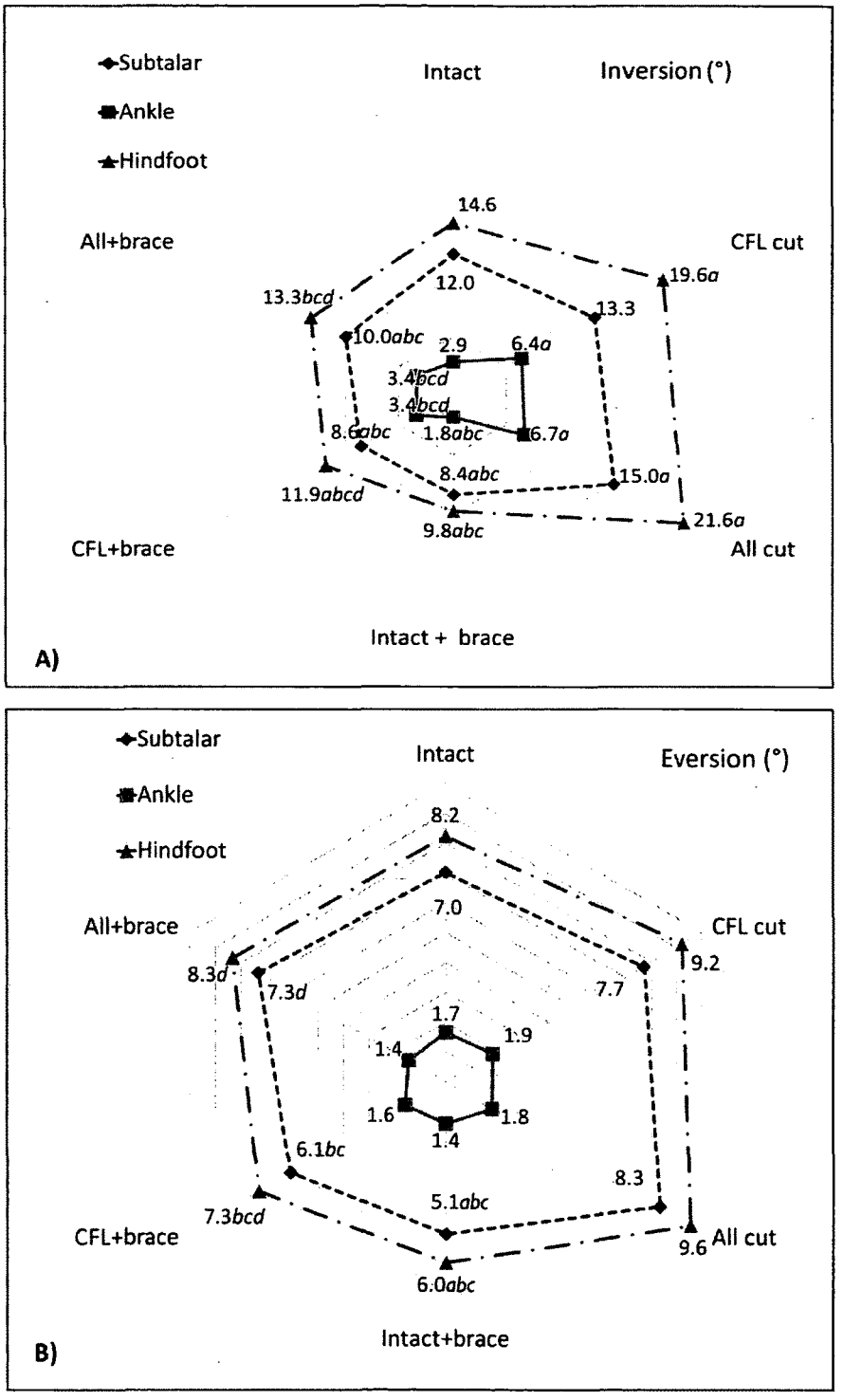

Figure 4-1: A) Inversion range of motion and B) Eversion range of motion at the subtalar, ankle and hindfoot for the intact, CFL cut, CFL+cervical +ITCL cut conditions with and without an ankle brace independently of sagittal foot position. a means significantly different from intact. b means significantly different from CFL. c means significantly different from All cut. d means significant difference between brace conditions (compared to intact with brace).

Significant position main effect (Figure 4-2) was also detected for inversion at the subtalar joint ($F(2)=7.708$, $p=0.005$), ankle joint ($F(2)=6.341$, $p=0.009$) and hindfoot ($F(2)=17.595$, $p=<0.001$) and for eversion at the subtalar joint ($F(2)=15.752$, $p=<0.001$) and hindfoot ($F(2)=12.347$, $p=0.001$). Positioning the foot in maximum dorsiflexion significantly reduced subtalar ($p=0.003$, $d=1.37$), ankle ($p=0.002$, $d=0.84$) and hindfoot ($p=0.001$, $d=1.72$) inversion motion compared to neutral. Having the foot in plantarflexion instead of neutral while applying inversion significantly reduced the range of motion at the subtalar joint ($p=0.004$, $d=1.00$). Eversion range of motion decreased with plantarflexion compared to neutral ($p=0.003$, $d=1.40$ for the subtalar joint and $p=0.005$, $d=1.2$ for the hindfoot) and dorsiflexion ($p=$, $d=1.80$ for the subtalar joint and $p=$, $d=1.00$ for the hindfoot).

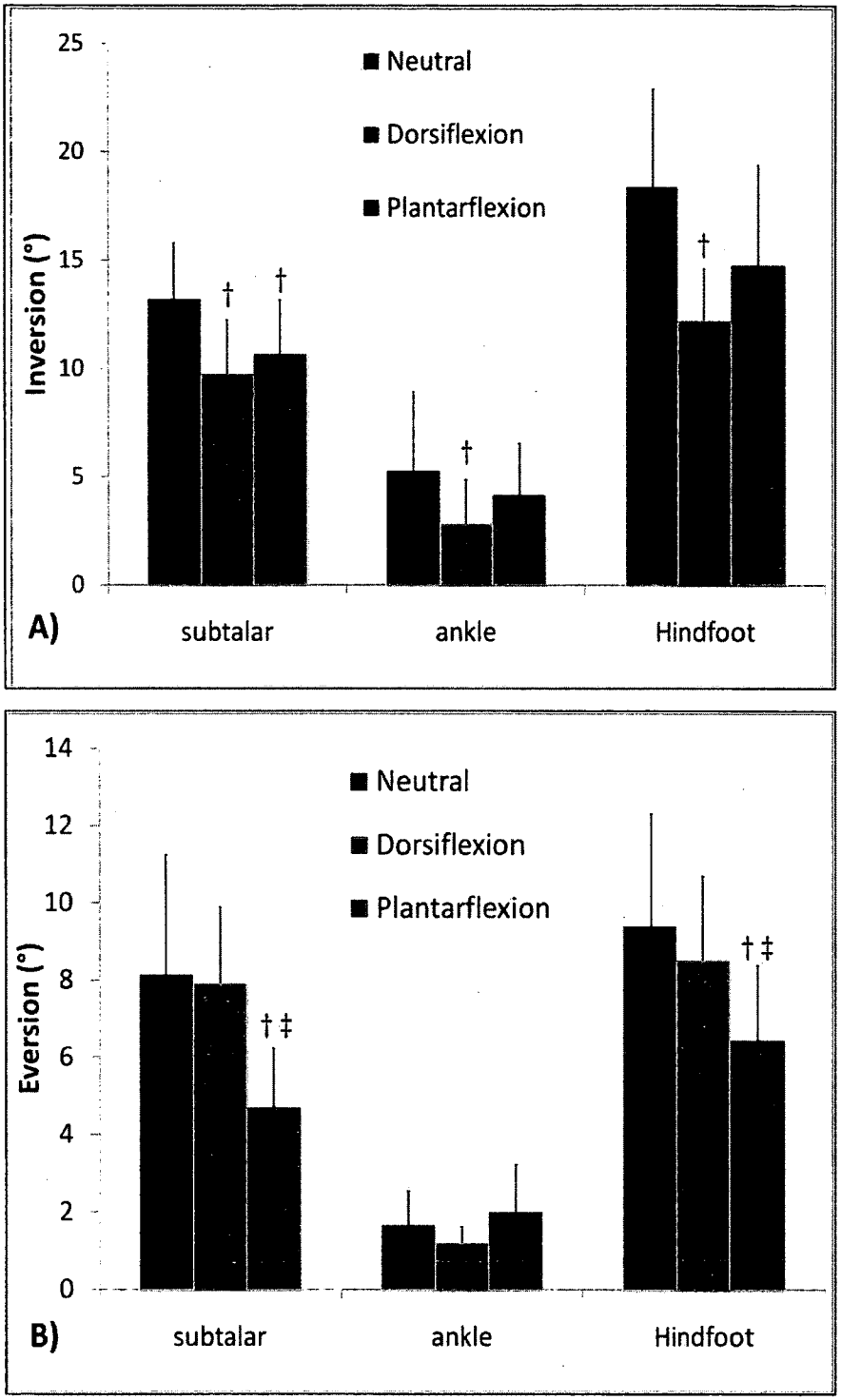

Figure 4-2: A) Inversion range of motion and B) Eversion range of motion at the subtalar joint, the ankle joint and hindfoot with the foot in neutral position, maximum dorsiflexion and maximum plantarflexion. † indicates significantly different from neutral and ‡ indicates significantly different from dorsiflexion.

No significant interaction for the applied moment was found between the ligament conditions (intact, CFL cut and CFL, cervical and ITCL cut) and bracing condition (with and without brace) for inversion and eversion and all sagittal foot positions (Table 4-2). A simple main effect was found on the bracing condition for inversion with the foot in a neutral position ($p<0.001$), maximum dorsiflexion ($p=0.001$) and maximum plantarflexion ($p<0.001$). A significant main effect was also detected on bracing for eversion in neutral ($p=0.001$), dorsiflexion ($p<0.001$) and plantarflexion ($p=0.003$). Moments applied on the foot wearing a brace were significantly higher than moments applied to the unbraced hindfoot.

Table 4-2: Mean moment (standard deviation) applied to the foot. (DF = Dorsiflexion, PF = Plantarflexion).

Moment	Intact		CFL cut		CFL+cevical+ITCLcut	
(N.m)	Barefoot	Bracing	Barefoot	Bracing	Barefoot	Bracing
Inversion	5.74 (1.52)	7.75 (1.91)	5.29 (1.30)	7.14 (1.26)	6.42 (1.21)	7.55 (1.90)
Eversion	6.76 (1.57)	7.53 (1.20)	6.83 (1.66)	8.58 (1.77)	7.18 (1.78)	8.42 (1.51)
DF+Inversion	5.45 (1.61)	6.84 (0.75)	5.48 (1.59)	6.38 (0.84)	4.62 (1.36)	7.36 (1.64)
DF+Eversion	6.45 (1.5)	7.78 (2.10)	5.61 (1.94)	9.57 (2.16)	6.25 (1.66)	9.25 (2.18)
PF+Inversion	6.11 (1.66)	6.59 (1.19)	6.00 (1.36)	7.31 (1.71)	5.77 (1.16)	6.68 (1.65)
PF+Eversion	5.64 (0.83)	6.74 (1.38)	5.89 (1.26)	7.22 (1.29)	6.00 (0.66)	7.60 (1.75)

4.2 Foot axes analysis

4.2.1 Mean Helical Axis

Intact condition

The mean helical axis (MHA) for the subtalar joint, the ankle joint and the hindfoot were calculated as described in the methods section. The inclination and deviation angles derived from these MHAs are reported in Table 4-3, Table 4-4 and Table 4-5. At the subtalar joint, the MHA was calculated for the dorsiflexed inversion/eversion motion (i.e., inversion-eversion with the foot placed in maximum dorsiflexion) and for inversion-eversion (Table 4-3). The mean inclination angle found for the dorsiflexed inversion/eversion motion was 49.71° (range: 40.99° – 60.06°) and

54.55° (range: 51.71° – 60.17°) for the inversion-eversion motion. The mean deviation angle for the MHA of the subtalar joint was 15.70° (range: 1.32° – 30.03°) for the dorsiflexed inversion/eversion motion and 17.47° (range: 2.77° – 32.31°) for inversion-eversion. The angular difference in the orientation of the MHA calculated from the dorsiflexed inversion/eversion and from inversion-eversion was small at the subtalar joint with a mean difference in inclination angle of -4.84° ± 4.30° (range: -10.72° – (-0.12°)) and a mean difference in deviation angle of -1.77° ± 9.50° (range: -16.77° – 8.75°) across specimens. The calculation of the angle between the dorsiflexed inversion/eversion MHA and the inversion-eversion MHA was 7.30° ranging from 1.96° to 11.13°.

Table 4-3: Inclination angle, deviation angle and the angle between the Mean Helical Axis calculated at the subtalar joint during inversion-eversion (Inv-Ev) and the dorsiflexed inversion/eversion (DF+Inv-Ev) motion.

Subtalar	Inclination angle (°)		Deviation angle (°)		Angle
Specimen#	DF+Inv-Ev	Inv-Ev	DF+Inv-Ev	Inv-Ev	between (°)
4	50.36	52.25	30.03	29.18	1.96
7	49.90	52.94	8.26	2.77	4.57
9	47.67	57.24	11.77	3.02	10.93
11	60.06	60.17	1.32	10.33	4.49
12	40.99	51.71	27.30	27.20	10.72
13	49.27	53	15.54	32.31	11.13
Mean ± SD	49.71 ± 6.13	54.55 ± 3.38	15.70 ± 11.11	17.47 ± 13.62	7.30 ± 4.08
Inman [71]	42 ± 9 (68.5 - 20.5)		23 ± 11 (47 - 4)		-

At the ankle joint, the MHA was calculated for plantarflexion-dorsiflexion and inversion-eversion (Table 4-4). The angular difference in the orientation of the MHA calculated from the plantarflexion-dorsiflexion and the inversion-eversion motion is higher at the ankle joint than the subtalar joint with a mean difference in inclination angle of 5.85° ± 21.55° (range: -25.53° –26.34°) and a mean difference in deviation angle of -33.58° ± 14.33° (range: -55.13° – (-14.69°)) across specimen. The calculation of the angle between the plantarflexion-dorsiflexion MHA and the inversion-eversion MHA showed a high difference in the orientation of the two axes with an average of 57.38° ranging from 30.09° to 89.10°.

Table 4-4: Inclination angle, deviation angle and angle between the Mean Helical Axis calculated at the ankle joint during inversion-eversion (Inv-Ev) and the plantarflexion-dorsiflexion (PF-DF).

Ankle	Inclination angle (°)		Deviation angle (°)		Angle
Specimen#	PF-DF	Inv-Ev	PF-DF	Inv-Ev	between (°)
4	26.08	51.61	17.28	54.52	58.75
7	32.30	7.20	1.58	16.27	30.09
9	28.18	11.44	6.08	34.85	48.43
11	43.62	17.28	31.08	86.21	58.55
12	31.93	24.70	15.06	57.06	89.10
13	44.67	59.45	25.51	49.16	59.35
				49.68	57.38
Mean ± SD	34.46 ± 7.86	28.61 ± 21.80	16.10 ± 11.20	±23.45	±19.17
Inman [71]	7.3 ± 3.7 ((-4)-16)		6 ± 7		-

At the hindfoot joint, the MHA was calculated for the dorsiflexed inversion/eversion motion, plantarflexion-dorsiflexion and inversion-eversion (Table 4-5).

Table 4-5: Inclination and deviation angles of the Mean Helical Axis calculated at the hindfoot joint during inversion-eversion (Inv-Ev), dorsiflexed inversion/eversion (DF+Inv-Ev) and plantarflexion-dorsiflexion (PF-DF).

Hindfoot	Inclination angle (°)			Deviation angle (°)		
Specimen#	DF+Inv-Ev	PF-DF	Inv-Ev	DF+Inv-Ev	PF-DF	Inv-Ev
4	42.21	20.17	37.38	7.44	19.03	9.99
7	43.47	28.42	49.13	1.40	18.06	29.83
9	37.84	10.46	39.80	18.44	12.77	26.23
11	43.44	49.25	49.28	2.56	40.40	7.47
12	27.48	24.63	29.08	15.82	24.17	26.80
13	35.62	35.86	43.02	0.80	31.01	24.23
Mean	38.35	28.13	41.28	7.74	24.24	20.76
SD	6.21	13.37	7.68	7.68	10.04	9.52

The differences in the MHA orientation between the subtalar joint and hindfoot joint for the dorsiflexed inversion/eversion motion and inversion-eversion are presented in Figure 4-3 as well as the differences between the MHA orientation of the ankle joint and hindfoot joint for plantarflexion-dorsiflexion and inversion-eversion.

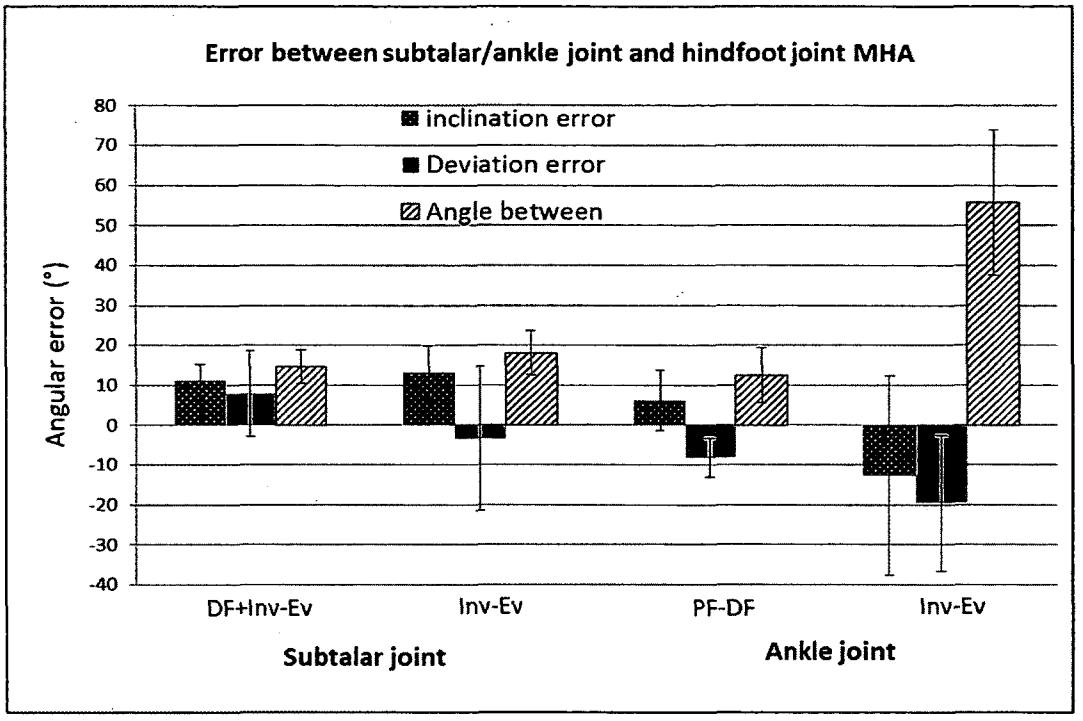

Figure 4-3: Error between the subtalar and hindfoot joint MHA orientation and error between the ankle joint and hindfoot joint MHA orientation represented by the difference in inclination angle, the difference in deviation angle and the angle between the MHA.

The differences in subtalar joint MHA and hindfoot joint MHA orientations for the dorsiflexed inversion/eversion motion are small enough to use the hindfoot MHA as an approximation of the subtalar joint axis for the optimization input. Similar differences in ankle joint MHA and hindfoot joint MHA orientations were found in plantarflexion-dorsiflexion; therefore, the hindfoot MHA will be used to approximate the ankle joint axis in the optimization input.

Calcaneofibular ligament (CFL) cut condition

The mean helical axis (MHA) for the subtalar joint, the ankle joint and the hindfoot was calculated after sectioning the calcaneofibular ligament (CFL). The inclination and deviation angles derived from these MHA are reported in (Table 4-6, Table 4-7 and Table 4-8). At the subtalar joint, the MHA was calculated for the dorsiflexed inversion/eversion motion and for inversion-eversion (Table 4-6). The mean inclination angle found for the dorsiflexed inversion/eversion motion was 43.89° (range:

39.32° – 49.30°) and 49.67° (range: 43.15° – 53.98°) for the inversion-eversion motion. The mean deviation angle for the MHA of the subtalar joint was 18.16° (range: 5.12° – 30.07) for the dorsiflexed inversion/eversion motion and 19.60° (range: 3.34° – 36.75°) for inversion-eversion. The difference in the orientation of the MHA calculated from the dorsiflexed inversion/eversion and the inversion-eversion motion remains small after the CFL was sectioned at the subtalar joint with a mean difference in inclination angle of -5.77° ± 3.98° (range: -13.48° – (-2.71°)) and a mean difference in deviation angle of -1.43° ± 3.86° (range: -6.67° – 1.80°) across specimen. The calculation of the angle between the dorsiflexed inversion/eversion MHA and the inversion-eversion MHA showed that the orientation of the two axes stays similar as the average angle between is 6.57° ranging from 3.70° to 13.53° after cutting the CFL. Only one specimen (#9) had more than 10° difference in inclination angle and angle between the MHA from the dorsiflexed inversion/eversion and inversion-eversion. Without this specimen the maximum difference in inclination angle would have been -6.47°, and the maximum angle between would have been 6.55°.

Table 4-6: Inclination angle, deviation angle and the angle between the Mean Helical Axis calculated at the subtalar joint during inversion-eversion (Inv-Ev) and the dorsiflexed inversion/eversion (DF+Inv-Ev) motion in CFL deficient feet.

Subtalar	Inclination angle (°)		Deviation angle (°)		Angle
Specimen#	DF+Inv-Ev	Inv-Ev	DF+Inv-Ev	Inv-Ev	between (°)
4	49.30	53.92	25.96	24.16	4.75
7	44.12	47.66	18.59	17.02	3.70
9	40.51	53.98	5.12	3.34	13.53
11	43.40	49.87	8.52	10.02	6.55
12	46.70	49.41	20.71	26.28	4.60
13	39.32	43.15	30.07	36.75	6.31
Mean ± SD	43.89 ±3.74	49.67 ± 4.08	18.16 ± 9.72	19.6 ± 12.02	6.57 ± 3.57
Intact	49.71 ±6.13	54.55 ± 3.38	15.70 ± 11.11	17.47 ± 13.62	7.30 ± 4.08

At the ankle joint, the MHA was calculated for plantarflexion-dorsiflexion and inversion-eversion after the CFL was sectioned (Table 4-7). The difference in the orientation of the MHA calculated from the plantarflexion-dorsiflexion and the inversion-eversion motion remains higher at the ankle joint than the subtalar joint after sectioning

the CFL with a mean difference in inclination angle of 12.79° ± 15.37° (range: -8.21° – 32.39°) and a mean difference in deviation angle of -40.60° (range: -64.35° – (-19.44°)) across specimen. The calculation of the angle between the plantarflexion-dorsiflexion MHA and the inversion-eversion MHA showed a high difference in the orientation of the two axes with an average of 50.96° ranging from 17.81° to 67.65°. No apparent difference is seen in the ankle MHA angular orientation calculated in plantarflexion-dorsiflexion between the intact condition and the CFL deficient foot. A slight difference can be observed between the intact and CFL deficient feet MHA orientation during inversion-eversion, but the standard deviations are too high to make the difference discernible.

Table 4-7: Inclination angle, deviation angle and angle between the Mean Helical Axis calculated at the ankle joint during inversion-eversion (Inv-Ev) and the plantarflexion-dorsiflexion (PF-DF) in CFL deficient feet.

Ankle	Inclination angle (°)		Deviation angle (°)		Angle
Specimen#	PF-DF	Inv-Ev	PF-DF	Inv-Ev	between (°)
4	28.99	24.91	20.69	61.51	36.44
7	36.78	4.39	10.53	29.97	55.84
9	32.47	40.69	2.41	22.17	17.81
11	36.31	19.96	21.73	86.07	64.30
12	25.55	20.57	12.42	57.43	63.73
13	40.91	13.78	26.79	81.00	67.65
Mean ±SD	33.50 ±5.62	20.72 ± 12.10	15.76 ± 8.92	56.36 ±26.01	50.96 ±19.76
Intact	34.46 ±7.86	28.61 ± 21.80	16.10 ±11.20	49.68 ±23.45	57.38 ±19.17

At the hindfoot joint, the MHA was calculated for the dorsiflexed inversion/eversion motion, plantarflexion-dorsiflexion and inversion-eversion after the CFL was sectioned (Table 4-8).

Table 4-8: Inclination and deviation angles of the Mean Helical Axis calculated at the hindfoot joint during inversion-eversion (Inv-Ev), dorsiflexed inversion/eversion (DF+Inv-Ev) and plantarflexion-dorsiflexion (PF-DF) in CFL deficient feet.

Hindfoot	Inclination angle (°)			Deviation angle (°)		
Specimen#	DF+Inv-Ev	PF-DF	Inv-Ev	DF+Inv-Ev	PF-DF	Inv-Ev
4	40.03	27.08	40.89	11.15	22.16	4.78
7	45.00	22.52	40.17	4.89	11.39	4.81
9	32.74	22.95	40.06	8.93	20.97	16.96
11	37.73	34.07	35.71	12.26	29.13	13.75
12	29.96	23.45	37.86	22.44	20.05	27.35
13	25.25	29.65	32.75	17.73	30.42	27.25
Mean	35.12	26.62	37.91	12.90	22.36	15.82
SD	7.19	4.59	3.16	6.29	6.9	10.12
Intact mean	38.35	28.13	41.28	7.74	24.24	20.76

The differences in the MHA orientation between the subtalar joint and hindfoot joint for the dorsiflexed inversion/eversion motion and inversion-eversion are presented in Figure 4-4 as well as the differences between the MHA orientation of the ankle joint and hindfoot joint for plantarflexion-dorsiflexion and inversion-eversion for CFL deficient feet.

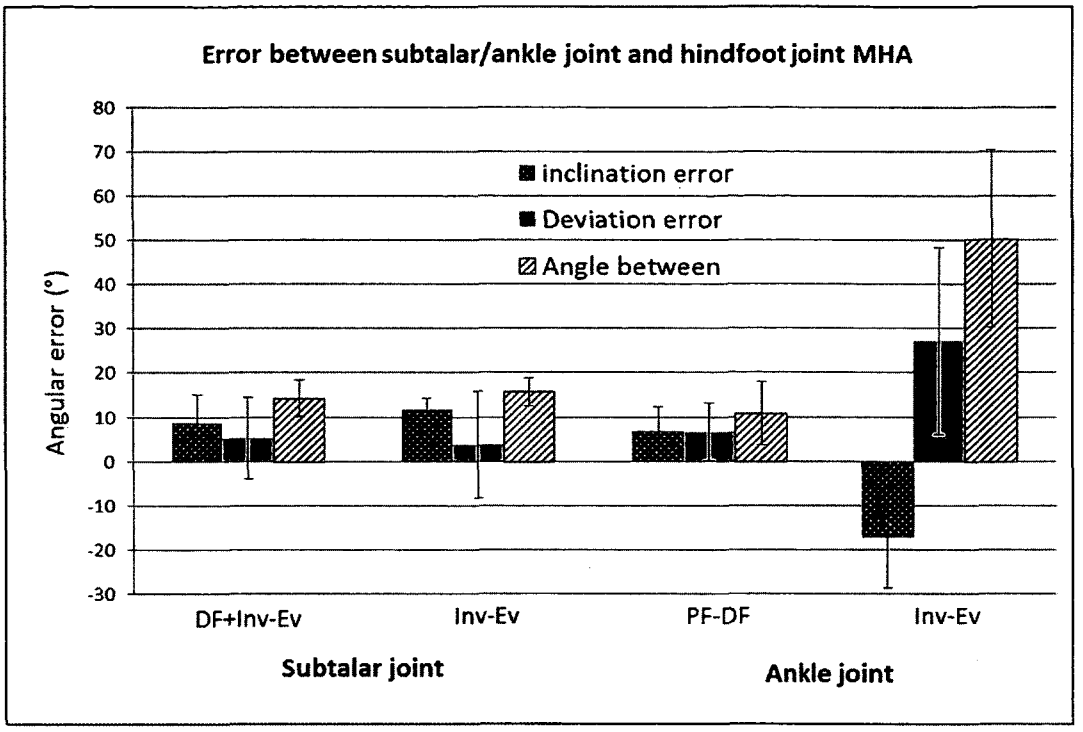

Figure 4-4: Error between the subtalar and hindfoot joint MHA orientation and error between the ankle joint and hindfoot joint MHA orientation represented by the difference in inclination angle, the difference in deviation angle and the angle between the MHA in CFL deficient feet.

The differences in subtalar joint MHA and hindfoot joint MHA orientations for the dorsiflexed inversion/eversion motion are small enough to use the hindfoot MHA as an approximation of the subtalar joint axis for the CFL deficient optimization input. Similar differences in ankle joint MHA and hindfoot joint MHA orientations were found after the CFL was sectioned in plantarflexion-dorsiflexion; therefore, the hindfoot MHA will be used to approximate the ankle joint axis in the optimization.

4.2.2 CFL, cervical and interosseous talocalcaneal ligaments (ALL) cut condition

The mean helical axis (MHA) for the subtalar joint, the ankle joint and the hindfoot were calculated after injury at the calcaneofibular ligament (CFL), the cervical ligament and the interosseous talocalcaneal ligament (ITCL); this condition will be more commonly named all ligaments cut. The inclination and deviation angles derived from these MHA are reported in (Table 4-9, Table 4-10 and Table 4-11). At the subtalar joint,

the MHA was calculated for the dorsiflexed inversion/eversion motion and for inversion-eversion (Table 4-9). The mean inclination angle found for the dorsiflexed inversion/eversion motion was 43.60° (range: 36.78° – 53.15°) and 48.04° (range: 41.48° – 54.36°) for the inversion-eversion motion. The mean deviation angle for the MHA of the subtalar joint was 11.30° (range: 0.24° – 28.64°) for the dorsiflexed inversion/eversion motion and 10.92° (range: 1.28° – 24.55°) for inversion-eversion. The difference in the orientation of the MHA calculated from the dorsiflexed inversion/eversion and the Inversion-Eversion motion remains small after sectioning all ligaments at the subtalar joint with a mean difference in inclination angle of -4.44° ± 5.03° (range: -10.31° – 2.88°) and a mean difference in deviation angle of 0.38° ± 5.27° (range: -7.03° – 6.43°) across specimen. The calculation of the angle between the dorsiflexed inversion/eversion MHA and the inversion-eversion MHA was 6.77° ranging from 3.59° to 10.38° after cutting all ligaments. One specimen (#9) has a 10° and more difference in inclination angle and angle between the MHA from the dorsiflexed inversion/eversion and inversion-eversion and is the same specimen we found having an abnormal difference after the CFL was sectioned. Without this specimen, the maximum absolute difference in inclination angle would be 8.91°, and the maximum angle between would be 9.42°.

Table 4-9: Inclination angle, deviation angle and the angle between the Mean Helical Axis calculated at the subtalar joint during inversion-eversion (Inv-Ev) and the dorsiflexed inversion/eversion (DF+Inv-Ev) motion in a CFL, cervical and ITCL deficient feet.

Subtalar	Inclination angle (°)		Deviation angle (°)		Angle
Specimen#	DF+Inv-Ev	Inv-Ev	DF+Inv-Ev	Inv-Ev	between (°)
4	43.73	50.40	12.94	16.77	7.15
7	36.78	45.69	28.64	24.55	9.42
9	44.05	54.36	0.24	1.62	10.38
11	44.30	46.04	18.80	12.37	4.85
12	53.15	50.27	1.93	8.96	5.22
13	39.55	41.48	5.26	1.28	3.59
Mean ± SD	43.60 ±5.56	48.04 ± 4.54	11.30 ± 11.01	10.92 ± 9	6.77 ± 2.70
CFL cut	43.89 ±3.74	49.67 ± 4.08	18.16 ± 9.72	19.6 ± 12.02	6.57 ± 3.57
Intact	49.71 ±6.13	54.55 ± 3.38	15.70 ± 11.11	17.47 ±13.62	7.30 ± 4.08

At the ankle joint, the MHA was calculated for plantarflexion-dorsiflexion and inversion-eversion after the CFL and intrinsic ligaments were sectioned (Table 4-10). The difference in the orientation of the MHA calculated from the plantarflexion-dorsiflexion and the inversion-eversion motion remains higher at the ankle joint than the subtalar joint after sectioning all ligaments with a mean difference in inclination angle of 16.57° ± 17.90° (range: -17.12° – 31.30°) and a mean difference in deviation angle of -35.26° ± 27.02° (range: -60.96° – 13.62°) across specimen. The calculation of the angle between the plantarflexion-dorsiflexion MHA and the inversion-eversion MHA showed a high difference in the orientation of the two axes with an average of 53.88° ranging from 22.42° to 89.69°. No apparent pattern is seen in the ankle MHA angular orientation calculated in plantarflexion-dorsiflexion between the intact condition, the CFL deficient foot and CFL, cervical and ITCL deficient foot.

Table 4-10: Inclination angle, deviation angle and angle between the Mean Helical Axis calculated at the ankle joint during inversion-eversion (Inv-Ev) and the plantarflexion-dorsiflexion (PF-DF) in CFL, cervical and ITCL deficient feet.

Ankle	Inclination angle (°)		Deviation angle (°)		Angle
Specimen#	PF-DF	Inv-Ev	PF-DF	Inv-Ev	between (°)
4	31.29	48.41	17.40	55.36	77.27
7	40.75	11.39	3.93	40.60	43.56
9	32.45	1.16	3.72	34.19	47.43
11	32.95	17.46	15.82	2.20	22.42
12	35.55	9.90	18.29	79.26	89.69
13	56.44	41.69	28.24	87.34	42.91
Mean	38.24	21.67	14.57	49.83	53.88
SD	9.53	18.97	9.4	31.31	24.85
CFL mean	33.50	20.72	15.76	56.36	50.96
Intact mean	34.46	28.61	16.10	49.68	57.38

At the hindfoot joint, the MHA was calculated for the dorsiflexed inversion/eversion motion, plantarflexion-dorsiflexion and inversion-eversion after all ligaments were sectioned (Table 4-11).

Table 4-11: Inclination and deviation angles of the Mean Helical Axis calculated at the hindfoot joint during inversion-eversion (Inv-Ev), dorsiflexed inversion/eversion (DF+Inv-Ev) and plantarflexion-dorsiflexion (PF-DF) in CFL, cervical and ITCL deficient feet.

Hindfoot	Inclination angle (°)			Deviation angle (°)		
Specimen#	DF+Inv-Ev	PF-DF	Inv-Ev	DF+Inv-Ev	PF-DF	Inv-Ev
4	32.64	33.32	34.26	0.09	14.34	11.99
7	46.26	33.00	42.16	1.55	7.98	13.56
9	30.11	14.05	40.74	7.06	19.07	24.58
11	35.96	29.45	34.14	16.78	22.23	10.72
12	41.23	37.75	35.94	12.05	30.60	11.16
13	29.35	42.56	24.27	5.12	24.44	1.67
Mean	35.92	31.69	35.25	7.11	19.78	12.28
SD	6.68	9.75	6.34	6.36	7.93	7.34
CFL mean	35.12	26.62	37.91	12.90	22.36	15.82
Intact mean	38.35	28.13	41.28	7.74	24.24	20.76

The differences in the MHA orientation between the subtalar joint and hindfoot joint for the dorsiflexed inversion/eversion motion and inversion-eversion are presented in Figure 4-5 as well as the differences between the MHA orientation of the ankle joint and hindfoot joint for plantarflexion-dorsiflexion and inversion-eversion after cutting all ligaments.

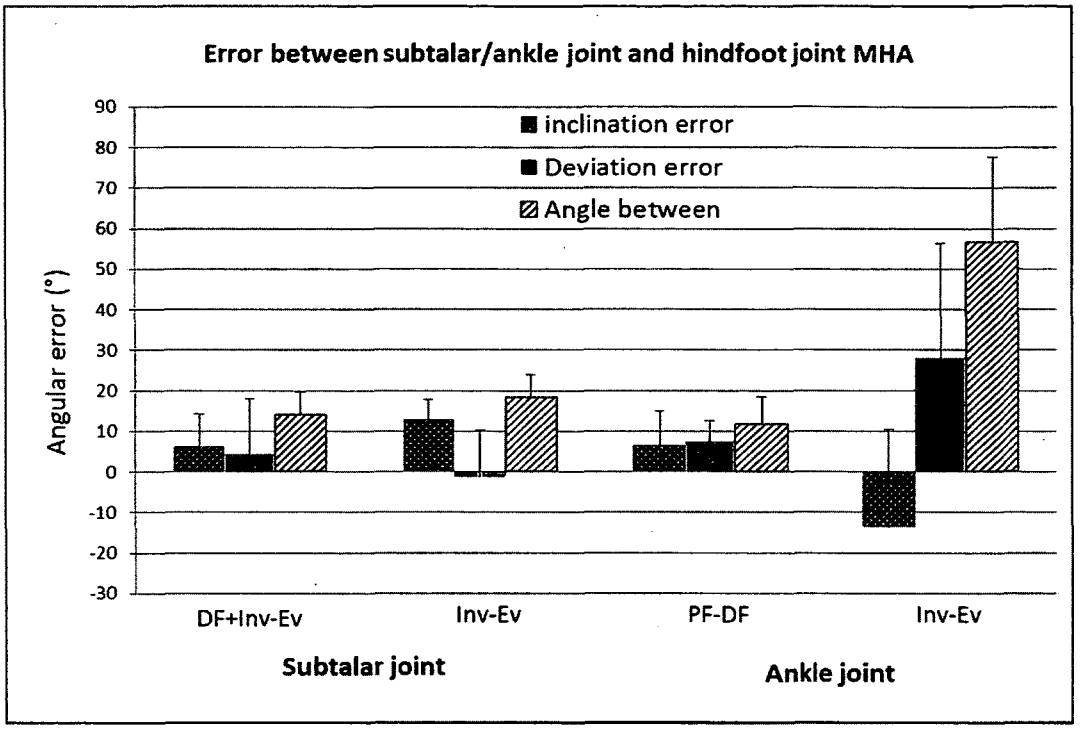

Figure 4-5: Error between the subtalar and hindfoot joint MHA orientation and error between the ankle joint and hindfoot joint MHA orientation represented by the difference in inclination angle, the difference in deviation angle and the angle between the MHA in CFL, cervical and ITCL deficient feet.

The differences in subtalar joint MHA and hindfoot joint MHA orientations for the dorsiflexed inversion/eversion motion can be considered small enough to use the hindfoot MHA as an approximation of the subtalar joint axis for the all cut condition optimization input. Similar differences in ankle joint MHA and hindfoot joint MHA orientations were found after all ligaments were sectioned in plantarflexion-dorsiflexion; therefore, the hindfoot MHA will be used to approximate the ankle joint axis in the optimization.

4.2.3 Optimization

To ensure the optimization algorithm was well implemented, the true rotation matrices representing the motion of the calcaneus with respect to the talus (i.e. subtalar motion) and the motion of the talus with respect to the tibia (i.e. ankle motion) were imported. Then, the output from these rotation matrices to the kinematics obtained from

the motion of the calcaneus and tibia with respect to the lab coordinate system were compared. The kinematics obtained through the optimization and the one from the experiments perfectly fit with a 10^{-6} type of error per frame.

Intact condition

The subtalar and ankle joint axes calculated for each specimen during inversion motion are displayed in Table 4-12 represented by the inclination and deviation angles. The optimized subtalar joint axis orientation looks similar to previous studies that used the same 2-hinge model optimization. The ankle joint axis orientation, on the other hand, has a considerably higher deviation angle compared to the ankle joint axis calculated previously.

Table 4-12: Inclination and deviation angles of the optimized subtalar and ankle joint axes for each specimen.

Specimen #	Inclination angle (°)		Deviation angle (°)	
	Subtalar joint	Ankle joint	Subtalar joint	Ankle joint
4	33.59	10.29	10.73	22.85
7	33.92	10.36	5.25	11.37
9	33.39	2.33	35.06	37.01
11	19.39	6.48	19.96	28.21
12	38.27	4.52	1.27	22.83
13	43.13	4.18	19.68	9.16
Mean ± SD	33.62 ± 7.93	6.36 ± 3.34	15.33 ± 12.25	21.90 ± 10.42
Lewis et al. [90]	36.5 ± 10.75	-1.53 ± 0.76	19.03 ± 8.70	4.07 ± 14.15
Van Den Bogert et al. [93]	35.3 ± 4.8	4.6 ± 7.4	18 ± 16.2	1 ± 15.1

Final values for the optimization objective function (Equation 36) divided by the number of frame were $3.3 \times 10^{-3} - 5.8 \times 10^{-3}$.

The mean inclination angle error between the subtalar joint MHA and the resulting subtalar joint axis from the optimization was 16.09° ± 13.31° (range: 2.73° – 40.67°) for the MHA calculated from the dorsiflexed inversion/eversion motion and 20.93° ± 10.86° (range: 9.86° – 40.78°) for the inversion-eversion MHA (Figure 4-6). The

mean deviation angle error between the subtalar joint MHA and the resulting subtalar joint axis from the optimization was low 0.38° ± 19.38° (range: -23.29° – 26.03°) but with a vast standard deviation for the MHA calculated from the dorsiflexed inversion/eversion motion and similar values occurred with the inversion-eversion MHA with 2.14° ± 21.31° (range: -32.04° – 25.93°). The angle between the subtalar joint MHA and the resulting subtalar joint axis from the optimization were in average 22.18° ± 11.64° (range: 6.77° – 42.79°) for the dorsiflexed inversion/eversion MHA and 25.30° ± 10.02° (range: 12.94° – 41.36°) for the inversion-eversion MHA. The high range in differences between the optimized subtalar joint axis and the MHAs are due to the extremely low optimized inclination angle from specimen #11. Without this specimen the inclination error would not have been higher than 20.93° (instead of 40.78°) and the maximum angle between would have been 32.24° (instead of 42.79°). Individual results can be found in Appendix 3.

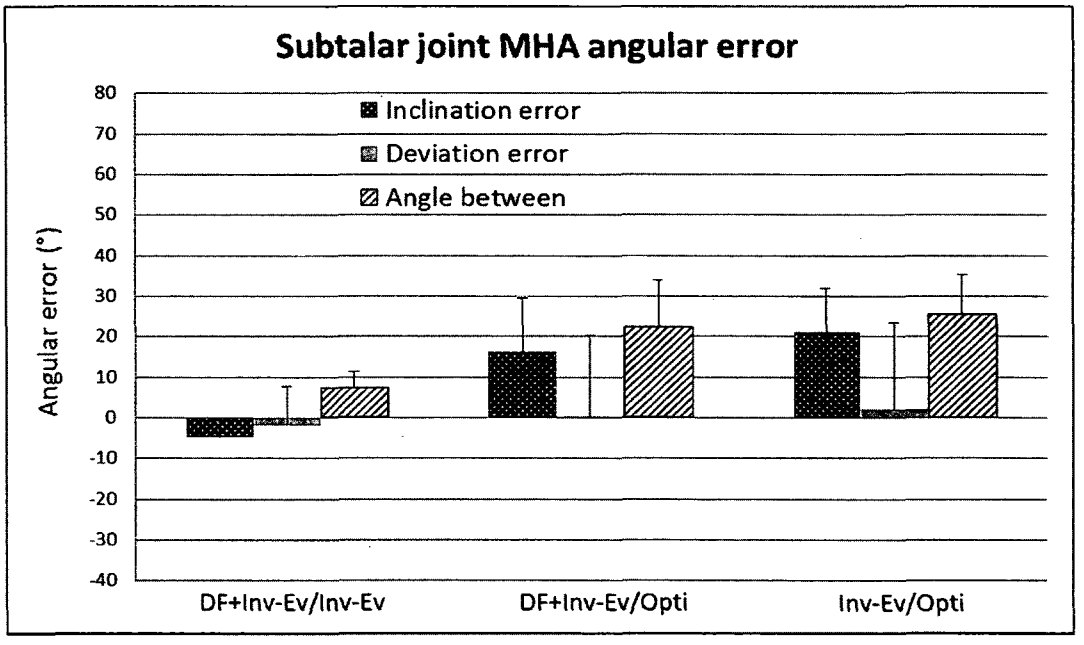

Figure 4-6: Angular error between the subtalar joint MHA calculated from the dorsiflexed inversion/eversion (DF+Inv-Ev) and inversion-eversion (Inv-Ev) and the subtalar joint axis resulting from optimization (Opti). The angular error was represented by the difference in inclination angle, the difference in deviation angle and the angle between the axes.

The mean inclination angle error between the ankle joint MHA and the resulting ankle joint axis from the optimization was 28.10° ± 9.28° (range: 15.79° – 40.49°) for the MHA calculated from plantarflexion-dorsiflexion and 22.25° ± 21.94° (range: -3.16° – 55.26°) for the inversion-eversion MHA (Figure 4-7). The mean deviation angle error between the ankle joint MHA and the resulting angle joint axis from the optimization was lower than the inclination error with -5.81° ± 15.61° (range: -30.94° – 16.36°) for the plantarflexion-dorsiflexion MHA and 27.77° ± 22.54° (range: -2.16° – 58°) for the inversion-eversion MHA. The angle between the ankle joint MHA and the resulting ankle joint axis from the optimization were in average 41.42° ± 10.69° (range: 24.98° – 57.85°) for the plantarflexion-dorsiflexion MHA and 39.35° ± 25.90° (range: 5.78° – 64.81°) for the inversion-eversion MHA. Individual results can be found in Appendix 3.

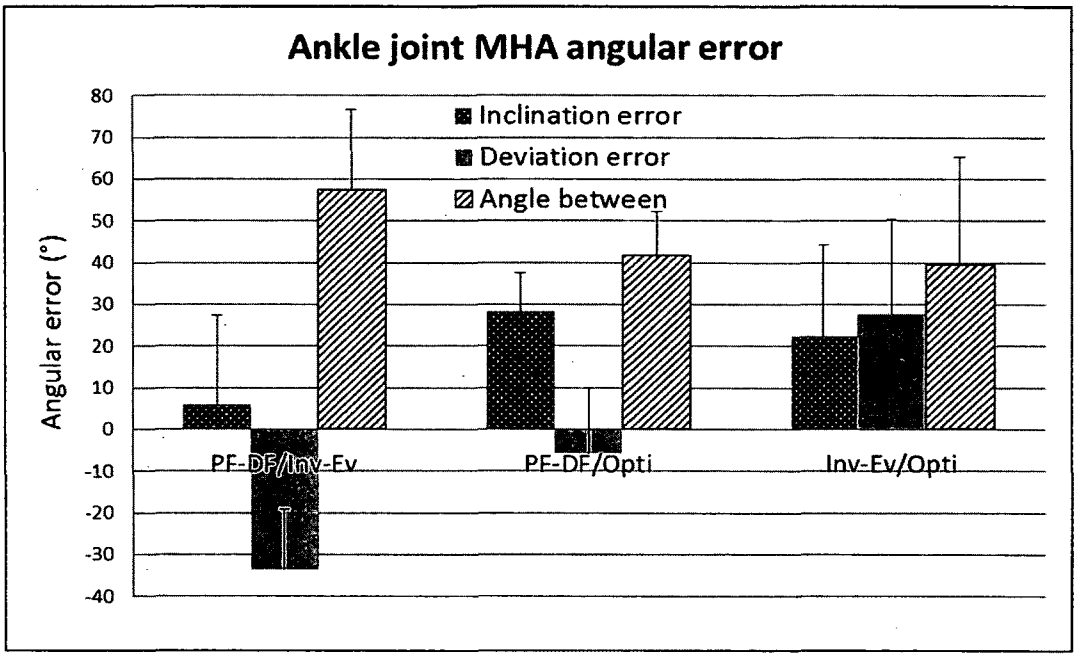

Figure 4-7: Angular error between the ankle joint MHA calculated from plantarflexion-dorsiflexion (PF-DF) and inversion-eversion (Inv-Ev) and the ankle joint axis resulting from optimization. The angular error was represented by the difference in inclination angle, the difference in deviation angle and the angle between the axes.

Angular error magnitudes were smaller for the subtalar joint than for the ankle joint. This could be explained by the high difference in the orientation of the MHA

calculated from plantarflexion-dorsiflexion and from inversion-eversion at the ankle joint as well as the high standard deviation across specimen associated with it.

Calcaneofibular ligament (CFL) cut condition

The subtalar and ankle joint axes calculated for each specimen during inversion motion on CFL deficient feet are displayed in Table 4-13 and are represented by the inclination and deviation angles. The optimized CFL deficient subtalar joint axis inclination angle looks similar to the optimized intact axis; however, the mean deviation angle is 8° higher in the CFL deficient axis than the intact subtalar axis. The CFL deficient ankle joint axis, on the other hand, has a higher inclination angle compared to the intact ankle joint axis with a similar deviation angle.

Table 4-13: Inclination and deviation angles of the optimized subtalar and ankle joint axes for each specimen after sectioning the CFL.

	Inclination angle (°)		Deviation angle (°)	
Specimen #	Subtalar joint	Ankle joint	Subtalar joint	Ankle joint
4	31.37	10.29	58.08	30.91
7	50.32	35.06	19.75	12.07
9	29.12	13.64	7.28	9.20
11	23.20	2.28	14.91	10.16
12	31.75	4.03	20.91	26.42
13	44.90	22.99	25.01	29.91
Mean ± SD	35.11 ± 10.30	14.71 ± 12.43	24.32 ± 17.61	19.78 ± 10.34
Intact	33.62 ± 7.93	6.36 ± 3.34	15.33 ± 12.25	21.90 ± 10.42

Final values for the optimization objective function (Equation 36) were 10 times higher after instability was created with values going from 2.3×10^{-3} to 35×10^{-3}.

The mean inclination angle error between the subtalar joint MHA calculated after sectioning the CFL and the resulting subtalar joint axis from the optimization was 8.78° ± 11.74° (range: -6.20° – 20.21°) for the MHA calculated from the dorsiflexed inversion/eversion motion and 14.56° ± 13.33° (range: -2.66° – 26.67°) for the inversion-eversion MHA (Figure 4-8). The mean deviation angle error between the subtalar joint MHA in CFL deficient feet and the resulting subtalar joint axis from the optimization was

-6.16° ± 13.24° (range: -32.12° – 5.06°) for the MHA calculated from the dorsiflexed inversion/eversion motion and -4.73° ± 15.68° (range: -33.92° – 11.73°) for the inversion-eversion MHA. The angle between the subtalar joint MHA and the resulting subtalar joint axis from the optimization were, on average, 15.05° ± 9.12° (range: 2.21° – 29.98°) for the dorsiflexed inversion/eversion MHA and 19.16° ± 11.45° (range: 3.21° – 33.08°) for the inversion-eversion MHA. Individual results can be found in Appendix 3.

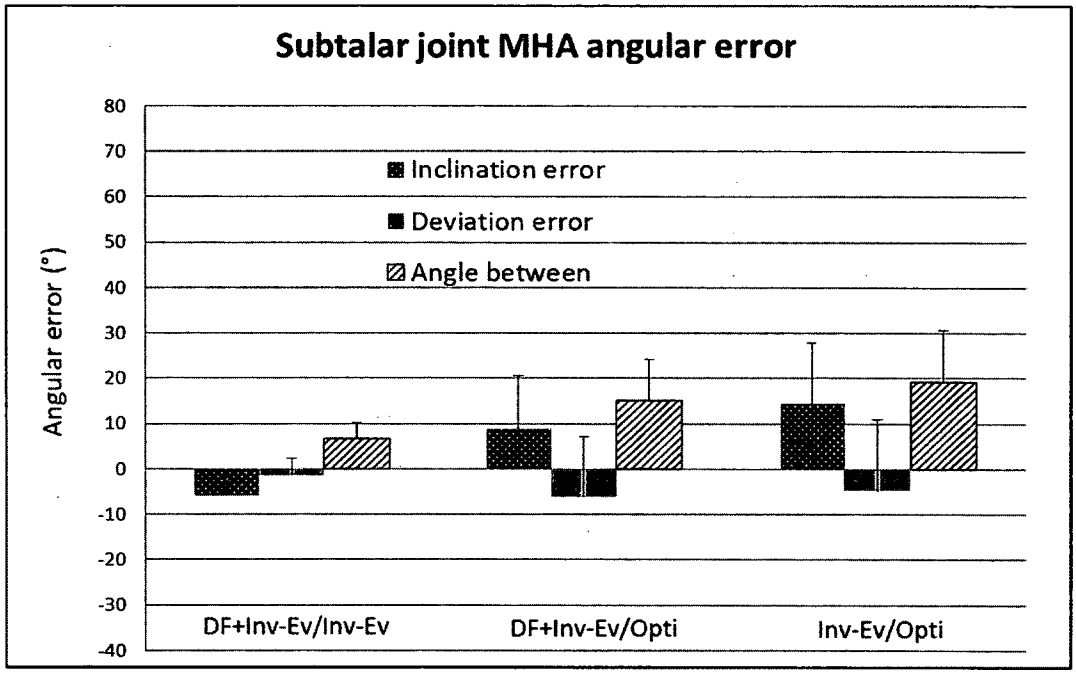

Figure 4-8: Angular error between the subtalar joint MHA calculated from the dorsiflexed inversion/eversion (DF+Inv-Ev) and inversion-eversion (Inv-Ev) and the subtalar joint axis resulting from optimization after sectioning the CFL. The angular error was represented by the difference in inclination angle, the difference in deviation angle and the angle between the axes.

The mean inclination angle error between the ankle joint MHA calculated after sectioning the CFL and the resulting ankle joint axis from the optimization was 18.79° ± 10.32° (range: 1.71° – 34.03°) for the plantarflexion-dorsiflexion MHA and 6° ± 21.64° (range: -30.68° – 27.05°) for the inversion-eversion MHA (Figure 4-9). The mean deviation angle error between the ankle joint MHA in CFL deficient feet and the resulting ankle joint axis from the optimization was -4.02° ± 8.90° (range: -14.01° – 11.57°) for the

plantarflexion-dorsiflexion and 36.58° ± 23.37° (range: 12.98° – 75.92°) for the inversion-eversion MHA. The angle between the CFL deficient ankle joint MHA and the resulting ankle joint axis from the optimization were in average 46.19° ± 24.93° (range: 18.34° – 82.75°) for the plantarflexion-dorsiflexion MHA and 53.59° ± 21.93° (range: 29.33° – 83.52°) for the inversion-eversion MHA. Individual results can be found in Appendix 3.

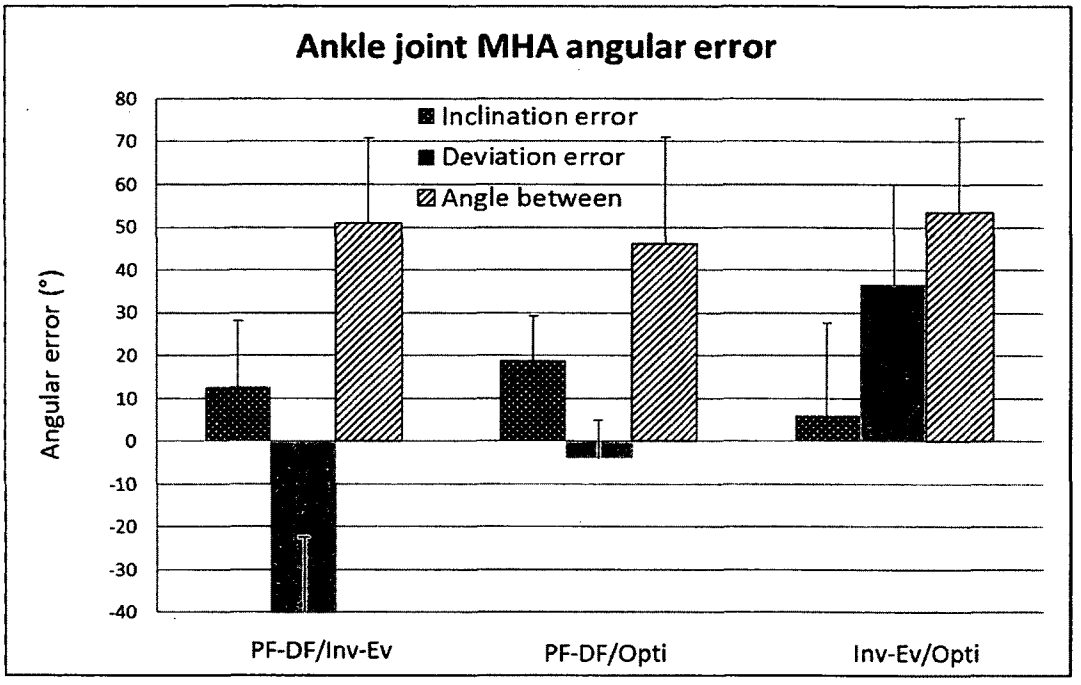

Figure 4-9: Angular error between the ankle joint MHA calculated from plantarflexion-dorsiflexion (PF-DF) and inversion-eversion (Inv-Ev) and the ankle joint axis resulting from optimization after sectioning the CFL. The angular error was represented by the difference in inclination angle, the difference in deviation angle and the angle between the axes.

CFL, cervical and interosseous talocalcaneal ligaments (ALL) cut condition

The subtalar and ankle joint axes inclination and deviation angles for each specimen during inversion motion on CFL, cervical ligament and interosseous talocalcaneal ligament (ITCL) deficient feet (this condition will be more commonly named all ligaments cut) are displayed in Table 4-14. The optimized all ligament cut subtalar joint axis inclination angle looks similar to the optimized intact and the optimized CFL cut axis with a higher standard deviation for the inclination angle. The

ankle joint axis, on the other hand, has a higher inclination angle compared to the intact and CFL cut ankle joint axis with a lower deviation angle.

Table 4-14: Inclination and deviation angles of the optimized subtalar and ankle joint axes for each specimen after sectioning the CFL and intrinsic ligaments.

	Inclination angle (°)		Deviation angle (°)	
Specimen #	Subtalar joint	Ankle joint	Subtalar joint	Ankle joint
4	52.02	36.88	21.86	21.69
7	6.71	23.07	8.59	0.50
9	38.72	23.59	44.22	5.32
11	34.46	5.16	24.01	25.26
12	0.84	1.23	21.29	1.51
13	45.29	41.71	14.46	19.69
Mean ± SD	29.67 ± 21.01	21.94 ± 16.30	22.40 ± 12.12	12.33 ± 11.09
CFL cut	35.11 ± 10.30	14.71 ± 12.43	24.32 ± 17.61	19.78 ± 10.34
Intact	33.62 ± 7.93	6.36 ± 3.34	15.33 ± 12.25	21.90 ± 10.42

Final values for the optimization objective function (Equation 36) were 2 times higher after additional instability was created with values going from 9.2×10^{-3} to 64×10^{-3}.

The mean inclination angle error between the subtalar joint MHA calculated after sectioning all ligaments and the resulting subtalar joint axis from the optimization was 13.92° ± 23.26° (range: -8.28° – 52.31°) for the MHA calculated from the dorsiflexed inversion/eversion motion and 18.37° ± 21.61° (range: -3.81° – 49.43°) for the inversion-eversion MHA (Figure 4-10). The mean deviation angle error between the subtalar joint MHA in CFL, cervical and ITCL deficient feet and the resulting subtalar joint axis from the optimization was -11.10° ± 20.80° (range: -43.98° – 20.05°) for the MHA calculated from the dorsiflexed inversion/eversion motion and -11.48° ± 18.79° (range: -42.59° – 15.96°) for the inversion-eversion MHA. The angle between the subtalar joint MHA and the resulting subtalar joint axis from the optimization were, on average, 30.90° ± 17.59° (range: 10.63° – 56.35°) for the dorsiflexed inversion/eversion MHA and 30.92° ± 16.97° (range: 12.03° – 52.18°) for the inversion-eversion MHA. Individual results can be found in Appendix 3.

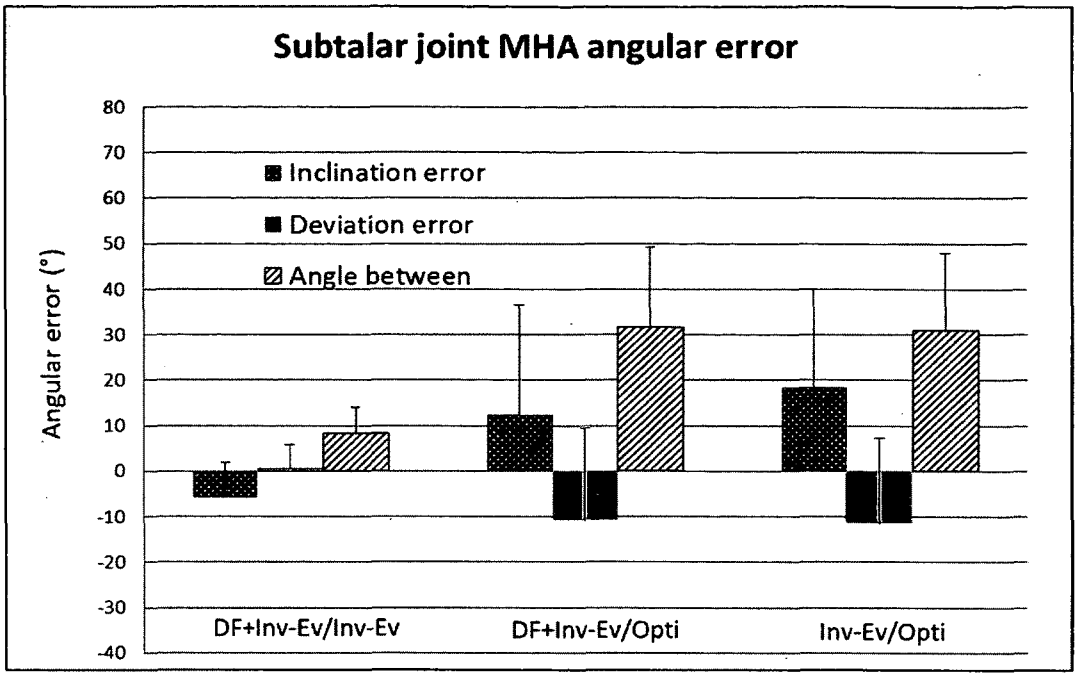

Figure 4-10: Angular error between the subtalar joint MHA calculated from the dorsiflexed inversion/eversion (DF+Inv-Ev) and inversion-eversion (Inv-Ev) and the subtalar joint axis resulting from optimization after sectioning all ligaments. The angular error was represented by the difference in inclination angle, the difference in deviation angle and the angle between the axes.

The mean inclination angle error between the ankle joint MHA calculated after sectioning the intrinsic ligaments in addition to the CFL and the resulting ankle joint axis from the optimization was 16.30° ± 14.11° (range: -5.58° – 34.32°) for the plantarflexion-dorsiflexion MHA and -0.27° ± 14.13° (range: -22.43° – 12.30°) for the inversion-eversion MHA (Figure 4-11). The mean deviation angle error between the ankle joint MHA in CFL, cervical and ITCL deficient feet and the resulting ankle joint axis from the optimization was 2.24° ± 9.45° (range: -9.43° – 16.78°) for the plantarflexion-dorsiflexion and 37.50° ± 35.47° (range: -23.05° – 77.75°) for the inversion-eversion MHA. The angle between the CFL, cervical and ITCL deficient ankle joint MHA and the resulting ankle joint axis from the optimization were in average 45.39° ± 18.12° (range: 17.91° – 68.29°) for the plantarflexion-dorsiflexion MHA and 53.27° ± 20.25° (range: 32.09° – 78.15°) for the inversion-eversion MHA. Individual results can be found in Appendix 3.

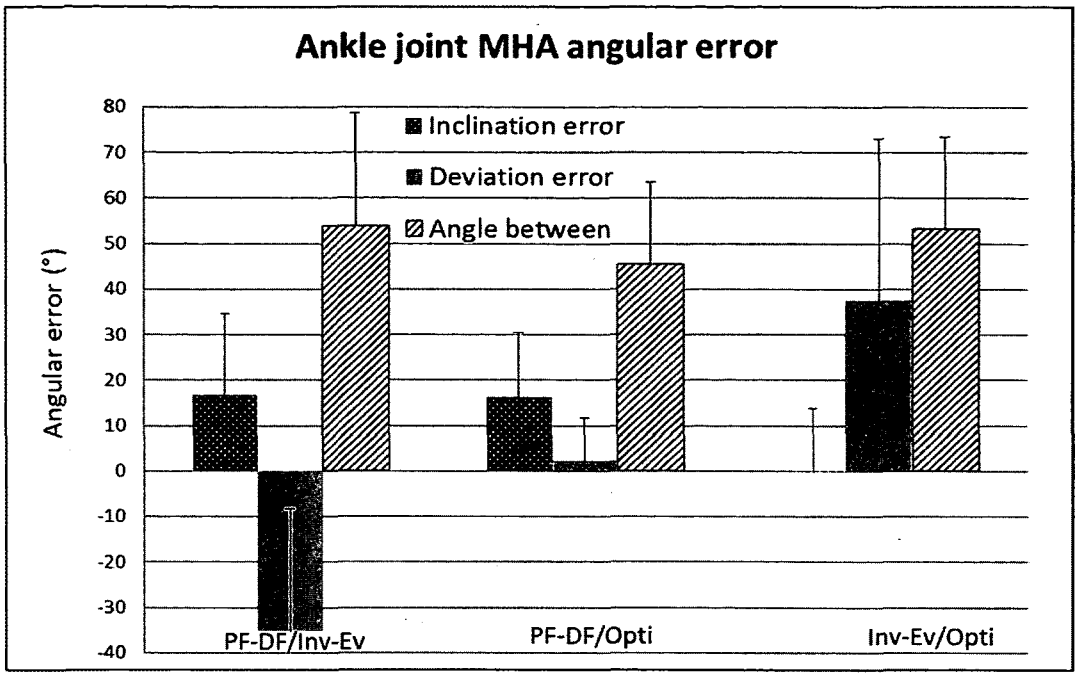

Figure 4-11: Angular error between the ankle joint MHA calculated from plantarflexion-dorsiflexion (PF-DF) and inversion-eversion (Inv-Ev) and the ankle joint axis resulting from optimization after sectioning the CFL, cervical and ITCL. The angular error was represented by the difference in inclination angle, the difference in deviation angle and the angle between the axes.

4.2.4 Statistical Analysis

No significant interaction was found in the inclination and deviation angles between the foot conditions (i.e., intact, CFL cut and all cut) and the subtalar joint axis (i.e., the mean helical axis calculated from inversion-eversion and the subtalar joint axis resulting from the optimization) (Figure 4-12 and Figure 4-13). For the inclination angle, the statistical results were (M=41.776, SE=1.519, F(2)=0.253, p=0.781, CI=[37.872,45.680]) and for the deviation angle (M=18.340, SE=2.060, F(2)=0.918, p=0.431, CI=[13.046,23.635]) . No significant interaction was found at the ankle joint between the foot conditions (i.e., intact, CFL cut and all cut) and the ankle joint axis (i.e., the mean helical axis calculated from inversion-eversion and the ankle joint axis resulting from the optimization) (Figure 4-14 and Figure 4-15). For the inclination angle, the statistical results were (M=19.002, SE=3.723, F(2)=2.62, p=0.122, CI=[9.432,28.572]) and for the deviation angle (M=34.979, SE=4.523, F(2)=0.214, p=0.811, CI=[23.351,46.606]) .

Significant condition main effect was present between the calculated MHA and the optimized subtalar joint axis inclination angle ($F(1)=21.143$, $p=0.006$) and between the calculated MHA and the optimized ankle joint axis deviation angle ($F(1)=29.846$, $p=0.003$). Therefore, the inclination angle between the optimized subtalar joint axis and the mean helical axis calculated from inversion-eversion were significantly different independently of the foot ligamentous condition ($p=0.006$). Also, a significant difference between the optimized ankle joint axis and the mean helical axis deviation angle was found ($p=0.003$).

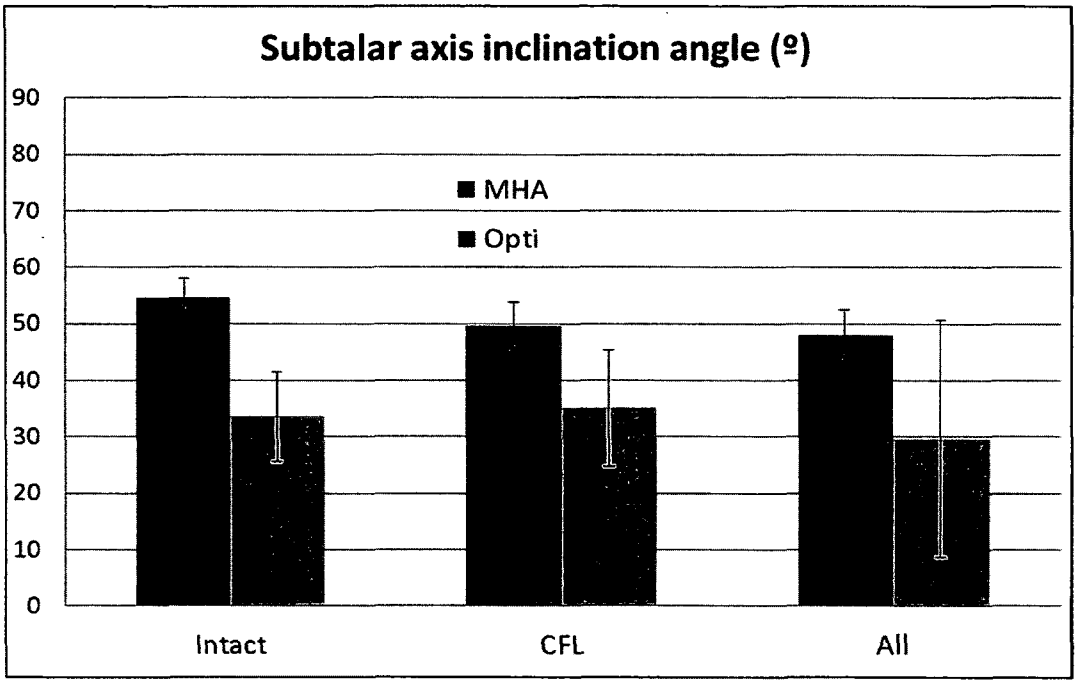

Figure 4-12: Subtalar joint axis inclination angle of the mean helical axis (MHA) calculated from inversion-eversion and the subtalar axis resulting from the optimization (Opti) in the intact condition, after sectioning the CFL and after sectioning all ligaments.

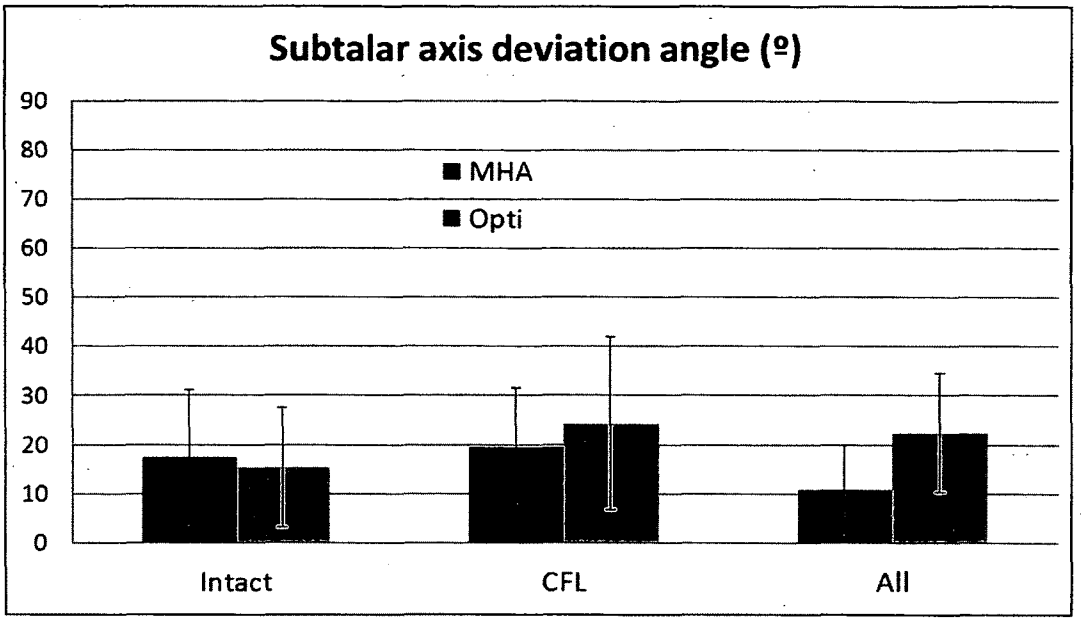

Figure 4-13: Subtalar joint axis deviation angle of the mean helical axis (MHA) calculated from inversion-eversion and the subtalar axis resulting from the optimization (Opti) in the intact condition, after sectioning the CFL and after sectioning all ligaments.

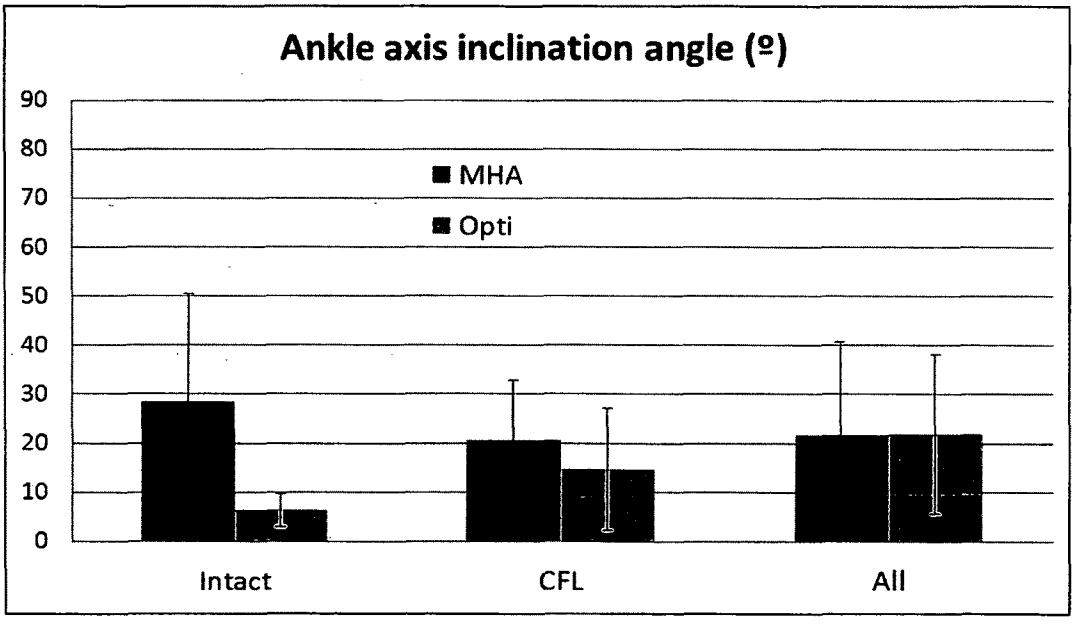

Figure 4-14: Ankle joint axis inclination angle of the mean helical axis (MHA) calculated from inversion-eversion and the subtalar axis resulting from the optimization (Opti) in the intact condition, after sectioning the CFL and after sectioning all ligaments.

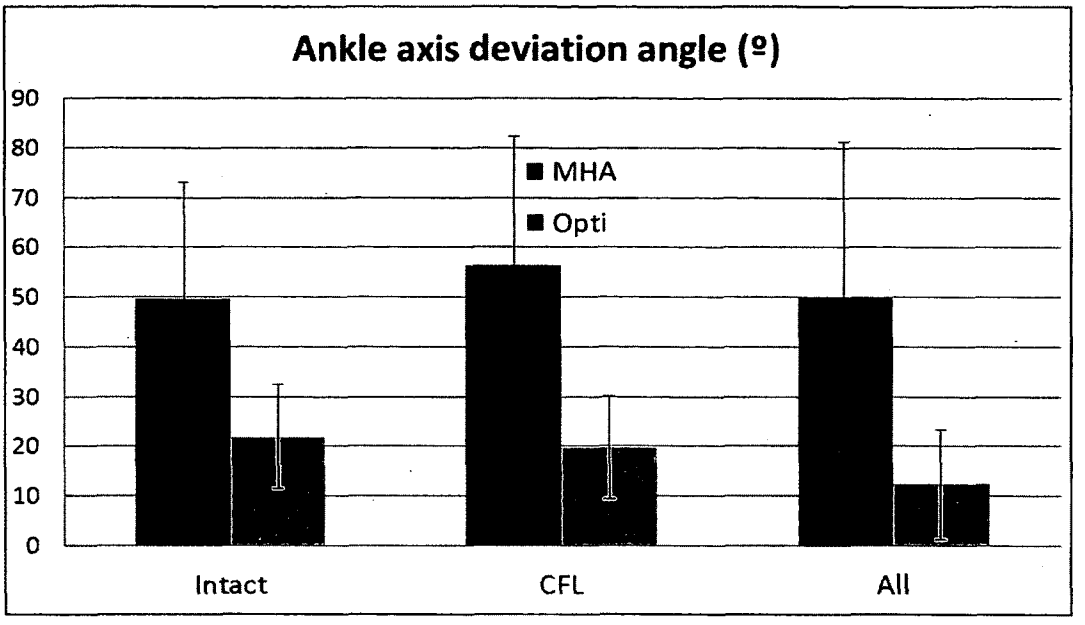

Figure 4-15: Ankle joint axis deviation angle of the mean helical axis (MHA) calculated from inversion-eversion and the subtalar axis resulting from the optimization (Opti) in the intact condition, after sectioning the CFL and after sectioning all ligaments.

5 DISCUSSION

The first purpose of this study was to investigate the three dimensional kinematics of the subtalar joint, ankle and hindfoot (i.e., motion of the calcaneus relative to the tibia) in the presence of isolated subtalar instability created by sectioning the calcaneofibular ligament (CFL) in isolation and in combination with the cervical and interosseous talocalcaneal ligaments (ITCL). The second purpose of this study was to investigate the effect of ankle braces on an intact, CFL deficient foot and after a total rupture of the intrinsic ligaments. The third purpose of this study was to determine if subtalar instability can be detected after applying inversion motion to the foot by only measuring the motion of the calcaneus and tibia. As motion of the talus cannot be isolated, the optimization method will determine the orientation of the subtalar joint axis by using the kinematics of the calcaneus relative to the tibia.

5.1 Investigation of the 3D kinematics of the ankle and subtalar joints

The first purpose of this study was to investigate the three dimensional kinematics of the subtalar joint, ankle and hindfoot (i.e., motion of the calcaneus relative to the tibia). The first step was to assess the kinematics of the subtalar joint, ankle joint and hindfoot in the presence of isolated subtalar instability created by sectioning the calcaneofibular ligament (CFL) in isolation and in combination with the cervical and interosseous talocalcaneal ligaments (ITCL).

The CFL has been described as the main stabilizer of the subtalar joint [19-22] and an important structure in maintaining subtalar joint stability. However, some studies concluded that rupture of the CFL does not affect the stability between the talus and calcaneus but increased ankle joint motion [23-28]. All of the studies which concluded that rupture of the CFL affect ankle joint stability previously damaged the anterior talofibular ligament (ATFL) which is known as the main stabilizer of the ankle joint. The present study confirmed that tear of the CFL alone, leaving the ATFL intact, increases inversion motion at the ankle joint but not at the subtalar joint. In neutral sagittal position,

a 140% increase in inversion laxity was found at the ankle after sectioning the CFL. These results were similar to the previous studies that found a 128% [27], 150% [26] and 168% [24] increase in inversion after sectioning the ATFL and CFL. Only one study [29], to our knowledge, looked at the effect of isolated CFL sectioning on the ankle and found an average of 283% increase in maximum inversion using a closed kinetic chain device [29]. The present investigation and other studies [24, 26, 27] used an open kinetic chain device, which may account for the differences in percentage increase. Subtalar stability was not affected by sectioning of the CFL which contradicts previous studies that reported higher subtalar tilt on roentgenograms [19] and X-Rays [20] but did not demonstrate it with statistics nor report the actual increase. Two studies [21, 22] demonstrated statistically significant increases in subtalar inversion angle after sectioning the CFL alone; however, it was unclear if this is a repeatable result, as it falls within experimental error and may not be clinically detectable. Ankle inversion motion increased by 160% between intact and CFL cut in dorsiflexion, while it only increased by 85% in plantarflexion. Similarly, the ankle-subtalar joint complex was most stable in plantarflexion after the CFL was sectioned in a previous study [23]. Based on the results of this study, it appears injury to the CFL increases ankle inversion motion and creates a more unstable hindfoot in dorsiflexion.

Additional injury created at the cervical ligament and ITCL significantly increased subtalar motion. The ITCL is found in the sinus tarsi and provides a strong stabilization system for the subtalar joint [7, 26, 31-34, 79, 85]. Discrepancy exists in the literature about the percentage of inversion increase after sectioning the ITCL. After applying inversion to the foot, increases in subtalar joint motion ranging from 24%-94% [21, 26] were found in previous studies. A 94% increase in subtalar joint motion was found between intact and the sectioning of the ATFL, CFL, cervical and ITCL [26], while an increase of 24% of subtalar inversion/eversion was found after sectioning the CFL, the lateral talocalcaneal ligament, the inferior extensor retinaculum and the ITCL and a 27% increase after sectioning the bifurcate ligament, the inferior extensor retinaculum and ITCL[21]. The present study found a 32% increase in inversion at the subtalar joint compared to intact with the ankle in the neutral sagittal plane position. Similarly, a 45% increase in inversion at the subtalar joint was measured after sectioning

of the CFL, the cervical ligament and the ITCL [29]. Sectioning the entire ITCL is difficult as it is a dense, broad, and flat ligament with a bilaminar bundle that crosses the sinus tarsi obliquely and laterally [85], which combined with differences in the ligaments that were sectioned, may account for differences in the literature on the rotational increase after the ITCL was cut. Moreover, the present study loaded the Achilles tendon after sectioning it which could be another reason to explain the differences in inversion range of motion at the subtalar joint.

The second step was to evaluate how maximum inversion range of motion of the ankle and subtalar joint is affected by the position of the ankle in the sagittal plane. A 26%, 48% and 34% decrease in the subtalar joint, ankle joint and hindfoot inversion ROM, respectively were found after the foot was placed in dorsiflexion. The ankle joint motion was reduced by half, suggesting that having the foot in maximum dorsiflexion limits ankle motion independently of the foot condition. Dorsiflexion was therefore a good sagittal position to help isolate motion at the subtalar joint. With the foot held in plantarflexion, subtalar joint and hindfoot inversion and eversion ROM were significantly reduced. Plantarflexion did not affect ankle joint ROM because the anterior talofibular ligament intact helps stabilize the ankle in maximum plantarflexion [19]. Isolated injury at the CFL created a more unstable ankle joint in dorsiflexion than in neutral or plantarflexion. Due to its oblique posterior orientation, the CFL is fully stretched when the foot is in full dorsiflexion [78] which makes it the main stabilizer of the hindfoot when the foot is in dorsiflexion.

5.2 Assessment of the effects of a semi-rigid ankle brace

The second purpose of this study was to investigate the effect of ankle braces on an intact, CFL deficient foot and after a total rupture of the intrinsic ligaments. The use of a semi-rigid ankle brace reduced inversion range of motion for all joints. The angle of rotation at the hindfoot decreased of 26%, 34% and 40% when the foot was in neutral, dorsiflexion and plantarflexion, respectively, in the intact condition. When the effects of five different semi-rigid braces were examined in healthy volunteers wearing athletic shoes in inversion, an average of 57% decrease in inversion motion was observed at the

hindfoot [59]. Another in vivo study [52] measured a 48% decrease in inversion with a shoe alone and in combination with a semi-rigid brace. Wearing a shoe with an ankle brace decreased the inversion ROM of 20% compared to wearing a brace barefoot [53] which may explain the large differences between the literature and this study. Additionally, a 28% decrease in inversion using a semi-rigid brace in a simulated barefoot condition (i.e. they cut out the shoe in order to simulate a barefoot condition) was observed [53], which is closer to what the present study observed. Cadaver studies displayed a significant restriction in motion by using ankle stabilizer devices after ligament injuries. For example, a significant decrease in talar tilt and anterior drawer was measured after applying a brace on specimen with ATFL and CFL deficiencies [58]. The range of inversion of three ankle braces was evaluated on intact feet *in vitro* in neutral and 20° plantarflexion [50]. All braces significantly reduced the inversion rotation and positioning the foot in 20° plantarflexion decreased inversion compared to neutral. In the present study a similar pattern was observed with increased restriction of hindfoot inversion with the foot positioned in plantarflexion and smaller inversion stability with the foot in neutral.

Applying the brace to the CFL deficient ankle joint significantly reduced inversion ROM. The brace restricted motion of 46% in neutral, 53% in dorsiflexion and 43% in plantarflexion. The largest increase in ankle inversion after CFL injury occurred when the foot was in dorsiflexion, which is also the position of the CFL deficient braced foot where greatest restriction of ankle motion took place. This suggests that the brace has the most potential to restrict motion where the instability is the greatest. The semi-rigid brace significantly restrained inversion at the subtalar joint as well. A 30%, 36% and 34% of rotation decrease was found after applying a brace in intact, CFL cut and all ligaments cut, respectively. Similarly, a 34% decrease in subtalar inversion after applying the brace on a ligamentous deficient foot (CFL, cervical ligament and ITCL) was observed [29] along with a non-significant 39% decrease in ankle inversion between the ligamentous deficient foot and after applying the brace while the present study found a significant 49% decrease.

5.3 Toward in vivo approximation of the subtalar joint axis

The main goal of this study was to determine if subtalar instability can be detected after applying inversion motion to the foot by only measuring the motion of the calcaneus and tibia. As motion of the talus cannot be isolated, the optimization method will determine the orientation of the subtalar joint axis by using the kinematics of the calcaneus relative to the tibia. However, the optimization method is a two-hinge joint model which requires an initial guess for the orientation of the subtalar joint axis and for the ankle joint axis. In order to find an input as close as possible of the 'true' subtalar joint axis (i.e. the subtalar joint axis from inversion-eversion), a mean helical axis calculated from inversion-eversion with the foot placed in maximum dorsiflexion (dorsiflexed inversion-eversion) was calculated at the hindfoot. This motion passively locks the talus into the ankle mortise and therefore limits ankle joint motion thus allowing for the majority of the motion to occur at the subtalar joint. The 'true' ankle joint axis (i.e. the ankle joint axis from inversion-eversion) was approximated by the hindfoot mean helical axis calculated from plantarflexion-dorsiflexion. The first step of this aim was to ensure that the hindfoot mean helical axis from dorsiflexed inversion-eversion was a good approximation of the 'true' subtalar joint axis by 1) comparing the orientation of the 'true' subtalar joint axis with the mean helical axis calculated at the subtalar joint from dorsiflexed inversion-eversion and 2) comparing the subtalar mean helical axis to the hindfoot mean helical from dorsiflexed inversion-eversion. The second step was to compare the resulting subtalar joint axis and ankle joint axis from the optimization to the 'true' subtalar joint axis and the 'true' ankle joint axis. It was important to determine if the optimization method was capable of approximating the 'true' subtalar joint axis and the 'true' ankle joint axis. The third step was to use the optimization method on a ligamentous deficient hindfoot in order to see if the resulting subtalar and ankle joint axes orientation were capable in detecting instability at the subtalar and ankle joints.

5.3.1 Approximation of the subtalar joint axis and ankle joint axis using the mean helical axis method (MHA) in the intact condition

The first step in this process was to ensure that the subtalar joint mean helical axis (MHA) calculated during dorsiflexed inversion/eversion was similar to the one from inversion-eversion in the intact condition.

The subtalar joint MHA for the inversion-eversion motion (called 'true subtalar joint axis) was described in terms of inclination and deviation angles. These angles help in describing the orientation of a joint axis and make the comparison easier across studies. In inversion-eversion, the mean inclination angle found across specimens was 54.55° (51.71° – 60.17°), and the mean deviation angle was 17.47° (2.77° – 32.31°). These results were similar to the most referenced study that investigated the orientation of the subtalar joint axis [71], which reported a mean inclination angle of 42° (20.5° – 68.5°) and a mean deviation angle of 23° (4° – 47°) in 100 specimens from a static posture. The absolute angular difference between the 'true' subtalar axis and the subtalar MHA approximated from dorsiflexed inversion/eversion was 4.84° for the inclination angle and 6.83° for the deviation angle with an angle between the two axes of 7.3°. These differences were minimal compared to the high inter-specimen variability in the orientation of the subtalar joint axis which was 48° for the inclination angle and 43° for the deviation angle [71].

Because the hindfoot MHA calculated from dorsiflexed inversion/eversion was used as initial guess for the optimization method, the next comparison was to examine the differences between the MHA of the subtalar joint and hindfoot during the dorsiflexed inversion/eversion motion. The absolute angular differences were 11.36° (±3.86°) for the inclination angle and 7.96° (±10.70°) for the deviation angle with an angle between the two axes of 14.61°. The differences between the subtalar and hindfoot MHA from dorsiflexed inversion/eversion were higher than the differences between the 'true' subtalar axis and the subtalar MHA from dorsiflexed inversion/eversion. An average of 3° of ankle motion was found during dorsiflexed inversion/eversion which likely contributed to the difference between the hindfoot and subtalar joint MHA orientations.

When the same technique was used to approximate the subtalar joint axis using the kinematics from the tibia and calcaneus, Lewis et al. found a mean difference in inclination angle of 7.6° and a mean difference in deviation angle of 8.7° between the subtalar and hindfoot MHA but did not report the angle between the two axes [90]. Van Den Bogert et al. [93], who developed a similar optimization algorithm, performed a sensitivity analysis to compare the optimization outcome depending on the initial guesses. After conducting 36 optimizations with different initial guesses, 99% of them converged to the same global minimum, occasionally encountering local minimum leading to high residuals. Therefore, the angular differences between the hindfoot MHA from dorsiflexed inversion/eversion used as initial guess and the 'true' subtalar joint axis are reasonable enough to ensure that the optimization will converge to a global minimum for the specific specimen.

Once the initial guess for the subtalar joint axis was established, the same task was performed for the ankle joint axis. The ankle joint MHA calculated from inversion-eversion (called the 'true' ankle joint axis) was highly different than the ankle joint MHA from plantarflexion. As these two motions occur in two different planes, it was hypothesized that the resulting ankle joint axis would be oriented differently. In plantarflexion-dorsiflexion, the ankle MHA inclination angle was 34.46° and the deviation angle was 16.10°. Compared to the study conducted by Inman et al. [71] (7.3° inclination angle and 6° deviation angle), our ankle axis orientation is more oblique anteriorly and proximally. This difference was explained by Lundberg et al. that demonstrated a 37° difference in inclination angle between the ankle axis calculated in dorsiflexion and the ankle axis calculated from plantarflexion [125]. As the ankle MHA was calculated from both plantarflexion and dorsiflexion, it was reasonable that our ankle joint axis was different than the one from Inman et al. that determined its ankle axis when the foot was static [71]. Lundberg et al. also concluded that the ankle joint axis orientation was highly variable between 20° inversion and 20° eversion and also between individuals which explains the high standard deviation in the ankle MHA orientation from inversion-eversion found in the present study [125]. Even though the plantarflexion-dorsiflexion and inversion-eversion ankle MHA orientation can differ of up to 90°; the

inversion-eversion ankle joint axis cannot be measured in vivo without using imaging, which is time consuming and expensive. Therefore, the MHA from plantarflexion-dorsiflexion was used as an estimate for the inversion-eversion MHA. The absolute angular differences between the ankle and hindfoot MHAs in plantarflexion-dorsiflexion were in the same range as the differences between the subtalar and hindfoot MHAs in the dorsiflexed inversion/eversion motion. Therefore, the hindfoot MHA calculated from the dorsiflexed inversion/eversion motion and from plantarflexion-dorsiflexion will be used as initial guesses for the subtalar joint axis and ankle joint axis orientation respectively in the optimization input.

5.3.2 The resulting subtalar and ankle joint axes from the optimization method

The second step of this aim was to develop a two-hinge joint optimization to estimate the subtalar joint axis and ankle joint axis during an inversion motion applied to the hindfoot based on the kinematics of the calcaneus and the tibia using the approximated subtalar and ankle axes as initial guesses. The ankle and subtalar joint axes resulting from the optimization were similar to those previously reported [90, 93] (Table 5-1).

Table 5-1: Optimized subtalar joint axis inclination and deviation angle in the intact condition from previous studies.

Optimized Subtalar axis	Type of study	Motion optimized	Inclination angle (°)	Deviation angle (°)
Present study	In vitro	Inversion	33.62 ±7.93	15.33 ±12.25
Van den Bogert [93]	In vivo	8 motions[1]	35.3 ±4.8	18 ±16.2
Lewis et al. [90]	Mechanical linkage	plantarflexion/dorsiflexion inversion/eversion, and combinations of these motions	36.5 ±10.75	19.03 ±8.70
	In vitro		14.8 ±1.77	54.27 ±6.36

The optimized subtalar joint axis orientation from the present study was similar to the one determined by Van Den Bogert [93] and the mechanical linkage developed by Lewis et al.[90] but is different from the subtalar axis optimized from cadaver feet motions in the Lewis study. However, Lewis et al. [90] concluded that their optimization method was more accurate when implemented on the mechanical linkage than on the biological specimens. The differences between the actual and optimized axis were too high to validate the optimization in vitro.

Table 5-2: Optimized ankle joint axis inclination and deviation angle in the intact condition from previous studies

Optimized Ankle axis	Type of study	Motion optimized	Inclination angle (°)	Deviation angle (°)
Present study	Cadaver	Inversion	6.36 ±3.34	21.90 ±10.42
Van den Bogert [93]	In vivo	8 motions[1]	4.6 ±7.4	1 ±15.1
Lewis et al. [90]	Mechanical linkage	plantarflexion/dorsiflexion inversion/eversion, and combinations of these motions	-1.53 ±0.76	4.07 ±14.15
	In vitro		-0.17 ±2.96	22.57 ±3.52

[1] (1) plantar-dorsiflexion movement with the subtalar joint in neutral positions, (2) plantar-dorsiflexion with subtalar joint in everted position, (3) plantar-dorsiflexion with subtalar joint in inverted position, (4) pronation-supination movement with the talocrural joint in neutral position, (5) pronation-supination with talocrural joint in dorsiflexed position, (6) pronation-supination with talocrural joint in semi-plantarflexed position, (7) pronation-supination with talocrucral joint in full plantarflexed position, and finally (8) a full range circumduction movement of the foot, being a combined movement of the two joints along the perimeter of the range of motion.

The present optimization method overestimated the ankle inclination and deviation angles compared to previous studies [90, 93] (Table 5-2). These differences could be explained by the motion applied to the foot which was implemented. The present study looked at a single inversion motion while the other studies implemented a combination of frontal (inversion-eversion) and sagittal (plantarflexion-dorsiflexion) plane of motion to account for the two hinge joints motion [90, 93]. Ankle joint motion mainly happens in the sagittal plane while motion assessed in the present study (i.e. inversion) happens only in the frontal plane; therefore the optimization will most likely converge toward an ankle axis representing inversion motion instead of plantarflexion-dorsiflexion.

Because of the nature of the study, the orientation of the MHA of the subtalar joint ('true' subtalar joint axis) can be compared with the optimized subtalar joint axis. The optimized axis had an absolute error of 20.93° ±10.86° in inclination angle, a 16.86° ±10.88° absolute error in deviation angle and a total error magnitude of 25.30° ±10.02°. These average errors were high mainly because of one specimen that had an error of 40.67°, -32.04° and 41.36° in inclination, deviation and total magnitude respectively. These abnormal large errors were due to the specimen's high subtalar MHA inclination angle in inversion-eversion (60.06° compared to a mean of 49.71° across specimen) and its relatively low optimization resulting axis inclination angle (19.39° compared to a mean of 33.13° across specimen). This specimen had the highest subtalar MHA and the lowest resulting axis inclination angle. This specimen was an isolated case as the range of error without including this specimen was (-9.63° to 25.93°); however, only two specimens had their total error magnitude of less than 20°. Lewis et al. had similar errors between the axes resulting from optimization and the mean helical axes of the subtalar joint with more than 20° angular errors for all 3 specimens.

The absolute error magnitude between the ankle joint MHA orientation and the resulting optimization axis was, as expected, very high with a 23.31° ±20.59° error in inclination angle, a 28.5° ±21.43° error in deviation angle and a total error magnitude of 39.35° ±25.90°. These high errors can be explained by the discrepancy in the ankle MHA

orientation during inversion-eversion and the overestimation of the optimized ankle axis inclination and deviation angles.

5.3.3 Optimization method applied to a CFL deficient foot and after sectioning the intrinsic ligaments

The same process, comparing the optimized ankle and subtalar joint axes with the 'true' axes, was applied to the CFL deficient foot alone and after additional injury to the intrinsic ligaments.

The first step was ensure that the MHA calculated at the hindfoot during dorsiflexed inversion/eversion was still an acceptable initial guess for the subtalar joint axis in the optimization method even after instability was present. The differences between the MHA calculated at the subtalar joint during inversion-eversion (called the 'true' subtalar axis) and the optimization initial guess (i.e., the MHA calculated at the hindfoot during dorsiflexed inversion/eversion) were summarized in the Table 5-3.

Table 5-3: Differences between the 'true' subtalar joint axis and the optimization initial guess for the subtalar axis in intact, after sectioning the calcaneofibular ligament (CFL) and after additional sectioning to the cervical ligament and interosseous talocalcaneal ligament (all ligaments cut).

Subtalar joint	Differences in the 'true' subtalar axis and the optimization initial guess		
	Inclination angle	Deviation angle	Angle between the two axes
Intact	16.20° ±5.65	14.86° ±10.67	20.24° ±6.76
CFL cut	14.55° ±6.75	9.3° ±6.47	18.39° ±4.43
All ligaments cut	12.30° ±8.07	9.41° ±8.36	16.29° ±6.37

After adding instability to the hindfoot, the difference in the orientation of the 'true' subtalar joint axis and the hindfoot MHA from the dorsiflexed inversion-eversion motion slightly decreased. While rupture of the CFL increased ankle joint range of motion of 200% when the foot was dorsiflexed, it did not affect the differences in the orientation of the hindfoot MHA from dorsiflexed inversion/eversion and the 'true' subtalar axis. Sectioning the CFL affected the differences between the MHA calculated at the ankle joint during inversion-eversion (called the 'true' ankle axis) and the MHA

calculated at the hindfoot during plantarflexion-dorsiflexion used as initial guess for the ankle joint axis in the optimization method (Table 5-4). These differences were too small to influence the optimization method output at the ankle joint.

Table 5-4: Differences between the 'true' ankle joint axis and the optimization initial guess for the ankle axis in intact, after sectioning the calcaneofibular ligament (CFL) and after additional sectioning to the cervical ligament and interosseous talocalcaneal ligament (all ligaments cut).

Ankle joint	Differences in the 'true' ankle axis and the optimization initial guess		
	Inclination angle	Deviation angle	Angle between the two axes
Intact	18.21° ±14.34	26.04° ±15.44	60° ±16.33
CFL cut	11.82° ±7.34	34° ±20.76	55.34° ±16.22
All ligaments cut	15.05° ±9.19	36.72° ±17.93	56.01° ±20.48

Even after instability was created at the ankle and subtalar joint, the hindfoot MHA from dorsiflexed inversion/eversion was a good approximation of the subtalar joint axis orientation. As for the ankle joint MHA, sectioning the ligaments did not affect its plantarflexion-dorsiflexion orientation and the absolute angular differences between the hindfoot and ankle MHAs in plantarflexion-dorsiflexion were consistent across condition. The hindfoot MHA from plantarflexion-dorsiflexion for each condition was used as an initial guess for the ankle joint axis orientation in the optimization method.

Table 5-5: Inclination and deviation angles of the 'true' and optimized subtalar joint axes in intact, after sectioning the calcaneofibular ligament (CFL) and after additional sectioning to the cervical ligament and interosseous talocalcaneal ligament (all ligaments cut).

Subtalar joint	Optimized subtalar joint axis		'true' subtalar joint axis	
	Inclination angle (°)	Deviation angle (°)	Inclination angle (°)	Deviation angle (°)
Intact	33.62 ± 7.93	15.33 ± 12.25	54.55 ± 3.38	17.47 ± 13.62
CFL cut	35.11 ± 10.30	24.32 ± 17.61	49.67 ± 4.08	19.6 ± 12.02
All ligaments cut	29.67 ± 21.01	21.94 ± 16.30	48.04 ± 4.54	10.92 ± 9

The second step in using the optimization to detect instability at the hindfoot is to ensure that the optimized subtalar and ankle joint axis were consistent with the 'true'

subtalar and ankle joint axes. The CFL deficient and all ligament deficient subtalar joint axes resulting from the optimization had a similar inclination and deviation angle than the intact optimized subtalar joint axis (Table 5-5). While a 4.88° decrease in inclination angle was observed between intact and CFL cut at the 'true' subtalar axis, a 1.49° increase was found at the optimized axis between the same conditions. Also, when a 6.55° decrease in deviation angle was observed between intact and all ligaments cut at the 'true' subtalar axis, a 6.61° increase was found at the optimized subtalar axis between intact and all ligaments cut. These variations between the 'true' subtalar joint axis and optimized subtalar joint axis were confirmed statistically as a significant difference in the inclination angle was found between the 'true' and optimized subtalar joint axis independently of the ligament conditions.

Table 5-6: Inclination and deviation angles of the 'true' and optimized ankle joint axes in intact, after sectioning the calcaneofibular ligament (CFL) and after additional sectioning to the cervical ligament and interosseous talocalcaneal ligament (all ligaments cut).

Ankle joint	Optimized ankle joint axis		'true' ankle joint axis	
	Inclination angle (°)	Deviation angle (°)	Inclination angle (°)	Deviation angle (°)
Intact	6.36 ± 3.34	21.90 ± 10.42	28.61 ± 21.80	49.68 ± 23.45
CFL cut	14.71 ± 12.43	19.78 ± 10.34	20.72 ± 12.10	56.36 ± 26.01
All ligaments cut	21.94 ± 16.30	12.33 ± 11.09	21.67 ± 18.97	49.83 ± 31.31

The optimized ankle joint axis inclination angle increased with instability while its deviation angle decreased with instability (Table 5-6). Comparing the 'true' ankle axis with the optimized ankle axis; a 6.94° decrease in inclination angle was found at the 'true' ankle axis after sectioning all ligaments while a 15.04° increase was found at the optimized inclination angle. Also, a 6.68° increase in deviation angle was found at the 'true' ankle axis after sectioning the CFL alone while a 2.12° increase was found at the optimized ankle axis. Statistical analyses confirmed the differences in the orientation of the 'true' and optimized ankle joint axis with a significant difference found between the 'true' and optimized axes deviation angle at the ankle joint.

Statistical analyses did not demonstrate a change in subtalar or ankle joint axes orientation after instability was created. This could be due to the high inter-specimen variability, especially for the optimized subtalar joint axis compared to the 'true' subtalar joint axis. The standard deviation of the optimized subtalar axis increased with instability with an inter-specimen range of 23.74° in the inclination angle found for the intact condition compared to a range of 51.18° after all ligaments were cut. Likewise, for the optimized ankle joint axis inclination angle with an inter-specimen range of 8.03° found for the intact condition and a 40.48° range after all ligaments were cut. These high variations in the orientation of the optimized axes after instability might be due to the increase in the optimization residuals with a final objective function value 10 times higher after sectioning the CFL and 20 times higher after all ligaments were cut compared to the intact final objective function. This increase in optimization error means that the model kinematics had more difficulty to suit the experimental motion between the calcaneus and tibia. Due to errors brought by the instability at the hindfoot, the optimized subtalar and ankle joint axes are not a good representation of the 'true' subtalar and ankle axes after CFL injury alone and in combination to the cervical and interosseous talocalcaneal ligament. Therefore, the optimization method failed in detecting instability at the subtalar and ankle joints.

5.4 Limitations and future work

Limitations of this study include the cadaveric nature of the investigation as it is difficult to reproduce physiological conditions. First, the end range of motion will be different from a living person that will stop the examiner because of the pain versus a cadaver foot without muscle restriction or painful end point. Moreover, after applying a 3.4NM inversion moment on cadaver feet and on living individuals through an MRI a 3° higher range of inversion was noticed in vitro at the ankle joint with a similar subtalar joint rotation [68]. Second, after an acute sprain patients present signs of swelling, hematoma and pain which would not permit the same level of instability.

Even if the Achilles tendon was loaded, loading additional muscle may have helped in controlling joint motion as a two-hinge joint model and therefore reducing

optimization error. Another possibility to obtain a two-hinge joint motion at the hindfoot would be to place the foot in a closed kinetic chain device. Using a calculated mean helical axis to determine each joint axis conveys additional errors and might have altered the accuracy of the results. An alternative would be to use 3D imaging to determine the subtalar, ankle and hindfoot joint axes in each individual as it may be more representative to compare with the optimized axes.

Another limitation in the study of ankle brace restriction ROM is the use of an open kinetic chain device. People wear ankle braces in a closed kinetic chain condition and therefore might demonstrate different ROM. A future study should look at the differences in kinematics using a closed kinetic chain apparatus. Also, the present study looked at the passive inversion/eversion ROM while braces are used in more dynamic conditions therefore future studies should examine more dynamically induced inversion motion to determine if these results are replicated when functional conditions are simulated.

The optimization method had some limitations too. First, the two-hinge joint model was limited because the ankle and subtalar joint rotate in the three cardinal planes, not just about two hinges. Therefore, the optimization would not be able to find the two joint axes that best represent inversion motion. This limitation was most evident after creating injury to the ligaments which increase the three-dimensional motion of the hindfoot. Second, the optimization algorithm was not adequate if implemented clinically. The multiple transformations and Euler angle extraction for each frame makes the optimization not timely efficient needing at least an hour to converge. A reasonable time would be 10 minutes if the method was employed in clinical settings, however, since this method required additional work before moving to a clinical setting, this limitation does not need to be immediately addressed.

A step further in using the optimization method to differentiate between ankle and subtalar joint instability would be to determine the rotation around the optimized subtalar and ankle axis and how it changes with instability. Another technique to detect instability at the subtalar joint would be to look at the change in the hindfoot mean helical axis from

the dorsiflexed inversion/eversion motion as its orientation was closed to the subtalar mean helical axis. Future work would concentrate on using more than once cycle of dorsiflexed inversion-eversion to calculate the hindfoot mean helical axis until additional cycle no further change the orientation of the mean helical axis.

6 CONCLUSION

As hypothesized, this study demonstrated that ankle joint stability was affected by sectioning the CFL while subtalar motion did not significantly change. Additional sectioning of the cervical ligament and ITCL did not increase ankle joint motion but significantly increased subtalar joint inversion. Half of ankle joint inversion motion was reduced by placing the foot in maximum dorsiflexion; therefore this method could be used to evaluate subtalar joint motion in clinical settings to facilitate in detecting subtalar instability. After injury to the CFL alone or when combined with intrinsic ligaments, semi-rigid ankle braces limit inversion ROM at the ankle and subtalar joint which may be beneficial for clinical populations which exhibit these impairments. A future study would look at a more dynamic situation closer to what occur during an ankle sprain.

The subtalar joint axis resulting in the optimization from intact had similar orientation than the experimental axes which will help in implementing a subject-specific subtalar axis onto gait analysis studies. However, the optimization method was unsuccessful in determining the subtalar joint axis and the ankle joint axis after ligament injury due to arising problems from non-revolute behavior increasing with instability. Using the hindfoot mean helical axis as the subtalar and ankle joint axes initial guess in the optimization input 1) reduced the possibility of non-convergence of the optimization method; 2) reduced the inter-specimen variability compared to another study for the intact condition and 3) obtained more realistic subtalar and ankle joint axes than a previous in-vitro study. A future work would be to modify the optimization algorithm to obtain the angle of rotation around the subtalar joint axis and ankle joint axis instead of the orientation of the resulting axes. Looking at the optimized rotation angle will be less sensitive to the non-revolute behavior of the joints.

This study has several clinical implications which advance our knowledge of the pathomechanics, evaluation, and treatment of subtalar joint instabilities. First, the presence of detectable subtalar instability suggests an injury to the CFL and intrinsic ligaments is likely present. The presence of an isolated CFL tear created minimal changes

in subtalar stability. Second, placing the foot in maximal dorsiflexion range of motion and providing a manual stress test to the hindfoot can reduce motion at the ankle joint may permit instability at the subtalar joint to be more easily detected during evaluation. Future research is needed to determine the sensitivity and specificity of this method of evaluation for identifying subtalar instability but we believe this provides an easily incorporated method to begin progress in this area. Finally, braces designed to restore or maintain stability at the ankle joint can also be beneficial in the presence of subtalar instability. This study focused on a semi-rigid brace for a combination of clinical and methodological reasons. Future studies should determine if lace-up braces which are also commonly used in clinical practice demonstrate similar capabilities at the subtalar joint. While this study was performed in a cadaveric model with several limitations, we believe this study provides several new directions to advance clinical practice associated with subtalar stability.

REFERENCES

1. Levangie, P.K. and C.C. Norkin, *Joint structure and function : a comprehensive analysis*. 2005, Philadelphia, PA: F.A. Davis Co.
2. Wilkerson, G. *Inversion ankle sprains: Seeking optimal support*. 2011; Available from: http://lowerextremityreview.com/article/inversion-ankle-sprains-seeking-optimal-support.
3. McPoil, T.G. and H.G. Knecht, *Biomechanics of the foot in walking: a function approach*. J Orthop Sports Phys Ther, 1985. **7**(2): p. 69-72.
4. Waterman, B.R., et al., *Epidemiology of Ankle Sprain at the United States Military Academy*. The American Journal of Sports Medicine, 2010. **38**(4): p. 797-803.
5. Fong, D.T., et al., *Understanding acute ankle ligamentous sprain injury in sports*. Sports Med Arthrosc Rehabil Ther Technol, 2009. **1**: p. 14.
6. Rubin, G., *The subtalar joint and the symptom of turning over on the ankle: A new method of evaluation utilizing tomography*. American Journal of Orthopedics, 1962: p. 16-19.
7. Pisani, G., P.C. Pisani, and E. Parino, *Sinus tarsi syndrome and subtalar joint instability*. Clin Podiatr Med Surg, 2005. **22**(1): p. 63-77, vii.
8. Borrelli, A.H., *Planar dominance. A major determinant in flatfoot stabilization*. Clin Podiatr Med Surg, 1999. **16**(3): p. 407-21.
9. Michelson, J., et al., *Posterior tibial tendon dysfunction in rheumatoid arthritis*. Foot Ankle Int, 1995. **16**(3): p. 156-61.
10. Wikstrom, E.A., et al., *Self-assessed disability and functional performance in individuals with and without ankle instability: a case control study*. J Orthop Sports Phys Ther, 2009. **39**(6): p. 458-67.
11. Valderrabano, V., et al., *Ligamentous posttraumatic ankle osteoarthritis*. Am J Sports Med, 2006. **34**(4): p. 612-20.
12. Anandacoomarasamy, A. and L. Barnsley, *Long term outcomes of inversion ankle injuries*. Br J Sports Med, 2005. **39**(3): p. e14; discussion e14.
13. Gillespie, H.S. and P. Boucher, *Watson-Jones repair of lateral instability of the ankle*. J Bone Joint Surg Am, 1971. **53**(5): p. 920-4.
14. Hertel, J., et al., *Talocrural and subtalar joint instability after lateral ankle sprain*. Med Sci Sports Exerc, 1999. **31**(11): p. 1501-8.
15. Meyer, J.M., et al., *The subtalar sprain. A roentgenographic study*. Clin Orthop Relat Res, 1988(226): p. 169-73.
16. Riegler, H.F., *Reconstruction for lateral instability of the ankle*. J Bone Joint Surg Am, 1984. **66**(3): p. 336-9.
17. Chrisman, O.D. and G.A. Snook, *Reconstruction of lateral ligament tears of the ankle. An experimental study and clinical evaluation of seven patients treated by a new modification of the Elmslie procedure*. J Bone Joint Surg Am, 1969. **51**(5): p. 904-12.
18. Keefe, D.T. and S.L. Haddad, *Subtalar instability. Etiology, diagnosis, and management*. Foot Ankle Clin, 2002. **7**(3): p. 577-609.
19. Leonard, M.H., *Injuries of the lateral ligaments of the ankle; a clinical and experimental study*. J Bone Joint Surg Am, 1949. **31A**(2): p. 373-7.

20. Laurin, C.A., R. Ouellet, and R. St-Jacques, *Talar and subtalar tilt: an experimental investigation.* Can J Surg, 1968. **11**(3): p. 270-9.
21. Weindel, S., et al., *Subtalar instability: a biomechanical cadaver study.* Arch Orthop Trauma Surg, 2010. **130**(3): p. 313-9.
22. Kjaersgaard-Andersen, P., J.O. Wethelund, and S. Nielsen, *Lateral talocalcaneal instability following section of the calcaneofibular ligament: a kinesiologic study.* Foot Ankle, 1987. **7**(6): p. 355-61.
23. Hollis, J.M., R.D. Blasier, and C.M. Flahiff, *Simulated lateral ankle ligamentous injury. Change in ankle stability.* Am J Sports Med, 1995. **23**(6): p. 672-7.
24. Rosenbaum, D., et al., *Tenodeses destroy the kinematic coupling of the ankle joint complex. A three-dimensional in vitro analysis of joint movement.* J Bone Joint Surg Br, 1998. **80**(1): p. 162-8.
25. Cass, J.R., B.F. Morrey, and E.Y. Chao, *Three-dimensional kinematics of ankle instability following serial sectioning of lateral collateral ligaments.* Foot Ankle, 1984. **5**(3): p. 142-9.
26. Choisne, J., et al., *Influence of kinematic analysis methods on detecting ankle and subtalar joint instability.* J Biomech, 2012. **45**(1): p. 46-52.
27. Ringleb, S.I., et al., *The effect of ankle ligament damage and surgical reconstructions on the mechanics of the ankle and subtalar joints revealed by three-dimensional stress MRI.* J Orthop Res, 2005. **23**(4): p. 743-9.
28. Martin, L.P., et al., *Elongation behavior of calcaneofibular and cervical ligaments in a closed kinetic chain: pathomechanics of lateral hindfoot instability.* Foot Ankle Int, 2002. **23**(6): p. 515-20.
29. Kamiya, T., et al., *Mechanical stability of the subtalar joint after lateral ligament sectioning and ankle brace application: a biomechanical experimental study.* Am J Sports Med, 2009. **37**(12): p. 2451-8.
30. Fujii, T., et al., *Ankle stability in simulated lateral ankle ligament injuries.* Foot Ankle Int, 2010. **31**(6): p. 531-7.
31. Kjaersgaard-Andersen, P., et al., *The stabilizing effect of the ligamentous structures in the sinus and canalis tarsi on movements in the hindfoot. An experimental study.* Am J Sports Med, 1988. **16**(5): p. 512-6.
32. Knudson, G.A., et al., *Subtalar joint stability. Talocalcaneal interosseous ligament function studied in cadaver specimens.* Acta Orthop Scand, 1997. **68**(5): p. 442-6.
33. Tochigi, Y., et al., *Influence of the interosseous talocalcaneal ligament injury on stability of the ankle-subtalar joint complex--a cadaveric experimental study.* Foot Ankle Int, 2000. **21**(6): p. 486-91.
34. Tochigi, Y., et al., *The role of the interosseous talocalcaneal ligament in subtalar joint stability.* Foot Ankle Int, 2004. **25**(8): p. 588-96.
35. Kerkhoffs, G.M., L. Blankevoort, and C.N. van Dijk, *A measurement device for anterior laxity of the ankle joint complex.* Clin Biomech (Bristol, Avon), 2005. **20**(2): p. 218-22.
36. Pearce, T.J. and R.E. Buckley, *Subtalar joint movement: clinical and computed tomography scan correlation.* Foot Ankle Int, 1999. **20**(7): p. 428-32.

37. Christensen, J.C., G.L. Dockery, and J.M. Schuberth, *Evaluation of ankle ligamentous insufficiency using the Telos ankle stress apparatus.* J Am Podiatr Med Assoc, 1986. **76**(9): p. 527-31.
38. Cass, J.R. and H. Settles, *Ankle instability: in vitro kinematics in response to axial load.* Foot Ankle Int, 1994. **15**(3): p. 134-40.
39. Harper, M.C., *Stress radiographs in the diagnosis of lateral instability of the ankle and hindfoot.* Foot Ankle, 1992. **13**(8): p. 435-8.
40. Frost, S.C. and A. Amendola, *Is stress radiography necessary in the diagnosis of acute or chronic ankle instability?* Clin J Sport Med, 1999. **9**(1): p. 40-5.
41. Broden, B., *Roentgen examination of the subtaloid joint in fractures of the calcaneus.* Acta radiol, 1949. **31**(1): p. 85-91.
42. Louwerens, J.W., et al., *Stress radiography of the talocrural and subtalar joints.* Foot Ankle Int, 1995. **16**(3): p. 148-55.
43. Sijbrandij, E.S., et al., *Assessing the subtalar joint: the Broden view revisited.* Foot Ankle Int, 2001. **22**(4): p. 329-34.
44. van Hellemondt, F.J., et al., *Stress radiography and stress examination of the talocrural and subtalar joint on helical computed tomography.* Foot Ankle Int, 1997. **18**(8): p. 482-8.
45. Sheehan, F.T., A.R. Seisler, and K.L. Siegel, *In vivo talocrural and subtalar kinematics: a non-invasive 3D dynamic MRI study.* Foot Ankle Int, 2007. **28**(3): p. 323-35.
46. Ishii, T., et al., *Subtalar stress radiography using forced dorsiflexion and supination.* J Bone Joint Surg Br, 1996. **78**(1): p. 56-60.
47. Thermann, H., H. Zwipp, and H. Tscherne, *Treatment algorithm of chronic ankle and subtalar instability.* Foot Ankle Int, 1997. **18**(3): p. 163-9.
48. Lynch, S.A. and P.A. Renstrom, *Treatment of acute lateral ankle ligament rupture in the athlete. Conservative versus surgical treatment.* Sports Med, 1999. **27**(1): p. 61-71.
49. Shapiro, M.S., et al., *Ankle sprain prophylaxis: an analysis of the stabilizing effects of braces and tape.* Am J Sports Med, 1994. **22**(1): p. 78-82.
50. Tohyama, H., et al., *Stabilizing effects of ankle bracing under a combination of inversion and axial compression loading.* Knee Surg Sports Traumatol Arthrosc, 2006. **14**(4): p. 373-8.
51. Lee, W.C., et al., *Comparison of custom-moulded ankle orthosis with hinged joints and off-the-shelf ankle braces in preventing ankle sprain in lateral cutting movements.* Prosthet Orthot Int, 2012. **36**(2): p. 190-5.
52. Zhang, S., et al., *Efficacy of an ankle brace with a subtalar locking system in inversion control in dynamic movements.* J Orthop Sports Phys Ther, 2009. **39**(12): p. 875-83.
53. Eils, E., et al., *Passive stability characteristics of ankle braces and tape in simulated barefoot and shoe conditions.* Am J Sports Med, 2007. **35**(2): p. 282-7.
54. Tang, Y.M., et al., *A study of semi-rigid support on ankle supination sprain kinematics.* Scand J Med Sci Sports, 2010. **20**(6): p. 822-6.
55. Siegler, S., et al., *The three-dimensional passive support characteristics of ankle braces.* J Orthop Sports Phys Ther, 1997. **26**(6): p. 299-309.

56. Ubell, M.L., et al., *The effect of ankle braces on the prevention of dynamic forced ankle inversion.* Am J Sports Med, 2003. **31**(6): p. 935-40.
57. Nishikawa, T., et al., *Protection and performance effects of ankle bracing.* Int Orthop, 2000. **24**(5): p. 285-8.
58. Bruns, J. and H. Staerk, *Mechanical ankle stabilisation due to the use of orthotic devices and peroneal muscle strength. An experimental investigation.* Int J Sports Med, 1992. **13**(8): p. 611-5.
59. Eils, E., et al., *Comprehensive testing of 10 different ankle braces. Evaluation of passive and rapidly induced stability in subjects with chronic ankle instability.* Clin Biomech (Bristol, Avon), 2002. **17**(7): p. 526-35.
60. Thonnard, J.L., et al., *Stability of the braced ankle. A biomechanical investigation.* Am J Sports Med, 1996. **24**(3): p. 356-61.
61. Beimers, L., et al., *In-vivo range of motion of the subtalar joint using computed tomography.* J Biomech, 2008. **41**(7): p. 1390-7.
62. Lundberg, A., et al., *Kinematics of the ankle/foot complex: plantarflexion and dorsiflexion.* Foot Ankle, 1989. **9**(4): p. 194-200.
63. Lundberg, A. and O.K. Svensson, *The axes of rotation of the talocalcaneal and talonavicular joints.* The Foot, 1993. **3**(2): p. 65-70.
64. Lundberg, A., et al., *Kinematics of the ankle/foot complex--Part 2: Pronation and supination.* Foot Ankle, 1989. **9**(5): p. 248-53.
65. Lundberg, A., et al., *Kinematics of the ankle/foot complex--Part 3: Influence of leg rotation.* Foot Ankle, 1989. **9**(6): p. 304-9.
66. Sheehan, F.T., *The instantaneous helical axis of the subtalar and talocrural joints: a non-invasive in vivo dynamic study.* J Foot Ankle Res, 2010. **3**: p. 13.
67. Siegler, S., J. Chen, and C.D. Schneck, *The three-dimensional kinematics and flexibility characteristics of the human ankle and subtalar joints--Part I: Kinematics.* J Biomech Eng, 1988. **110**(4): p. 364-73.
68. Siegler, S., et al., *Mechanics of the ankle and subtalar joints revealed through a 3D quasi-static stress MRI technique.* J Biomech, 2005. **38**(3): p. 567-78.
69. Close, J.R., et al., *The function of the subtalar joint.* Clin Orthop Relat Res, 1967. **50**: p. 159-79.
70. Piazza, S.J., *Mechanics of the subtalar joint and its function during walking.* Foot Ankle Clin, 2005. **10**(3): p. 425-42, v.
71. Inman, V.T., *The joints of the ankle.* 1976, Baltimore: Williams and Wilkins.
72. Brantigan, J.W., L.R. Pedegana, and F.G. Lippert, *Instability of the subtalar joint. Diagnosis by stress tomography in three cases.* J Bone Joint Surg Am, 1977. **59**(3): p. 321-4.
73. Hyer, C.F., et al., *Evaluation of the anterior and middle talocalcaneal articular facets and the Evans osteotomy.* J Foot Ankle Surg, 2002. **41**(6): p. 389-93.
74. Karlsson, J., B.I. Eriksson, and P.A. Renstrom, *Subtalar ankle instability. A review.* Sports Med, 1997. **24**(5): p. 337-46.
75. Harper, M.C., *The lateral ligamentous support of the subtalar joint.* Foot Ankle, 1991. **11**(6): p. 354-8.
76. Zwipp, H., S. Rammelt, and R. Grass, *Ligamentous injuries about the ankle and subtalar joints.* Clin Podiatr Med Surg, 2002. **19**(2): p. 195-229, v.

77. Leardini, A., et al., *The role of the passive structures in the mobility and stability of the human ankle joint: a literature review.* Foot Ankle Int, 2000. **21**(7): p. 602-15.
78. Bonnel, F., et al., *Chronic ankle instability: biomechanics and pathomechanics of ligaments injury and associated lesions.* Orthop Traumatol Surg Res, 2010. **96**(4): p. 424-32.
79. Sarrafian, S.K., *Biomechanics of the subtalar joint complex.* Clin Orthop Relat Res, 1993(290): p. 17-26.
80. Manter, J.T., *Movements of the subtalar and transverse tarsal joints.* The Anatomical Record, 1941. **80**(4): p. 397-410.
81. Leardini, A., et al., *Kinematics of the human ankle complex in passive flexion; a single degree of freedom system.* J Biomech, 1999. **32**(2): p. 111-8.
82. Leardini, A., R. Stagni, and J.J. O'Connor, *Mobility of the subtalar joint in the intact ankle complex.* J Biomech, 2001. **34**(6): p. 805-9.
83. Tuijthof, G.J., et al., *Determination of consistent patterns of range of motion in the ankle joint with a computed tomography stress-test.* Clin Biomech (Bristol, Avon), 2009. **24**(6): p. 517-23.
84. Trouilloud, *Variations du ligament calcaneofibulaire. Application a la cinematique de la cheville.* Bull Assoc Anat, 1988. **72**: p. 31-35.
85. Barg, A., et al., *Subtalar instability: diagnosis and treatment.* Foot Ankle Int, 2012. **33**(2): p. 151-60.
86. Root, M.L., *Axis of motion of the subtalar joint: An anatomical study.* Journal of the American Podiatry Association, 1966. **56**(4): p. 149-155.
87. Engsberg, J.R., *A biomechanical analysis of the talocalcaneal joint--in vitro.* J Biomech, 1987. **20**(4): p. 429-42.
88. Lewis, G.S., K.A. Kirby, and S.J. Piazza, *Determination of subtalar joint axis location by restriction of talocrural joint motion.* Gait Posture, 2007. **25**(1): p. 63-9.
89. Lewis, G.S., et al., *In vivo tests of an improved method for functional location of the subtalar joint axis.* J Biomech, 2009. **42**(2): p. 146-51.
90. Lewis, G.S., H.J. Sommer, 3rd, and S.J. Piazza, *In vitro assessment of a motion-based optimization method for locating the talocrural and subtalar joint axes.* J Biomech Eng, 2006. **128**(4): p. 596-603.
91. Kirby, K.A., *Methods for determination of positional variations in the subtalar joint axis.* J Am Podiatr Med Assoc, 1987. **77**(5): p. 228-34.
92. Phillips, R.D. and R.H. Lidtke, *Clinical determination of the linear equation for the subtalar joint axis.* J Am Podiatr Med Assoc, 1992. **82**(1): p. 1-20.
93. van den Bogert, A.J., G.D. Smith, and B.M. Nigg, *In vivo determination of the anatomical axes of the ankle joint complex: an optimization approach.* J Biomech, 1994. **27**(12): p. 1477-88.
94. Freeman, M.A., *Instability of the foot after injuries to the lateral ligament of the ankle.* J Bone Joint Surg Br, 1965. **47**(4): p. 669-77.
95. Bahr, R., et al., *Mechanics of the anterior drawer and talar tilt tests. A cadaveric study of lateral ligament injuries of the ankle.* Acta Orthop Scand, 1997. **68**(5): p. 435-41.

96. Fujii, T., et al., *The manual stress test may not be sufficient to differentiate ankle ligament injuries.* Clin Biomech (Bristol, Avon), 2000. **15**(8): p. 619-23.
97. Lapointe, S.J., et al., *Changes in the flexibility characteristics of the ankle complex due to damage to the lateral collateral ligaments: an in vitro and in vivo study.* J Orthop Res, 1997. **15**(3): p. 331-41.
98. Ahovuo, J., E. Kaartinen, and P. Slatis, *Diagnostic value of stress radiography in lesions of the lateral ligaments of the ankle.* Acta radiol, 1988. **29**(6): p. 711-4.
99. Becker, H.P., et al., *Stress diagnostics of the sprained ankle: evaluation of the anterior drawer test with and without anesthesia.* Foot Ankle, 1993. **14**(8): p. 459-64.
100. Blanshard, K.S., et al., *A radiological analysis of lateral ligament injuries of the ankle.* Clin Radiol, 1986. **37**(3): p. 247-51.
101. Chandnani, V.P., et al., *Chronic ankle instability: evaluation with MR arthrography, MR imaging, and stress radiography.* Radiology, 1994. **192**(1): p. 189-94.
102. Johannsen, A., *Radiological diagnosis of lateral ligament lesion of the ankle. A comparison between talar tilt and anterior drawer sign.* Acta Orthop Scand, 1978. **49**(3): p. 295-301.
103. Raatikainen, T., M. Putkonen, and J. Puranen, *Arthrography, clinical examination, and stress radiograph in the diagnosis of acute injury to the lateral ligaments of the ankle.* Am J Sports Med, 1992. **20**(1): p. 2-6.
104. van Dijk, C.N., et al., *Diagnosis of ligament rupture of the ankle joint. Physical examination, arthrography, stress radiography and sonography compared in 160 patients after inversion trauma.* Acta Orthop Scand, 1996. **67**(6): p. 566-70.
105. Rijke, A.M. and P.A. Vierhout, *Graded stress radiography in acute injury to the lateral ligaments of the ankle.* Acta radiol, 1990. **31**(2): p. 151-5.
106. Baker, R., *ISB recommendation on definition of joint coordinate systems for the reporting of human joint motion-part I: ankle, hip and spine.* J Biomech, 2003. **36**(2): p. 300-2; author reply 303-4.
107. Saltzman, C.L., et al., *Reliability of standard foot radiographic measurements.* Foot Ankle Int, 1994. **15**(12): p. 661-5.
108. Kato, T., *The diagnosis and treatment of instability of the subtalar joint.* J Bone Joint Surg Br, 1995. **77**(3): p. 400-6.
109. Löfvenberg, R., J. Kärrholm, and A. Lundberg, *Subtalar stability in chronic lateral instability of the ankle.* The Foot, 1992. **2**(1): p. 39-43.
110. Yamamoto, H., et al., *Subtalar instability following lateral ligament injuries of the ankle.* Injury, 1998. **29**(4): p. 265-8.
111. Hertel, J., *Immobilisation for acute severe ankle sprain.* Lancet, 2009. **373**(9663): p. 524-6.
112. Bruns, J., J. Scherlitz, and S. Luessenhop, *The stabilizing effect of orthotic devices on plantar flexion/dorsal extension and horizontal rotation of the ankle joint. An experimental cadaveric investigation.* Int J Sports Med, 1996. **17**(8): p. 614-8.
113. Dhakal, A., *Develpment of a technique to diagnose subtalar joint*, in *Mechanical engineering department*2008, Old Dominion University: Norfolk. p. 155.
114. Dhakal, A., *Development of a technique to diagnose subtalar joint instability*, in *Mechanical Engineering*2008, Old Dominion University. p. 151.

115. Wu, G., et al., *ISB recommendation on definitions of joint coordinate system of various joints for the reporting of human joint motion--part I: ankle, hip, and spine.* Journal of Biomechanics, 2002. **35**(4): p. 543-548.
116. Schon, L.C., T.O. Clanton, and D.E. Baxter, *Reconstruction for subtalar instability: a review.* Foot Ankle, 1991. **11**(5): p. 319-25.
117. Wu, G., et al., *ISB recommendation on definitions of joint coordinate system of various joints for the reporting of human joint motion--part I: ankle, hip, and spine. International Society of Biomechanics.* J Biomech, 2002. **35**(4): p. 543-8.
118. Zatsiorsky, V.M., *Kinematics of human motion.* 1998, Champaign, IL: Human Kinetics.
119. Cappozzo, A. and N. Berme, *Rigid body mechanics as applied to human movement studies*, in *Biomechanics of human movement : applications in rehabilitation, sports and ergonomics*, A. Capozzo, Editor. 1990, Bertec Corporation: Worthington, Ohio. p. 89-102.
120. Kinzel, G.L., A.S. Hall, Jr., and B.M. Hillberry, *Measurement of the total motion between two body segments. I. Analytical development.* J Biomech, 1972. **5**(1): p. 93-105.
121. Spoor, C.W. and F.E. Veldpaus, *Rigid body motion calculated from spatial co-ordinates of markers.* J Biomech, 1980. **13**(4): p. 391-3.
122. Woltring, H.J., *Representation and calculation of 3-D joint movement.* Human Movement Science, 1991. **10**(5): p. 603-616.
123. Woltring, H.J., *3-D attitude representation of human joints: a standardization proposal.* J Biomech, 1994. **27**(12): p. 1399-414.
124. Sommer, H.J. and N.R. Miller, *A Technique for Kinematic Modeling of Anatomical Joints.* Journal of Biomechanical Engineering-Transactions of the Asme, 1980. **102**(4): p. 311-317.
125. Lundberg, A., et al., *The axis of rotation of the ankle joint.* J Bone Joint Surg Br, 1989. **71**(1): p. 94-9.

APPENDIX 1: OPTIMIZATION ALGORITHM

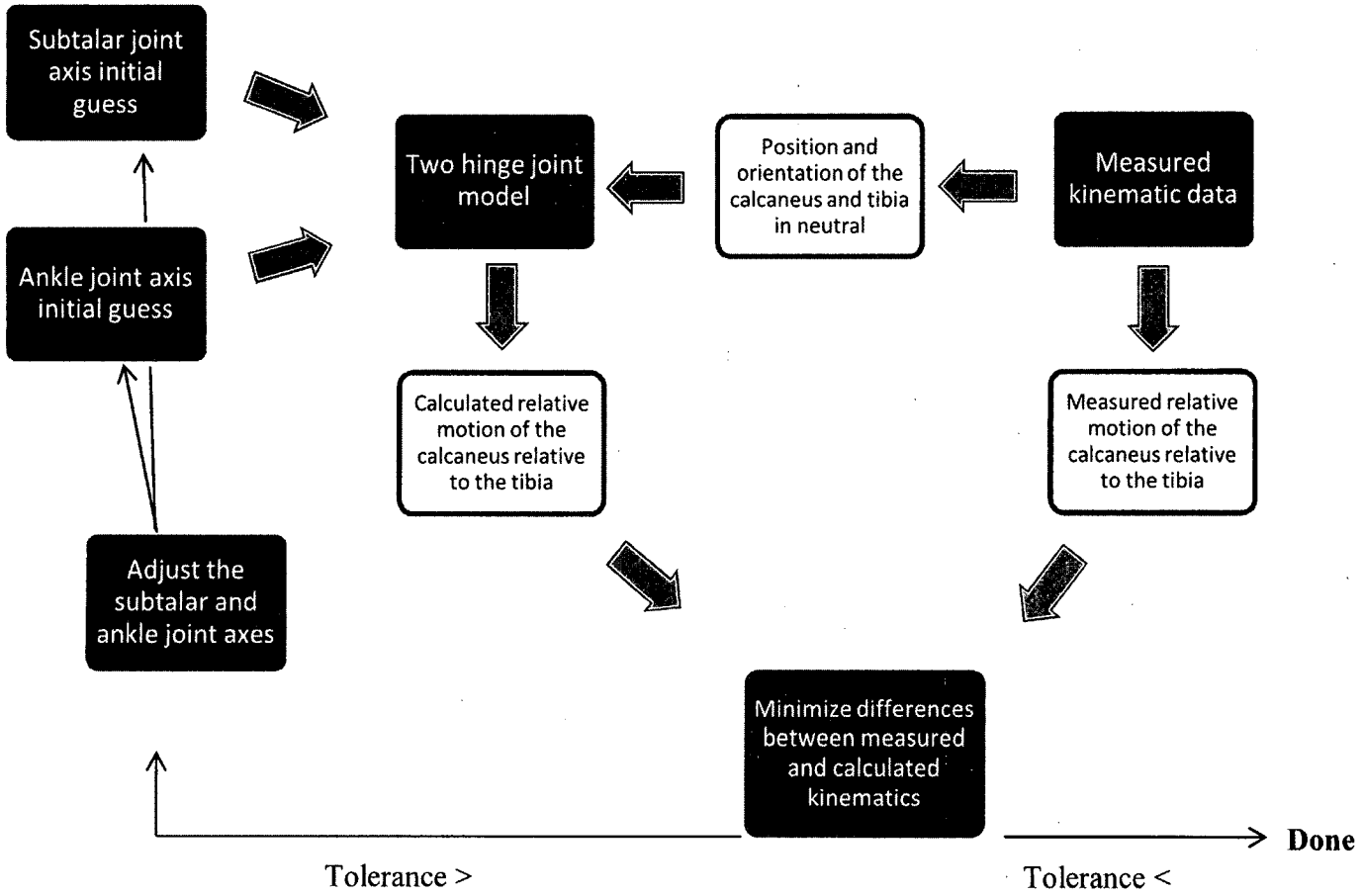

Figure A1-6-1: Flow chart of the optimization procedure

APPENDIX 2: FOOT KINEMATICS ANALYSIS

INDIVIDUAL RESULTS

A2.1 Subtalar joint angle of rotation

Table A2-1: Subtalar joint inversion range of motion in degree for the intact condition, after sectioning the calcaneofibular ligament (CFL) and after sectioning the CFL, cervical and interosseous talocalcaneal ligament (ITCL) while the foot was barefoot and after placing an ankle brace

Inversion	Intact		CFL cut		CFL, cervical and ITCL cut	
	Barefoot	Bracing	Barefoot	Bracing	Barefoot	Bracing
2	10.06	6.92	19.57	7.63	20.49	15.22
4	16.08	10.44	16.36	10.64	20.62	10.43
7	9.66	7.97	11.35	8.36	9.28	9.84
8	19.19	10.91	19.65	10.98	21.95	16.06
9	13.55	14.41	16.45	13.51	17.52	15.28
10	11.87	10.86	10.67	8.82	18.27	10.64
11	10.24	8.28	9.91	7.25	12.10	6.76
12	12.78	11.28	14.26	13.77	20.84	14.28
13	17.68	10.74	18.42	10.06	18.52	14.42

Table A2-2: Subtalar joint eversion range of motion in degree for the intact condition, after sectioning the calcaneofibular ligament (CFL) and after sectioning the CFL, cervical and interosseous talocalcaneal ligament (ITCL) while the foot was barefoot and after placing an ankle brace

Eversion	Intact		CFL cut		CFL, cervical and ITCL cut	
	Barefoot	Bracing	Barefoot	Bracing	Barefoot	Bracing
2	-13.22	-7.90	-9.03	-5.26	-13.01	-12.21
4	-6.77	-6.59	-8.73	-7.66	-6.91	-8.80
7	-5.76	-4.82	-9.91	-7.11	-7.85	-8.60
8	-6.26	-4.53	-5.83	-8.28	-9.23	-9.41
9	-15.41	-13.55	-18.03	-13.95	-16.13	-13.83
10	-8.90	-2.69	-11.61	-5.58	-7.25	-7.30
11	-8.44	-3.72	-10.82	-4.23	-9.35	-4.91
12	-8.76	-8.09	-7.34	-6.97	-7.22	-9.72
13	-3.38	-2.54	-4.37	-4.13	-5.10	-2.58

Table A2-3: Subtalar joint inversion range of motion in degree with the foot placed in maximum dorsiflexion for the intact condition, after sectioning the calcaneofibular ligament (CFL) and after sectioning the CFL, cervical and interosseous talocalcaneal ligament (ITCL) while the foot was barefoot and after placing an ankle brace

Dorsiflexion	Intact		CFL cut		CFL, cervical and ITCL cut	
+ Inversion	Barefoot	Bracing	Barefoot	Bracing	Barefoot	Bracing
2	14.02	11.73	20.96	6.18	19.90	13.44
4	7.30	6.53	13.71	7.07	13.56	7.34
7	5.62	5.11	10.41	5.48	6.45	4.29
8	14.43	11.59	12.73	9.40	15.93	9.66
9	10.49	5.46	5.62	9.17	10.74	3.99
10	9.27	4.77	11.48	7.36	9.80	9.14
11	10.93	8.04	7.43	6.91	11.23	6.98
12	8.88	7.70	10.07	9.02	11.97	10.63
13	11.86	8.72	13.59	8.54	12.18	11.29

Table A2-4: Subtalar joint eversion range of motion in degree with the foot placed in maximum dorsiflexion for the intact condition, after sectioning the calcaneofibular ligament (CFL) and after sectioning the CFL, cervical and interosseous talocalcaneal ligament (ITCL) while the foot was barefoot and after placing an ankle brace

Dorsiflexion	Intact		CFL cut		CFL, cervical and ITCL cut	
+ Eversion	Barefoot	Bracing	Barefoot	Bracing	Barefoot	Bracing
2	-9.28	-4.06	-7.81	-12.46	-11.91	-11.28
4	-7.97	-6.42	-6.59	-8.03	-9.06	-8.15
7	-6.64	-5.86	-5.08	-5.20	-9.47	-11.65
8	-7.39	-3.95	-10.59	-6.61	-10.44	-8.01
9	-12.41	-10.24	-13.56	-8.78	-15.95	-10.68
10	-8.90	-2.50	-2.82	-3.72	-9.20	-3.96
11	-6.48	-3.73	-11.14	-4.62	-10.53	-5.10
12	-7.34	-6.73	-9.14	-8.81	-9.79	-10.18
13	-7.20	-4.37	-6.89	-6.30	-6.49	-5.50

Table A2-5: Subtalar joint inversion range of motion in degree with the foot placed in maximum plantarflexion for the intact condition, after sectioning the calcaneofibular ligament (CFL) and after sectioning the CFL, cervical and interosseous talocalcaneal ligament (ITCL) while the foot was barefoot and after placing an ankle brace

Plantarflexion + Inversion	Intact		CFL cut		CFL, cervical and ITCL cut	
	Barefoot	Bracing	Barefoot	Bracing	Barefoot	Bracing
2	11.25	0.03	14.89	5.68	18.30	8.53
4	13.34	8.24	14.49	10.27	17.43	9.67
7	9.90	8.36	11.93	5.75	11.10	7.77
8	17.59	7.84	12.52	8.91	16.08	9.68
9	14.06	14.26	16.77	12.21	21.79	13.19
10	7.42	5.09	9.31	7.28	11.16	7.98
11	10.32	5.07	12.23	4.88	8.79	4.25
12	13.81	9.37	13.45	8.87	15.73	11.57
13	11.73	7.23	9.86	7.38	13.55	7.58

Table A2-6: Subtalar joint eversion range of motion in degree with the foot placed in maximum plantarflexion for the intact condition, after sectioning the calcaneofibular ligament (CFL) and after sectioning the CFL, cervical and interosseous talocalcaneal ligament (ITCL) while the foot was barefoot and after placing an ankle brace

Plantarflexion + Eversion	Intact		CFL cut		CFL, cervical and ITCL cut	
	Barefoot	Bracing	Barefoot	Bracing	Barefoot	Bracing
2	-5.20	-2.41	-5.87	-4.59	-7.04	-8.24
4	-6.35	-5.94	-6.16	-5.35	-4.53	-5.21
7	-2.92	-4.19	-5.19	-2.25	-6.27	-3.28
8	-5.37	-4.20	-6.99	-5.58	-8.04	-6.26
9	-4.37	-5.23	-9.01	-5.19	-6.79	-7.32
10	-6.46	-5.09	-7.67	-4.60	-5.68	-5.83
11	-3.70	-3.20	-2.84	-4.06	-5.46	-4.39
12	-3.26	-2.82	-2.46	-2.79	-3.51	-3.04
13	-1.16	-2.04	-2.43	-1.47	-2.85	-2.11

A2.2 Ankle joint angle of rotation (°)

Table A2-7: Ankle joint inversion range of motion in degree for the intact condition, after sectioning the calcaneofibular ligament (CFL) and after sectioning the CFL, cervical and interosseous talocalcaneal ligament (ITCL) while the foot was barefoot and after placing an ankle brace

Inversion	Intact		CFL cut		CFL, cervical and ITCL cut	
	Barefoot	Bracing	Barefoot	Bracing	Barefoot	Bracing
2	1.68	1.98	11.22	3.11	12.65	5.40
4	0.26	0.32	3.56	2.08	3.06	2.46
7	7.21	4.77	13.08	10.59	11.60	7.72
8	1.72	0.34	7.29	0.87	9.14	1.93
9	9.19	6.33	17.23	10.27	19.49	11.44
10	2.58	1.74	5.36	0.65	3.45	1.20
11	1.87	0.14	4.84	1.56	5.09	1.73
12	5.34	4.86	7.49	7.90	9.44	7.13
13	1.07	0.62	3.90	2.72	3.87	2.44

Table A2-8: Ankle joint eversion range of motion in degree for the intact condition, after sectioning the calcaneofibular ligament (CFL) and after sectioning the CFL, cervical and interosseous talocalcaneal ligament (ITCL) while the foot was barefoot and after placing an ankle brace

Eversion	Intact		CFL cut		CFL, cervical and ITCL cut	
	Barefoot	Bracing	Barefoot	Bracing	Barefoot	Bracing
2	-1.52	-0.41	-1.49	-1.39	-1.07	-2.00
4	-1.43	-0.99	-1.98	-0.58	-1.16	-0.57
7	-0.40	-1.84	-1.90	-0.39	-2.87	-0.50
8	-3.74	-1.16	-0.97	-0.73	-1.28	-2.94
9	-2.37	-0.74	-0.12	-1.34	-1.44	-0.95
10	-1.14	-2.55	-1.10	-1.10	-1.88	-1.27
11	-1.56	-1.15	-1.42	-1.44	-1.14	-0.84
12	-3.60	-3.19	-5.28	-5.68	-3.15	-2.49
13	-1.47	-1.27	-2.17	-0.62	-2.28	-1.81

Table A2-9: Ankle joint inversion range of motion in degree with the foot placed in maximum dorsiflexion for the intact condition, after sectioning the calcaneofibular ligament (CFL) and after sectioning the CFL, cervical and interosseous talocalcaneal ligament (ITCL) while the foot was barefoot and after placing an ankle brace

Dorsiflexion	Intact		CFL cut		CFL, cervical and ITCL cut	
+ Inversion	Barefoot	Bracing	Barefoot	Bracing	Barefoot	Bracing
2	0.38	0.22	7.99	3.18	3.51	2.03
4	0.27	0.46	1.95	0.59	2.02	0.80
7	4.90	2.28	6.71	3.57	13.20	3.17
8	2.65	1.64	1.89	1.12	2.03	1.48
9	3.50	2.47	10.13	6.32	12.20	5.43
10	0.69	0.00	2.27	0.26	2.16	0.80
11	1.58	0.27	3.57	0.24	3.06	0.16
12	1.76	0.67	4.76	3.45	7.64	0.70
13	0.95	0.54	3.99	1.48	1.34	1.01

Table A2-10: Ankle joint eversion range of motion in degree with the foot placed in maximum dorsiflexion for the intact condition, after sectioning the calcaneofibular ligament (CFL) and after sectioning the CFL, cervical and interosseous talocalcaneal ligament (ITCL) while the foot was barefoot and after placing an ankle brace

Dorsiflexion	Intact		CFL cut		CFL, cervical and ITCL cut	
+ Eversion	Barefoot	Bracing	Barefoot	Bracing	Barefoot	Bracing
2	-2.21	-1.14	-1.28	-2.88	-1.14	-3.23
4	-0.92	-1.13	-1.78	-2.18	-2.81	-1.04
7	0.00	-1.69	-0.83	-0.67	-0.79	-1.23
8	-1.11	-2.63	-0.55	-0.97	-1.58	-0.03
9	-0.99	-0.07	-1.49	-0.99	-2.15	-0.84
10	-0.57	-1.34	-1.21	-0.62	-1.22	-0.74
11	-0.32	-0.93	-0.51	-1.17	-1.45	-0.92
12	-2.57	-1.19	-1.29	-1.92	-1.00	-1.16
13	-0.63	-0.67	-0.61	-0.37	-1.53	-0.51

Table A2-11: Ankle joint inversion range of motion in degree with the foot placed in maximum plantarflexion for the intact condition, after sectioning the calcaneofibular ligament (CFL) and after sectioning the CFL, cervical and interosseous talocalcaneal ligament (ITCL) while the foot was barefoot and after placing an ankle brace

Plantarflexion + Inversion	Intact		CFL cut		CFL, cervical and ITCL cut	
	Barefoot	Bracing	Barefoot	Bracing	Barefoot	Bracing
2	2.35	3.32	10.17	3.76	9.04	7.52
4	2.91	0.20	5.00	2.56	5.12	3.54
7	2.99	2.10	2.86	2.78	1.78	1.48
8	3.43	0.60	8.87	2.66	6.43	0.54
9	5.98	5.10	11.77	8.25	13.93	7.69
10	2.38	1.07	2.42	1.71	3.22	1.83
11	1.66	0.78	3.20	1.39	2.65	1.18
12	6.47	5.08	7.64	5.03	7.61	5.97
13	1.99	1.24	3.50	3.16	5.27	4.16

Table A2-12: Ankle joint eversion range of motion in degree with the foot placed in maximum plantarflexion for the intact condition, after sectioning the calcaneofibular ligament (CFL) and after sectioning the CFL, cervical and interosseous talocalcaneal ligament (ITCL) while the foot was barefoot and after placing an ankle brace

Plantarflexion + Eversion	Intact		CFL cut		CFL, cervical and ITCL cut	
	Barefoot	Bracing	Barefoot	Bracing	Barefoot	Bracing
2	-5.00	-2.37	-8.24	-3.85	-3.70	-1.31
4	-0.90	-1.94	-2.23	-1.28	-1.30	-1.72
7	-1.18	-1.15	-0.61	-0.47	-1.19	-1.08
8	-1.76	-1.10	-2.18	-2.16	-2.97	-1.97
9	-3.58	-0.89	-2.58	-1.56	-2.55	-0.98
10	-0.73	-0.99	-0.85	-1.71	-0.99	-1.51
11	-1.04	-0.56	-0.91	-1.16	-0.74	-1.67
12	-3.32	-3.77	-4.31	-4.41	-4.53	-3.59
13	-0.84	-1.09	-2.11	-0.63	-1.46	-1.57

A2.3 Hindfoot joint angle of rotation (°)

Table A2-13: Hindfoot inversion range of motion in degree for the intact condition, after sectioning the calcaneofibular ligament (CFL) and after sectioning the CFL, cervical and interosseous talocalcaneal ligament (ITCL) while the foot was barefoot and after placing an ankle brace

Inversion	Intact		CFL cut		CFL, cervical and ITCL cut	
	Barefoot	Bracing	Barefoot	Bracing	Barefoot	Bracing
2	11.49	8.92	30.13	10.84	32.51	20.70
4	16.03	10.60	20.17	12.91	24.37	12.88
7	16.49	12.67	24.04	19.08	20.61	17.20
8	19.79	11.02	26.82	12.05	30.84	18.41
9	22.54	20.67	33.36	23.69	36.70	26.39
10	14.41	11.55	15.86	9.51	21.67	11.83
11	12.00	8.16	14.86	8.56	17.13	8.49
12	18.34	16.63	21.88	22.03	29.98	21.18
13	18.78	11.28	22.51	12.76	22.69	16.89

Table A2-14: Hindfoot eversion range of motion in degree for the intact condition, after sectioning the calcaneofibular ligament (CFL) and after sectioning the CFL, cervical and interosseous talocalcaneal ligament (ITCL) while the foot was barefoot and after placing an ankle brace

Eversion	Intact		CFL cut		CFL, cervical and ITCL cut	
	Barefoot	Bracing	Barefoot	Bracing	Barefoot	Bracing
2	-14.58	-6.49	-10.23	-6.34	-13.36	-13.14
4	-8.05	-7.09	-10.60	-7.97	-7.86	-9.35
7	-5.80	-5.75	-11.74	-7.35	-10.46	-8.39
8	-9.89	-4.87	-6.50	-8.94	-8.37	-10.65
9	-17.22	-13.38	-16.71	-14.15	-17.28	-13.43
10	-10.07	-5.20	-12.61	-6.28	-9.10	-8.25
11	-9.77	-4.76	-12.10	-5.47	-10.37	-5.70
12	-12.28	-11.42	-12.69	-12.69	-10.29	-11.77
13	-4.59	-3.67	-6.60	-4.72	-7.15	-4.31

Table A2-15: Hindfoot inversion range of motion in degree with the foot placed in maximum dorsiflexion for the intact condition, after sectioning the calcaneofibular ligament (CFL) and after sectioning the CFL, cervical and interosseous talocalcaneal ligament (ITCL) while the foot was barefoot and after placing an ankle brace

Dorsiflexion	Intact		CFL cut		CFL, cervical and ITCL cut	
+ Inversion	Barefoot	Bracing	Barefoot	Bracing	Barefoot	Bracing
2	12.57	11.77	28.86	9.79	22.98	15.32
4	7.35	5.71	15.71	7.59	15.57	8.11
7	10.48	7.17	16.66	8.74	19.33	7.27
8	15.45	9.25	14.36	10.42	17.98	10.85
9	13.79	7.65	15.63	15.29	22.88	9.41
10	9.62	4.43	13.42	7.21	12.21	9.93
11	12.53	7.35	10.57	6.76	13.89	6.68
12	10.68	7.43	14.82	12.70	19.51	11.26
13	12.65	8.58	17.76	9.10	13.62	12.21

Table A2-16: Hindfoot eversion range of motion in degree with the foot placed in maximum dorsiflexion for the intact condition, after sectioning the calcaneofibular ligament (CFL) and after sectioning the CFL, cervical and interosseous talocalcaneal ligament (ITCL) while the foot was barefoot and after placing an ankle brace

Dorsiflexion	Intact		CFL cut		CFL, cervical and ITCL cut	
+ Eversion	Barefoot	Bracing	Barefoot	Bracing	Barefoot	Bracing
2	-10.05	-4.64	-8.19	-15.11	-12.77	-13.54
4	-8.83	-6.94	-8.34	-10.20	-11.86	-8.98
7	-3.38	-7.05	-5.53	-4.97	-10.01	-12.61
8	-7.39	-4.72	-9.86	-7.60	-8.57	-6.94
9	-12.62	-8.84	-14.99	-8.75	-17.96	-11.51
10	-9.26	-3.84	-3.96	-4.60	-10.77	-4.86
11	-6.54	-3.78	-11.49	-5.05	-10.89	-5.32
12	-9.60	-7.91	-10.38	-10.58	-10.69	-10.52
13	-6.95	-4.81	-7.63	-5.60	-5.91	-5.99

Table A2-17: Hindfoot inversion range of motion in degree with the foot placed in maximum plantarflexion for the intact condition, after sectioning the calcaneofibular ligament (CFL) and after sectioning the CFL, cervical and interosseous talocalcaneal ligament (ITCL) while the foot was barefoot and after placing an ankle brace

Plantarflexion + Inversion	Intact		CFL cut		CFL, cervical and ITCL cut	
	Barefoot	Bracing	Barefoot	Bracing	Barefoot	Bracing
2	13.41	2.25	24.47	9.39	27.02	15.80
4	16.92	9.12	20.12	13.12	23.12	13.29
7	12.64	10.14	14.75	8.52	12.34	8.93
8	21.23	8.34	21.82	11.77	23.12	10.24
9	20.01	19.15	28.35	20.25	35.33	20.63
10	9.68	6.09	11.54	8.77	14.18	9.64
11	11.94	5.65	15.40	6.31	11.44	5.40
12	20.19	14.62	21.08	13.82	23.29	17.21
13	13.79	8.44	13.45	10.63	19.03	11.66

Table A2-18: Hindfoot eversion range of motion in degree with the foot placed in maximum plantarflexion for the intact condition, after sectioning the calcaneofibular ligament (CFL) and after sectioning the CFL, cervical and interosseous talocalcaneal ligament (ITCL) while the foot was barefoot and after placing an ankle brace

Plantarflexion + Eversion	Intact		CFL cut		CFL, cervical and ITCL cut	
	Barefoot	Bracing	Barefoot	Bracing	Barefoot	Bracing
2	-10.12	-5.24	-13.60	-8.50	-9.90	-9.28
4	-7.07	-7.54	-8.45	-6.44	-5.73	-6.72
7	-3.82	-5.10	-5.58	-2.26	-7.19	-4.04
8	-6.95	-5.25	-8.68	-7.21	-10.81	-8.35
9	-7.69	-5.70	-10.59	-6.34	-7.95	-7.71
10	-6.95	-6.01	-8.28	-6.13	-6.38	-7.23
11	-4.69	-3.65	-3.54	-5.00	-5.97	-6.02
12	-6.23	-6.38	-6.31	-7.02	-7.49	-6.31
13	-1.72	-3.07	-4.29	-2.07	-4.00	-3.56

A2.4 Moments (N.m)

Table A2-19: Moment (N.m) applied to the foot during inversion for the intact condition, after sectioning the calcaneofibular ligament (CFL) and after sectioning the CFL, cervical and interosseous talocalcaneal ligament (ITCL) while the foot was barefoot and after placing an ankle brace

Inversion	Intact		CFL cut		CFL, cervical and ITCL cut	
	Barefoot	Bracing	Barefoot	Bracing	Barefoot	Bracing
2	5.39	7.29	5.20	5.80	6.70	5.07
4	7.44	9.75	6.66	9.83	7.54	8.93
7	7.08	8.72	5.54	7.08	6.02	9.04
8	5.62	5.58	4.33	5.75	5.28	7.05
9	4.59	4.42	4.25	5.83	4.91	5.02
10	7.40	10.52	4.41	6.77	8.50	8.43
11	5.01	6.50	6.69	6.99	7.19	8.87
12	5.03	7.48	4.94	7.66	4.99	6.14
13	7.11	7.88	7.50	7.77	7.25	10.64

Table A2-20: Moment (N.m) applied to the foot during eversion for the intact condition, after sectioning the calcaneofibular ligament (CFL) and after sectioning the CFL, cervical and interosseous talocalcaneal ligament (ITCL) while the foot was barefoot and after placing an ankle brace

Eversion	Intact		CFL cut		CFL, cervical and ITCL cut	
	Barefoot	Bracing	Barefoot	Bracing	Barefoot	Bracing
2	-4.61	-6.81	-5.36	-6.61	-6.98	-9.23
4	-7.44	-9.42	-8.89	-10.89	-8.60	-9.53
7	-6.00	-7.82	-6.24	-6.20	-6.16	-5.72
8	-6.61	-6.03	-6.69	-9.08	-7.38	-10.14
9	-4.38	-7.56	-6.03	-8.27	-5.59	-6.93
10	-7.85	-6.81	-6.29	-10.19	-9.87	-8.45
11	-6.15	-7.82	-8.39	-10.68	-5.63	-9.50
12	-7.19	-8.12	-6.78	-7.88	-5.88	-7.99
13	-7.83	-9.13	-9.52	-9.55	-10.16	-9.87

Table A2-21: Moment (N.m) applied to the foot during inversion with the foot placed in maximum dorsiflexion for the intact condition, after sectioning the calcaneofibular ligament (CFL) and after sectioning the CFL, cervical and interosseous talocalcaneal ligament (ITCL) while the foot was barefoot and after placing an ankle brace

Dorsiflexion	Intact		CFL cut		CFL, cervical and ITCL cut	
+ Inversion	Barefoot	Bracing	Barefoot	Bracing	Barefoot	Bracing
2	3.35	7.38	3.81	5.79	4.72	6.52
4	5.84	7.20	6.69	6.76	5.52	5.62
7	7.21	6.61	7.15	7.45	2.26	4.56
8	4.13	5.80	4.66	6.18	4.56	7.03
9	5.97	7.27	4.52	6.06	4.60	6.84
10	7.84	8.31	7.08	5.44	5.53	8.27
11	5.38	6.45	4.83	8.00	5.53	8.00
12	5.10	6.40	6.21	5.40	5.85	7.40
13	6.73	7.07	7.15	6.13	5.51	9.77

Table A2-22: Moment (N.m) applied to the foot during eversion with the foot placed in maximum dorsiflexion for the intact condition, after sectioning the calcaneofibular ligament (CFL) and after sectioning the CFL, cervical and interosseous talocalcaneal ligament (ITCL) while the foot was barefoot and after placing an ankle brace

Dorsiflexion	Intact		CFL cut		CFL, cervical and ITCL cut	
+ Eversion	Barefoot	Bracing	Barefoot	Bracing	Barefoot	Bracing
2	-3.77	-5.56	-2.60	-8.80	-4.94	-5.38
4	-9.21	-12.56	-7.84	-13.10	-8.65	-13.42
7	-6.94	-7.05	-3.34	-7.65	-4.78	-7.90
8	-6.53	-7.66	-6.85	-10.23	-7.10	-9.82
9	-5.56	-7.00	-5.14	-7.60	-5.53	-7.61
10	-7.23	-7.17	-4.32	-11.03	-7.38	-10.87
11	-5.22	-8.70	-4.60	-6.30	-7.64	-8.52
12	-6.17	-7.43	-8.58	-10.40	-7.77	-8.59
13	-7.84	-9.50	-6.73	-12.07	-5.08	-9.96

Table A2-23: Moment (N.m) applied to the foot during inversion with the foot placed in maximum plantarflexion for the intact condition, after sectioning the calcaneofibular ligament (CFL) and after sectioning the CFL, cervical and interosseous talocalcaneal ligament (ITCL) while the foot was barefoot and after placing an ankle brace

Plantarflexion + Inversion	Intact		CFL cut		CFL, cervical and ITCL cut	
	Barefoot	Bracing	Barefoot	Bracing	Barefoot	Bracing
2	2.92	4.23	5.67	4.91	4.85	5.91
4	6.11	7.34	7.38	8.96	5.95	8.47
7	7.29	7.37	8.44	9.93	5.63	7.89
8	4.46	5.24	4.31	4.69	4.76	5.04
9	4.71	7.29	4.21	7.28	5.81	5.40
10	7.51	8.16	6.02	7.51	6.77	7.44
11	6.07	6.30	7.25	6.74	4.72	8.29
12	6.46	6.94	5.22	6.28	5.34	6.26
13	8.45	7.19	5.99	8.63	8.53	8.39

Table A2-24: Moment (N.m) applied to the foot during eversion with the foot placed in maximum plantarflexion for the intact condition, after sectioning the calcaneofibular ligament (CFL) and after sectioning the CFL, cervical and interosseous talocalcaneal ligament (ITCL) while the foot was barefoot and after placing an ankle brace

Plantarflexion + Eversion	Intact		CFL cut		CFL, cervical and ITCL cut	
	Barefoot	Bracing	Barefoot	Bracing	Barefoot	Bracing
2	-5.16	-6.80	-7.67	-7.44	-5.88	-8.23
4	-6.19	-10.03	-7.12	-8.59	-6.05	-7.43
7	-5.64	-5.65	-6.89	-6.83	-7.44	-6.24
8	-4.83	-5.69	-4.42	-5.76	-5.37	-6.91
9	-4.54	-5.31	-6.24	-6.94	-5.58	-5.92
10	-7.52	-7.12	-5.59	-7.53	-5.97	-6.81
11	-5.93	-6.25	-4.32	-9.46	-5.42	-7.78
12	-5.41	-6.81	-5.83	-6.44	-5.53	-6.77
13	-5.36	-7.78	-6.71	-8.04	-6.87	-7.77

APPENDIX 3: MEAN HELICALAXIS ANALYSIS INDIVIDUAL RESULTS

A3.1 Subtalar joint

Table A3-1: Differences in inclination angle and deviation angle for the different intact subtalar joint axis (DF+InvEv = MHA from dorsiflexed inversion-eversion; InvEv = MHA from inversion-eversion and Opti = resulting axis from the optimization method)

Intact	Differences in inclination angle			Differences in deviation angle		
between	DF+InvEv InvEv	DF+InvEv Opti	InvEv Opti	DF+InvEv InvEv	DF+InvEv Opti	InvEv Opti
4	-1.89	16.77	18.66	0.84	19.29	18.45
7	-3.03	15.98	19.01	5.49	3.01	-2.48
9	-9.56	14.29	23.85	8.75	-23.29	-32.04
11	-0.12	40.67	40.78	-9.01	-18.64	-9.63
12	-10.72	2.73	13.44	0.10	26.03	25.93
13	-3.73	6.13	9.86	-16.77	-4.15	12.63

Table A3-2: Differences in inclination angle and deviation angle for the different calcaneofibular ligament (CFL) deficient subtalar joint axis (DF+InvEv = MHA from dorsiflexed inversion-eversion; InvEv = MHA from inversion-eversion and Opti = resulting axis from the optimization method)

CFL cut	Differences in inclination angle			Differences in deviation angle		
between	DF+InvEv InvEv	DF+InvEv Opti	InvEv Opti	DF+InvEv InvEv	DF+InvEv Opti	InvEv Opti
4	-4.62	17.93	22.56	1.80	-32.12	-33.92
7	-3.54	-6.20	-2.66	1.57	-1.17	-2.74
9	-13.48	11.38	24.86	1.78	-2.16	-3.94
11	-6.47	20.21	26.67	-1.51	-6.39	-4.89
12	-2.71	14.95	17.66	-5.57	-0.20	5.37
13	-3.83	-5.58	-1.75	-6.67	5.06	11.73

Table A3-3: Differences in inclination angle and deviation angle for the different subtalar joint axis after the CFL, cervical and interosseous talocalcaneal ligament (ITCL) were cut (DF+InvEv = MHA from dorsiflexed inversion-eversion; InvEv = MHA from inversion-eversion and Opti = resulting axis from the optimization method)

All cut	Differences in inclination angle			Differences in deviation angle		
between	DF+InvEv InvEv	DF+InvEv Opti	InvEv Opti	DF+InvEv InvEv	DF+InvEv Opti	InvEv Opti
4	-6.66	-8.28	-1.62	-3.83	-8.92	-5.09
7	-8.91	30.07	38.98	4.09	20.05	15.96
9	-19.42	-3.78	15.64	0.16	-42.43	-42.59
11	-1.74	9.84	11.58	6.43	-5.21	-11.64
12	2.88	52.31	49.43	-7.03	-19.36	-12.33
13	-1.93	-5.74	-3.81	3.98	-9.19	-13.18

A3.2 Ankle joint

Table A3-4: Differences in inclination angle and deviation angle for the different intact ankle joint axis (PFDF = MHA from plantarflexion-dorsiflexion; InvEv = MHA from inversion-eversion and Opti = resulting axis from the optimization method)

Intact	Differences in inclination angle			Differences in deviation angle		
between	PFDF InvEv	PFDF Opti	InvEv Opti	PFDF InvEv	PFDF Opti	InvEv Opti
4	-25.53	15.79	41.32	-37.24	-5.57	31.67
7	25.10	21.94	-3.16	-14.69	-9.79	4.90
9	16.75	25.86	9.11	-28.78	-30.94	-2.16
11	26.34	37.14	10.80	-55.13	2.87	58.00
12	7.23	27.41	20.18	-42.00	-7.77	34.23
13	-14.78	40.49	55.26	-23.65	16.36	40.01

Table A3-5: Differences in inclination angle and deviation angle for the different CFL deficient ankle joint axis (PFDF = MHA from plantarflexion-dorsiflexion; InvEv = MHA from inversion-eversion and Opti = resulting axis from the optimization method)

CFL cut	Differences in inclination angle			Differences in deviation angle		
between	PFDF InvEv	PFDF Opti	InvEv Opti	PFDF InvEv	PFDF Opti	InvEv Opti
4	4.08	18.70	14.62	-40.82	-10.22	30.60
7	32.39	1.71	-30.68	-19.44	-1.54	17.90
9	-8.21	18.83	27.05	-19.76	-6.78	12.98
11	16.35	34.03	17.68	-64.35	11.57	75.92
12	4.98	21.52	16.54	-45.01	-14.01	31.01
13	27.13	17.93	-9.21	-54.21	-3.12	51.10

Table A3-6: Differences in inclination angle and deviation angle for the different ankle joint axis after the CFL, cervical and interosseous talocalcaneal ligament (ITCL) were cut (PFDF = MHA from plantarflexion-dorsiflexion; InvEv = MHA from inversion-eversion and Opti = resulting axis from the optimization method)

All cut	Differences in inclination angle			Differences in deviation angle		
between	PFDF InvEv	PFDF Opti	InvEv Opti	PFDF InvEv	PFDF Opti	InvEv Opti
4	-17.12	-5.58	11.53	-37.96	-4.28	33.67
7	29.36	17.67	-11.68	-36.67	3.43	40.10
9	31.30	8.86	-22.43	-30.48	-1.60	28.87
11	15.48	27.78	12.30	13.62	-9.43	-23.05
12	25.65	34.32	8.67	-60.96	16.78	77.75
13	14.75	14.73	-0.02	-59.10	8.55	67.65

JULIE CHOISNE

Educational background

Master in Mechanical Engineering, 09/2004 - 06/2009
Engineering School Leonard De Vinci (ESILV Paris) – France
Swiss Federal Institute of Technology Lausanne (EPFL) 09/2008 - 07/2009
Exchange student in Department of Material Science

Peer-reviewed publications

Choisne J, Ringleb SI, Samaan MA, Bawab SY, Naik D, Anderson CD. Influence of Kinematic Analysis Methods on Detecting Ankle and Subtalar joint Instability, *Journal of Biomechanics*, 45 (1), 2012, pp. 46-52
Choisne J, Hoch M, Bawab S, Alexander I, Ringleb S. The effects of a semi-rigid ankle brace on a simulated isolated subtalar joint instability, *Journal of Orthopedic Research*

Professional experience

Graduate Teaching Assistant, Dynamics 09/2011 - Present
Dr. Ringleb, ODU, Norfolk, VA
Doctoral Research Assistant in Mechanical Engineering 09/2009 – 09/2011
Dr. Ringleb, ODU, Norfolk, VA
Graduate Teaching Assistant, Nanomaterials Spring 2009
Prof. Hofmann, EPFL, Switzerland
Internship in the Aerospace R&D department 09/2007 – 02/2008
Hispano Suiza (Safran Group), Colombes, France
Internship in the rail train R&D department Summer 2006
Paulstra Vibrachoc (Hutchinson Group), Levallois, France

Grants and awards

- The ISB Congress Travel Grant, *International Society of Biomechanics* (2013)
- The ASB Graduate Student Grant-In-Aid, *American Society of Biomechanics* (2012)
- The ISB Matching Dissertation Grant, *International Society of Biomechanics* (2012)
- Graduate Teaching Assistantship, *Old Dominion University, Frank Batten College of Engineering* (Fall 2011)
- Graduate Student Travel Award, *Old Dominion University* (Summer 2010)
- Dean Fellowship Award, *Old Dominion University, Frank Batten College of Engineering* (2009)